MEASUREMENT OF QUANTUM AND PARTICLE ENERGIES WITH SCINTILLATION COUNTERS.

by

R.C. Bannerman,
Department of Natural Philosophy,
University of Glasgow.

Presented as a thesis for the degree of Ph.D.
in the University of Glasgow.
May, 1952.

ProQuest LLC.
789 East Eisenhower Parkway
P.O. Box 1346
Ann Arbor, MI 48106 – 1346

Preface.

In this thesis I have given an account of work carried out with scintillation counters on the measurement of quantum and particle energies. The main application has been to the measurement of β-ray and ϒ-ray energies as a means of determining the decay schemes of radioactive isotopes.

In Part I a general introduction to the subject of energy measurement is given which includes a critical survey of other techniques and an indication of the scope for new ones. This part is taken from a variety of sources, including Moon's "Artificial Radioactivity" (Moon 1949) and a number of original papers which are referred to in the text. Part II is a more detailed introduction dealing with the scintillation counter itself, and it is drawn from the now fairly extensive literature on the subject.

Part III contains a description of the scintillation counter as developed by the writer for use in β- and ϒ-ray energy measurements. Part IV deals with an original application of the Compton effect to ϒ-ray spectroscopy, which was suggested by Dr. S.C. Curran and developed and used by the writer. In Part V, the techniques used in studying decay schemes and the results obtained for three different sources are described. One of the techniques

used here, the integrated spectrum method, is a new application of a 4π counting geometry to such problems. In the work on La^{140} the writer was assisted in the interpretive aspects of the problem by Mr. G.M. Lewis and Dr. S.C. Curran, while in the case of RaD the approach to the problem and the interpretation of results was carried out jointly with Dr. S.C. Curran. In the work on Sm^{153} the writer had the benefit of helpful discussion with Dr. S.C. Curran. All the experimental work described in Parts III, IV and V was carried out solely by the writer.

In Appendix I an account is given of some early work on α-particle detection, and the latter part of this work which involved the use of the H.T. Set was carried out in collaboration with members of that group. In this connection I wish to thank Dr. J.G. Rutherglen for the use of the illustration of Figure 1, Appendix I. In Appendix II details are given of methods evolved by the writer for handling and cleaning the phosphor crystals, while in Appendix III a more detailed account of the electronic equipment is given than is included in the main body of the thesis. Although the circuits described in Appendix III represent no original work on the part of the writer, it is considered that a description of their mode of operation forms an essential part of the thesis.

In conclusion I would like to thank Professor P.I. Dee for his continued interest and encouragement, and Dr. S.C.

Curran for many helpful suggestions and discussions. I am indebted to the Department of Scientific and Industrial Research and to the Nuffield Foundation for financial support during the period of this work.

May, 1952. R.C.B.

Contents.

Part I. General Introduction. 1.

1. The Purpose of Energy Measurements. 1.

2. Experimental Techniques. 3.

(a) Crystal Diffraction.
(b) Absorption Measurements.
(c) The Cloud Chamber.
(d) The Photographic Plate.
(e) The Nuclear Photo-Effect.
(f) The Proportional Counter.
(g) Magnetic Spectrometers.
(h) Coincidence Techniques.

3. The Field of Application. 13.

(a) Nuclear Reactions.
(b) Natural Radioactivity.
(c) Artificial Radioactivity.

Part II. The Scintillation Counter. 18.

1. Historical Development. 18.

2. Design Considerations. 23.

3. The Process of Energy Measurement. 31.

(a) The Measurement of Particle Energies.
(b) The Measurement of Quantum Energies.

Part III. The Scintillation Counter. (continued) 40.

1. Description of Equipment. 40.

(a) The Scintillation Counter.
(b) Electronic Equipment.

2. Performance of the Scintillation Counter. 54.

(a) Energy Response and Resolution.
(b) The Photomultiplier Tubes.
(c) Merits and Demerits as a Spectrometer.

Part IV. The Compton Coincidence Spectrometer. 69.

1. The Theory of the Spectrometer. 69.

2. Description and Performance of the Spectrometer. 81.

Part V. The Study of Decay Schemes. 85.

1. The Techniques Employed. 85.

(a) The γ-Ray Spectrum.
(b) The γ-γ Coincidence Spectrum.
(c) The β-Ray Spectrum.
(d) The β-γ Coincidence Spectrum.
(e) The Integrated Spectrum.

2. The Decay Scheme of La^{140}. 95.

3. The Decay Scheme of RaD. 108.

4. The Decay Scheme of Sm^{153}. 125.

5. Conclusion. 140.

(a) Improvements in Technique.
(b) Future Work.

Appendix I. The Detection of α-Particles. 145.

1. The Nature of the Problem. 145.

2. Description of the α-Particle Counter. 146.

3. Experimental Results. 149.

Appendix II. The Cleaning of Phosphor Crystals. 153.

Appendix III. Electronic Equipment. 159.

References. 169.

Part I. General Introduction.

1. The Purpose of Energy Measurements.

It has been pointed out many times that the state of nuclear physics at the present day bears a strong resemblance to the state of atomic physics at the end of last century. In the latter case a large amount of spectroscopic data had been amassed on the radiations emitted by excited atoms and some empirical relations had been established connecting their wavelengths. These results were later explained by theories based on the original concepts of Rutherford and Bohr, and now a very full understanding of the outer electronic structure of the atom has been attained.

Arguing along somewhat similar lines, we would expect that the collection of similar data on the radiations from excited nuclei would lead first to empirical relationships, and ultimately to a solution of the problem of the structure of the nucleus and the nature of nuclear forces. The parallel is not completely exact because the structure of the nucleus presents an extremely complex many-body problem, in contrast to the relatively simple structure of the electronic shells. However, the principles of quantum mechanics would lead us to expect that the total energy of the nucleons could only assume certain discrete values, similar to the electron "energy levels". This assumption has been confirmed by a large body of experimental evidence, including the phenomena

of resonance absorption of protons and neutrons, and the emission of α-particles and γ-rays of well-defined energies. The emission of β-particles is an apparent exception to this rule but can be reconciled with the energy level hypothesis. The properties of these levels, such as the energy above the ground state, the angular momentum and the parity, will depend upon the forces between the nucleons and the structure of the nucleus. Thus it is clearly desirable to obtain as detailed a knowledge as possible of these properties, in order to provide a basis for comparison between theoretical predictions and experimental results.

There are several ways of obtaining this information, and one of the most generally used is the study of the radiations, both particles and quanta, which are emitted from an excited nucleus. The properties of the emitted radiations which can be measured include the energy, the relative intensity, and the correlation both in space and in time of different particles and quanta. It is with such problems of measurement that we shall be concerned in the remainder of this thesis.

2. Experimental Techniques.

The techniques which have been used up to the present to examine radiations have been concerned largely with the determination of energy and of relative intensity, such as in the measurement of β-ray and ϒ-ray spectra (Moon 1949). The emphasis on coincidence work, particularly when combined with accurate determination of the energy of the coincident radiations, has not been so great. We shall now consider briefly some of the existing techniques.

(a) Crystal Diffraction.

This method, which is really an extension of the optical and X-ray technique, is capable of determining ϒ-ray energies to a considerable degree of accuracy, since it measures wavelengths in terms of the crystal lattice spacing. The limitations of this method are that it demands a very strong source and that there is an upper limit to the energy at which it can be used, on account of the very small glancing angles involved which diminish with increasing energy. One of the highest energy lines which has been investigated by this method is the 1.33 MeV ϒ-ray from Co^{60} (Lind, Brown and DuMond 1949), and a source of the order of 1 Curie was used to obtain an accuracy of 1 part in 10,000. Thus for energies much in excess of 1 MeV and where only small sources are available, other methods must be used.

(b) Absorption Measurements.

This method has been used extensively in the past to determine the range, and hence the energy, of most types of radiation, including protons, α-particles and β-rays. To obtain absolute measurements the range-energy relationship for the particles in question must be known. For heavy particles, protons and α-particles, the effects of range straggling limit the accuracy to about 1%, but for β-rays the errors due to straggling are much more serious. However if special precautions are taken, much useful information on β-ray spectrum shapes and end-points can be obtained (Feather 1938).

γ-ray energies can be determined by measuring the absorption coefficient in various materials, but where more than one γ-ray is present in the same energy region, the method breaks down completely. Energy determination is also made difficult at energies much greater than ~1 MeV by the fact that in this region the absorption coefficient changes too slowly with energy to provide much information. There is also the difficulty that, since the absorption coefficient has a minimum value, it is necessary to determine it in more than one material to avoid ambiguity (McMillan 1934).

γ-ray energies can also be determined by measuring the range of the secondary electrons by the coincidence absorption method. In this the secondary particles produced in a "converter" are caused to pass right through one

thin-walled Geiger counter into a second counter. The range of the particles is then found by placing sheets of absorber between the counters and plotting the coincidence counting rate against the absorber thickness. When the absorber thickness is greater than the range of the secondary particles, no further drop in the coincidence counting rate can take place. This method is capable of determining the energy of a single γ-ray line to a few percent over a wide range of energies, but breaks down due to poor resolution when two γ-rays of comparable energy are present. With high energy γ-rays, pair production and bremsstrahlung can cause serious trouble.

(c) The Cloud Chamber.

The cloud chamber's usefulness is limited by the short β-particle range in the gas and its very low stopping power for γ-rays. In addition, the straggling of the β-particles makes the measurement of track lengths and curvatures difficult, and the interpretation of results from a large number of photographs is slow and tedious. On the other hand it is possible to observe the coincident emission of particles, e.g. positron-electron pairs, and to carry out measurements of their energies. This method has been used by Delsasso et al. (1937), among others, to measure high energy γ-radiation. A useful application of the cloud chamber is to the study of β-particles of energy less than

~50 keV, particularly if the source can be introduced into the chamber in gaseous form, e.g. in the study of the RaD β-spectrum by Richardson and Leigh-Smith (1937).

(d) The Photographic Plate.

This method is similar in principle to the cloud chamber. Development of the plate produces grains of silver at points where ionisation has occurred, and so reveals the tracks of charged particles in the emulsion. From a measurement of the track length and the grain density along the track it is possible in many cases both to identify the particle and to determine its energy. The greatly increased stopping power of the emulsion over the gas of the cloud chamber allows the photographic plate to be used in the examination of particles of several MeV in energy. The method, however, suffers from the limitations in energy resolution due to straggling which are inherent in an absorption technique.

(e) The Nuclear Photo-Effect.

This method of measuring γ-ray energies is analogous to the photoelectric effect in that a proton or neutron is ejected from the nucleus with the energy of the γ-ray minus the binding energy of the particle. The application of the method, however, is rather restricted. It is limited on the low energy side by the fact that the nucleus most commonly used (deuterium) has a threshold at ~~2.18~~ 2.23 MeV, while on the high energy side the cross-section for the effect falls off

with increasing energy. The method has, however, the great advantage of making it possible to detect a very weak high energy radiation in the presence of intense radiation of a lower energy.

(f) The Proportional Counter.

This counter, which uses the process of gas multiplication to produce an output proportional to the amount of ionisation caused by the radiation, has been developed lately into one of the most useful methods of measuring particle and quantum energies. The lower limit to the energy range is in practice about 200 eV, although theoretically this should correspond to the energy required to produce one ion pair in the gas, i.e. $\sim$30 eV. The upper limit is set by the path length in the gas and if pressures of $\sim$5 atmospheres are used the range can be extended to $\sim$200 keV. This can be further increased by the use of magnetic fields to confine the particles within the counting volume (Curran, Cockroft and Insch 1950). The counter, however, suffers from the usual defects of a gas-filled tube, a low stopping power for γ-rays and the problem of using thin windows with particle radiations. The latter drawback can be overcome in certain cases by mounting the source inside the counter or by using a gaseous source. A detailed description of the present design of counter is given by Cockroft and Curran (1951).

(g) Magnetic Spectrometers.

The method of magnetic analysis has so far provided the most accurate means of determining both quantum and particle energies, except at very low energies where the proportional counter can be used. Of the many varied and specialised types, some of the most commonly used are the semi-circular, the magnetic lens and the double-focusing spectrometers. An excellent survey of these is given by Persico and Geoffrion (1950).

The magnetic spectrometer is usually designed to deal with β-particles but the method can also be applied to protons and α-particles. It is normally used with a resolution of 1 or 2%, a transmission factor (solid angle) of 1% or less, and a source area of ~ 1 cm^2. The performance is good up to very high energies but is limited on the low energy side by the problem of detecting the resolved β-particles. The two principal methods of detection are the photographic plate and the Geiger counter. The former requires only a single exposure with a fixed magnetic field to record a complete spectrum, but is non-linear for a wide range of intensities and so cannot give an accurate spectrum shape. It is also relatively insensitive to electrons below $\sim$10 to 20 keV. The Geiger counter, on the other hand, detects individual electrons and therefore enables relative intensities to be measured accurately. It however suffers from the problem of requiring thin windows to detect low

energy electrons, and its lower limit is similar to that of the photographic plate. Attempts have been made to overcome this difficulty, among them the use of post-focusing acceleration (Butt 1950) which is designed to impart sufficient energy to the electrons to enable them to enter the counter. Two other disadvantages are that the use of a finite slit width in front of the counter reduces the resolving power, and that to cover a whole spectrum the magnetic field must be varied.

The determination of γ-ray energies is usually carried out by examining the secondary photoelectrons arising from either internal or external conversion. In the first case the photoelectrons are observed as sharp lines superimposed upon the ordinary β-spectrum. If internal conversion is not strong enough or does not occur, the second method is used. Here the β-particles from the source are absorbed in some dense material, preferably of low atomic number (e.g. Cu), and the photoelectrons are ejected from a thin "radiator" of either lead or platinum foil. The photoelectron peaks are now observed against a background of Compton electrons produced by the γ-rays in the copper absorber. The lower energy limit of this method is again set by the problem of detecting low energy electrons, while the upper limit is set by the behaviour of the photoelectric cross-section which becomes vanishingly small at energies much above 1 MeV. The overall efficiency of this method is naturally much

poorer than that which makes use of internal conversion electrons.

Recently a spectrometer has been developed by Walker and McDaniel (1948) which extends the range of γ-ray measurement to 20 MeV and above. This method makes use of the pair-production effect in a thin lead "radiator", and detects coincidences between the positron and electron produced, at the same time measuring the total energy from their curvatures in a magnetic field. This method can only be used, of course, above ~ 2 MeV, and since the pair-production cross-section increases with energy it provides a complementary technique to the photoelectric conversion method.

(h) Coincidence Techniques.

A description of some of the earlier coincidence techniques is to be found in Moon (1949). The detectors used were Geiger counters and the methods have been applied to the study of both β-γ and γ-γ time correlations. Since the source strength is limited by the resolving time, $\sim 10^{-6}$ to 10^{-7} sec. in most cases, and since the stopping power of Geiger counters for γ-radiation is low ($< 1\%$), these methods are not very efficient, particularly for γ-γ coincidence work. In addition, the Geiger counter provides no direct information on the γ-ray energies involved and these have to be determined by coincidence absorption measurements. If a number of γ-rays are in

coincidence then this method becomes difficult and unreliable. An alternative method of determining the γ-ray energy from the experimentally determined efficiencies of the counters has been described by Dunworth (1940).

More accurate and reliable methods are those which make use of energy sensitive detectors in the coincidence arrangement. The detector normally employed is the magnetic spectrometer, and examples of its use are given by Feather, Kyles and Pringle (1948) and by Slätis and Siegbahn (1949). The former authors used a double β-ray spectrometer in the field of a permanent magnet, and were thus able to detect coincidences between electrons of known energy. The method was applied to sources with internally converted γ-rays, and it was possible to obtain the β-spectrum in coincidence with a given γ-ray by detecting coincidences of the form β-e^-. The solid angles used varied from 10^{-2} to 10^{-3}. This method, although defining the coincident energies reliably and accurately, is thus seen to be restricted to a specific type of source and to have a poorer solid angle than is desirable for general coincidence work. In the method described by Slätis and Siegbahn a single β-ray spectrometer was used and β-γ coincidences were obtained by placing a Geiger counter near the source-holder of the spectrometer. In this case the γ-ray detector is not energy-sensitive, but if the decay is simple the β-spectrum in coincidence with a γ-ray can be isolated. Here again

Refer also to Bothe & Maass-Leibnitz, Zeit. Phys. 104 604. 1937.

the solid angles are very small and the method somewhat restricted.

It will be noted that the main disadvantage of these two methods is the small solid angles available, and that the use of the double spectrometer is confined to the detection of β-e^- coincidences. The effective solid angle of such a device would be prohibitive if it were applied to the study of γ-γ coincidences, particularly if the γ-rays were not internally converted.

3. The Field of Application.

The field in which any newly developed technique of energy measurement can be applied is very wide, but can be subdivided into three main sections, (a) nuclear reactions, (b) natural radioactivity, and (c) artificial radioactivity. The particular aspects of each section which offer the greatest scope will usually be those which have been the least investigated, i.e. those aspects for which existing techniques are least well suited. With this consideration in mind, we will now discuss in turn the possibilities of each section.

(a) Nuclear Reactions.

The main body of the work in this field has been on the study of the reactions produced in light nuclei (up to $Z \sim 10$) when subjected to bombardment by heavy particles (protons, deuterons, etc.). A very full summary of recent work has been given by Hornyak et al. (1950). It is to be noted here that excitation of a light nucleus by particle capture normally results in the formation of a compound nucleus in a highly excited state. The reaction products are therefore very energetic and may range from a few MeV up to ~ 20 MeV. In addition, there is the added difficulty of working close to the target and of detecting the reaction products against a background of elastically scattered bombarding particles many orders of magnitude greater in intensity. The study of

nuclear reactions, therefore, has its own specific problems, in addition to those usually associated with particle and quantum energy measurements.

Magnetic analysis provides one of the most satisfactory methods at the moment of determining the energies of the charged particles produced, since it has a high resolution and also provides a means of suppressing the background of elastically scattered particles. The method however suffers from the problem of thin window techniques, and the solid angle is low. For the determination of γ-ray energies, the pair spectrometer developed by Walker and McDaniel (1948) provides good resolution over the required range, but again has a poor geometry. There is thus scope for the development of techniques of comparable energy resolution, but which will provide increased solid angles of acceptance. This would enable much lower yield reactions to be studied and would allow a greater application of coincidence and angular correlation methods.

(b) Natural Radioactivity.

A detailed summary of the state of knowledge regarding the radiations from the natural radioactive elements has been given recently by Feather (1949). More recent work is to be found in Nuclear Data (1950) and its supplements. In contrast to the previous case, all β- and γ-radiations emitted by radioactive decay processes are to be found within the range extending from a few keV up to a maximum

of $\sim$3 MeV, although α-particle energies tend to lie in the 4 - 10 MeV range.

Information on the α-particle emitters is now fairly complete and offers little scope for new techniques. A rather similar situation exists with regard to the γ-rays emitted by these elements, and the present state of knowledge is closely related to the accuracy and efficiency of present-day spectrometers. It is to be noted here that the elements of the radioactive series have a high atomic number and consequently the emitted γ-rays normally have a high internal conversion coefficient. It is thus possible to obtain much stronger conversion electron sources than are obtainable by the external conversion technique, and spectrometers of increased resolution can be used. In the classical work of Ellis and Skinner (1924) the absolute accuracy of the results is quoted as 1 part in 500, while recently a new method has been described by Craig (1952) for which accuracies of up to 1 part in 10,000 are claimed. Information is thus fairly complete above about 50 keV, while below this level some work has been done using crystal diffraction techniques (Frilley et al. 1951) and with the proportional counter (Curran, Angus and Cockroft 1949), particularly on the radiations from RaD. However the position as regards the mode of decay of this element, to cite a particular example, is still very unsatisfactory.

It is when we turn to the results on β-spectra that we

find the greatest possibilities for future work. Out of the 42 natural radioactive elements listed in his review, Feather mentions only 5 for which the information regarding the β-spectra can be considered as complete. The need in this field is for an accurate and efficient β-γ coincidence technique to permit the isolation of the components of a complex β-decay and the accurate determination of their end-point energies and relative intensities. This calls for the same qualities as were considered desirable in the previous section on nuclear reactions, an equivalent energy resolution and a greatly improved effective solid angle.

(c) Artificial Radioactivity.

The most up-to-date and useful survey of this very extensive field is to be found in Nuclear Data (1950) and its regularly issued supplements. The range of energy of the radiations emitted by this radioactive group is similar in extent to the range of the natural emitters, and so the previous remarks on the limitations of existing techniques and the openings for new ones again apply. Further, the very weak specific activity of some of the artificial radio-elements makes an increased sensitivity very desirable for straightforward examination of spectra, as well as for coincidence work. The field here is so vast that it can be said of very few isotopes that the amount of reliable work carried out on them justifies the acceptance of the existing decay schemes as the complete and final answer.

To sum up, it appears that in all three sections there is wide scope for improved coincidence techniques which will combine accurate energy determination with information on the time and/or space correlation of the emitted radiations. The effective solid angle of existing spectrometers, particularly for γ-rays, is too low to allow the use of two such instruments in coincidence, so that the most immediate benefit is to be gained from an increase in solid angle and γ-ray efficiency. This will also provide advantages in the straightforward examination of weak sources or low yield reactions. The lower limits of β- and γ-ray energy measurements could also be extended with advantage in the study of radioactive sources, both natural and artificial.

Part II. The Scintillation Counter.

1. Historical Development.

The scintillation counter was one of the earliest devices used in the study of radioactivity. As the spinthariscope it consisted of a zinc sulphide screen which was observed by eye through a low power microscope, and with this simple equipment it was possible to observe the scintillations produced by α-particles or protons when they struck the screen. An idea of the procedure used can be gained from the following description given by Rutherford (1919).

> "In these experiments, two workers are required, one to remove the source of radiation and to make experimental adjustments, and the other to do the counting. Before beginning to count, the observer rests his eyes for half an hour in a dark room and should not expose his eyes to any but a weak light during the whole time of counting. The experiments were made in a large darkened room with a small dark chamber attached to which the observer retired when it was necessary to turn on the lights for experimental adjustments. It was found convenient in practice to count for 1 minute and then rest for an equal interval, the times and data being recorded by the assistant. As a rule, the eye becomes fatigued after an hour's counting and the results become erratic and unreliable. It is not desirable to count for more than 1 hour per day, and preferably only a few times per week."

The average counting rate in these experiments varied between 15 and 40 per minute, so that not more than 4,000 counts could be recorded per week. By contrast, present day scintillation counters have been used up to counting rates of $\sim 10^6$ per second. It is not surprising then that when

Geiger counters and ion chambers came into general use this rather laborious technique fell into abeyance.

The scintillation counter was re-established as a useful tool in nuclear physics by Curran and Baker (1944), who used a photomultiplier tube to record the scintillations, in place of the human eye. This first counter was used to detect α-particles which were made to strike a layer of ZnS adhering to the envelope of the photomultiplier tube opposite the cathode. The application of this technique to other types of radiation is described by Coltman and Marshall (1947), but apart from the detection of heavy particles it was not very successful due to the nature of the phosphor.

The next advance was made by Kallmann (1947) who used large blocks of naphthalene as a phosphor for the detection of β- and γ-rays. This step may well be described as the first stage in the evolution of the scintillation counter as a γ-ray spectrometer of high stopping power. This development was immediately taken up and verified by Deutsch (1948) and many others, and a search began for new and improved phosphors. The first reference to the use of anthracene was made by Bell (1948), and to the use of NaI(Tl) in polycrystalline form by Hofstadter (1948).

In addition to the investigation of the scintillation counter itself, some of the earliest work using this new technique was carried out by De Benedetti et al. (1948),

and Brady and Deutsch (1948). The former authors used an anthracene scintillation counter to replace Geiger counters in the "self-delayed coincidence" method of detecting short-lived isomers. A considerable improvement in resolving time was obtained over the 10^{-4} sec. of the Geiger counters. Brady and Deutsch applied naphthalene scintillation counters to the measurement of the angular correlation between successive γ-ray quanta, and obtained a 100-fold increase in the coincidence counting rate over previous experiments with Geiger counters. This application was extended by Deutsch and Metzger (1948) into an elegant method for determining the correlation between direction and polarisation of successive γ-ray quanta.

All the above authors made use of the two immediately obvious properties of the scintillation counter; its high efficiency for γ-rays and its short resolving time. The first tentative attempts at energy measurement were carried out by Taschek and Gittings (1948) on the low energy β-spectrum of tritium. It was not until 1949, however, that the first reliable results were obtained by Bell and Cassidy. The β-spectrum of Be^{10} was measured using a scintillation counter calibrated with the radiations from Cs^{137}, and a Kurie plot of the data was found to give a straight line from the end-point at 566 keV down to $\sim$380 keV.

Most of the work at this stage was still on β-particles and electrons, since only organic phosphors with a low

atomic number were available in a form suitable for energy measurement. A little γ-ray spectroscopy was carried out by measuring the edges of the Compton distributions produced in the crystal, and a description of this technique is given in a survey article by Jordan and Bell (1949).

In 1950 large single crystals of NaI(Tl) began to be used for γ-ray spectroscopy, and results were published almost simultaneously by Pringle, Roulston and Taylor (1950), Johansson (1950), and McIntyre and Hofstadter (1950). This early γ-ray spectroscopy is well summarised in an article by Hofstadter and McIntyre (1950a).

This initial development of the phosphor aspect of the counter soon created a demand for improved photomultiplier tubes designed specifically for scintillation counting. This demand was met by the manufacturers in the form of the end-window photocathode type of tube, with a low noise level and a high gain. Examples of these are the R.C.A. 5819 and the various E.M.I. types (VX 5031, 5311, 6262, etc.). An account of the early development of the electron multiplier tube is given by Zworykin and Rajchman (1939), while in an excellent article by Morton (1948) the application of present day tubes to scintillation counting is discussed at length.

From this point onwards there has been only one major advance, the discovery of liquid phosphors (Kallmann 1950), comparable to the three mentioned above; (a) the application of the photomultiplier tube to the detection of scintillations

by Curran and Baker, (b) the discovery of naphthalene as a phosphor by Kallmann, and (c) the use of NaI(Tl) in γ-ray spectroscopy by Hofstadter. Most of the work has been in the nature of consolidation and of application to specific nuclear problems. The scintillation counter now offers a detector which is fast, has a high stopping power for γ-radiation and possesses a moderately good energy resolution. It is thus ideally suited for coincidence work involving energy measurements.

2. Design Considerations.

We shall now consider in some detail the various factors which are involved in the proper construction of a scintillation counter for use as an energy measuring device. A schematic diagram of such a counter is illustrated in Figure II.1, and we shall begin with the source of radiation and follow through the successive stages which lead to the production of a voltage pulse of a shape and amplitude suitable for analysis.

The conditions necessary for such a counter are (a) uniformity of response, (b) high energy efficiency, and (c) proportionality. The first criterion requires that particles (including secondaries produced by γ-rays) of equal energy should produce pulses of the same amplitude, thus ensuring good energy resolution. Condition (b) obtains the maximum signal from a given particle energy, and leads to a good signal-to-noise ratio (see below) and an extended lower limit to the energy range. Condition (b) also affects the first requirement (a) because of the statistical nature of the energy resolution (see below). Condition (c) normally depends solely on the nature of the phosphor. It is a desirable but not a necessary property, since the scintillation counter requires to be calibrated in any case.

The initial stage in the detection process is the

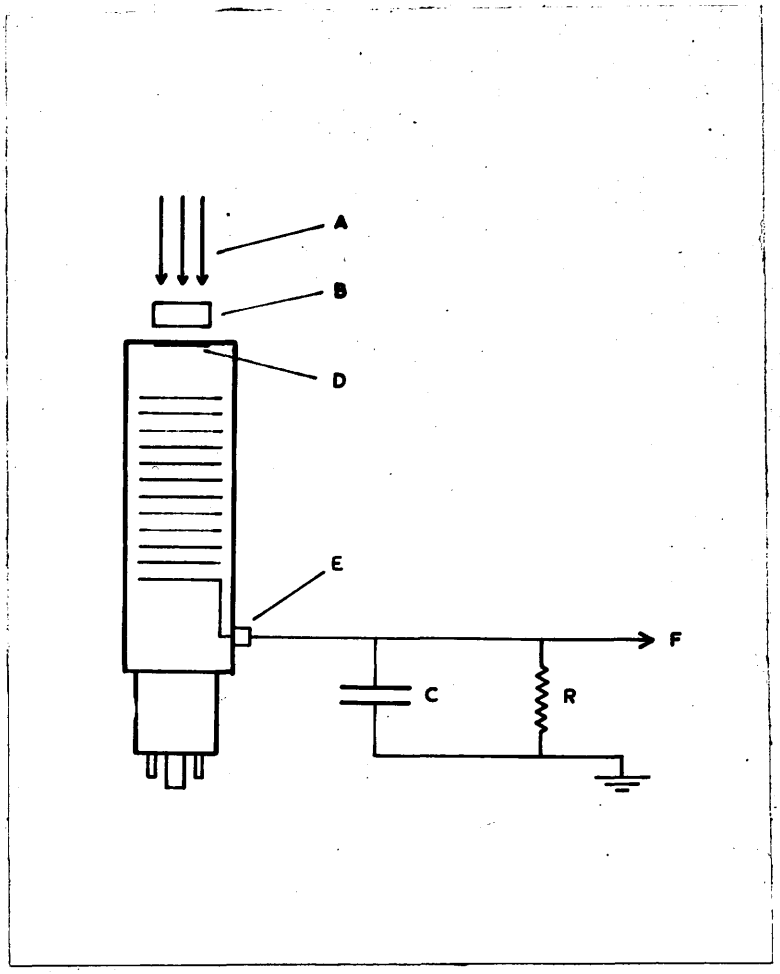

Figure II.1.

Schematic diagram of the scintillation counter.

A - incident radiation: B - phosphor crystal: D - photocathode: E - output terminal from photomultiplier tube: C - stray output capacitance: R - output resistance: F - lead to grid of cathode-follower valve.

interaction of the incident radiation with the phosphor crystal. This is considered in detail in the next section, but essentially it consists in the stopping of a particle (α-particle, β-particle or secondary electron) in the phosphor. This excites the fluorescence mechanism of the phosphor and a pulse of photons is produced in the crystal. The energy represented by this pulse is usually a few percent of the energy dissipated by the particle in the phosphor. This ratio is called the energy conversion efficiency or the physical light yield (Kallmann 1949). Its value affects both pulse height and uniformity, and in addition if it is independent of the incident particle energy the response will be proportional. The most efficient phosphor known is ZnS(Ag) which has a physical light yield of 30%, i.e. it requires only 10 eV in the phosphor to produce one photon of $\sim$3 eV. For organic phosphors this figure is nearer 100 eV per photon.

The decay of the excitation, i.e. the rate of production of photons, is approximately exponential and leads to the definition of a decay constant τ for each phosphor. This constant is a measure of the resolving time of the phosphor and sets the maximum permissible counting rate. A list of decay times for a number of commonly used phosphors is given by Jordan and Bell (1949).

The next stage from the phosphor to the photocathode of the multiplier can conveniently be divided into two parts;

(i) getting the light out of the phosphor, and (ii) collecting the light onto the photocathode surface. In part (i) the transparency, refractive index and structure of the phosphor are of importance in determining both the size and uniformity of the pulse. Since each is responsible for a reduction in light intensity, Kallmann (1949) has defined the technical light yield, as opposed to the physical light yield quoted above, as the fraction of the absorbed energy which is emitted from the phosphor in the form of light. The phosphor ZnS(Ag), for example, is quite opaque to its own radiation in thicknesses of 50 mg/cm^2. and over. The light intensity will therefore vary with the depth of the scintillation from the phosphor surface, becoming zero at depths greater than 50 mg/cm^2. On the other hand the organic phosphors, including liquids, and NaI(Tl) are perfectly clear up to thicknesses of 5 cm. and more, and the effect of an increasing absorption with depth will be negligible. Due to total internal reflection the refractive index restricts the escape of light, but this effect can be reduced by using some intervening optical medium, e.g. paraffin, between the crystal and the photomultiplier envelope. The structure of the phosphor also affects the technical light yield, since there will be a loss of light from diffuse scattering if the phosphor is in a polycrystalline or powder form - hence the insistence on large single crystals for use in energy measurements.

The geometry of light collection (ii) is partly

decided by the conditions of each individual experiment, but the optical coupling should be made as close as possible. Reflectors should be used round the crystal, and devices such as "light piping" which introduce light losses should be avoided. If the geometry is poor the effective solid angle of collection may vary with the position of the scintillation in the phosphor, thus destroying uniformity of response.

The light pulse is converted into a pulse of electrons at the photo-sensitive cathode surface. For the average photomultiplier tube about 10 photons are required to produce 1 electron, but if the emission spectrum of the phosphor does not match the response curve of the photo-cathode the conversion ratio will be much poorer. If the previous optical geometry is good, most of the pulse-height spread is introduced at this point by statistical fluctuations in the number of electrons ejected from the photocathode (Jordan and Bell 1949). A further spread is introduced by the nature of the secondary emission multiplication process, mainly in the first dynode stage. Morton (1948) has calculated that the percentage spread at the photocathode is increased by a factor $\left[G/(G-1)\right]^{1/2}$, where G is the gain per stage of the photomultiplier tube. For most tubes G varies between 3 and 4. It is therefore advantageous to have large light pulses from the phosphor, from considerations of uniformity as well as signal-to-noise ratio.

In addition to acting as the detector and amplifier of the phosphor scintillations, the photomultiplier tube contributes a certain amount of pulse noise which is appreciably above the noise level of the succeeding valve amplifier, and so is the deciding factor in estimating the signal-to-noise ratio of the counter. It is referred to as the dark current noise, since it is still observed when the tube is in complete darkness with no phosphor present. The dark current can be attributed to several causes (Morton and Mitchell 1949);

(a) Thermal emission of electrons from the sensitised cathode and dynode surfaces.

(b) Regenerative noise.

(c) Ionisation of residual gas in the tube.

(d) Cold discharge from points and irregularities on the dynode surfaces.

(e) Ohmic leakage.

The first cause (a) is usually the most important contributary factor but, in addition to choosing a "quiet" tube, it can be considerably reduced by cooling. Cause (b) becomes important in the new 14-stage high gain tubes (E.M.I. type 6262), where the large currents at the output stage produce light which is fed back via the glass envelope to the photocathode. Various methods have been evolved to prevent this feed-back. Any residual gas (c) will produce pulses by the movement of positive ions through the dynode system

towards the photocathode. Godfrey et al. (1951) have recently attributed the production of satellite pulses, pulses occurring in the photomultiplier tube about 1 μsec. after a signal or noise pulse, to this effect. Cold discharge only comes into consideration at very high operating voltages and ohmic leakage, although contributing about 99% of the total dark current, produces only small pulses well below the noise level of the amplifier and consequently can be neglected.

The shape of the photon pulse emitted by the phosphor is an exponential curve with a decay constant τ. This is converted into a similar pulse of electrons at the photocathode. The shape of this pulse will be altered in transit through the dynode system by the finite rise time and decay time of the photomultiplier tube. Allen and Engelder (1951) quote figures of 7.2×10^{-9} and 1.8×10^{-8} sec. respectively for the rise time and decay time of an E.M.I. 5311 tube. For relatively slow phosphors however, such as NaI(Tl) which has a value $\tau = 2.5 \times 10^{-7}$ sec., the effect on the pulse shape will be negligible.

To feed the maximum voltage pulse into the succeeding electronic circuits, the capacitance of the output stage must be kept to a minimum. This is shown as the condenser C in Figure II.1. It is made up of the capacitance of the photomultiplier collector and the input capacitance of the cathode-follower valve, plus the stray capacitance of the

connecting lead. This usually amounts to about 20 pF. The integrating circuit is made up of the grid resistor R of the cathode-follower valve and the stray capacitance C. This capacitance is charged up by the electron pulse from the photomultiplier tube and discharges through R. Since the value of C is fixed, R must be chosen to make the time constant RC greater than the decay constant τ of the phosphor, to avoid cutting the pulse height excessively. To a first approximation then, the voltage pulse appearing on the grid of the cathode-follower valve can be regarded as having a rise time τ and a decay time equal to the product RC.

If a fast phosphor is used to obtain a short resolving time, it is necessary to have a band-width with a high upper limit in the external stages of amplification. It is therefore advisable to reduce the external gain to a minimum and to obtain most of the amplification from the photomultiplier tube. However, if the multiplier is operated at too high a voltage excessive tube noise will be encountered and a compromise must be arrived at.

3. The Process of Energy Measurement.

In this section we shall consider the interaction of the incident radiation with the phosphor crystal and its bearing on the methods employed in energy measurement. Since quanta are detected by means of the secondary electrons which they produce in the crystal, the measurement of particle energies will be considered first.

(a) The Measurement of Particle Energies.

It has been shown by several workers, including Taylor et al. (1951) and Hopkins (1951), that the response of many phosphors is proportional over a wide range to the amount of energy dissipated in the phosphor by each particle. This has been corroborated by the writer for the response of anthracene and NaI(Tl) to electrons (see Part III.2a). There are therefore two problems to be considered in the measurement of particle energies, and in particular of electron energies. The first problem is getting the electron into the phosphor, and the second is to ensure that all the energy of the electron is then expended within the phosphor.

The first problem is only troublesome below about 20 keV, where the scattering of electrons becomes appreciable. A fraction of the incident electrons may then re-emerge from the phosphor crystal after only one or two collisions and these will not be recorded. Accurate measurement of relative intensities will therefore become difficult. This

effect does not enter where the secondaries of low energy quanta are concerned, since these are normally produced within the phosphor crystal.

As for the second problem, there is usually no difficulty in confining the electron range to within the limits of the phosphor crystal, since the range of a 2 MeV electron corresponds to approximately 1 cm. in anthracene or 0.25 cm. in NaI(Tl). The main source of energy loss will therefore be due to the escape from the crystal of bremsstrahlung produced by the electron. This will only be important for electrons of several MeV energy. It can therefore be said that in the medium energy range, 50 keV to 2 or 3 MeV say, the measurement of electron energies with scintillation counters presents no serious difficulty.

(b) The Measurement of Quantum Energies.

A knowledge of the energy of a γ-ray or X-ray can only be derived from measurement of the energy of the secondary electrons which are produced in the phosphor crystal. These electrons may arise from one or more of three processes; the photoelectric effect, the Compton effect, or pair production. Figure II.2 shows the cross-sections in iodine for these processes as a function of energy, and the region in which each process predominates is listed in Table II.1.

Table II.1. /

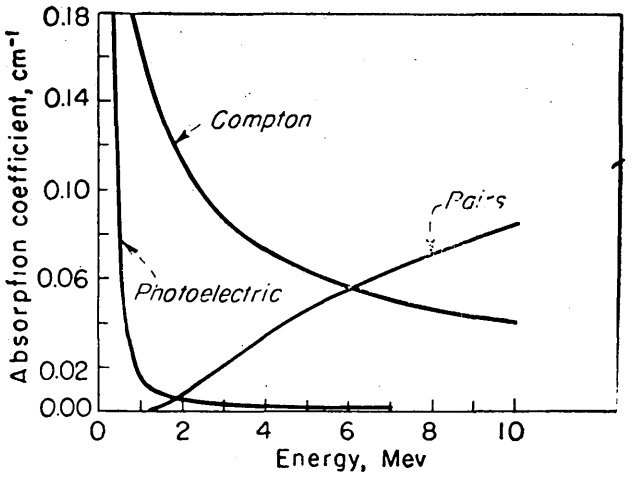

Theoretical cross-section curves for primary processes in iodine of NaI(Tl) To include the effect of sodium add 21% to Compton curve and 4% to pair curve

Figure II.2.

Taken from an article by Hofstadter and McIntyre (1950a).

Table II.1.

Phosphor	Photoelectric Effect	Compton Effect	Pair Production
Anthracene	< 20 keV	20 keV - 30 MeV	> 30 MeV
NaI(Tl)	< 250 keV	250 keV - 7 MeV	> 7 MeV

The predominant interaction process will therefore depend on the energy of the incident γ-ray and on the type of phosphor used as a detector. We shall now consider the electron distributions obtained from each of the three processes.

The Photoelectric Effect:- The energy of the photoelectron produced is equal to the incident quantum energy minus the binding energy of the shell (K, L, M ....) of the phosphor atom from which the electron has been ejected. The resultant K, L, M .... X-ray is absorbed simultaneously in the crystal, so that the full quantum energy is recorded. The photoelectric effect therefore produces a "line" in the spectrum whose position represents the total energy of the incident quantum. An exception to this arises at incident energies approaching that of the K-shell energy (West, Meyerhof and Hofstadter 1951). In this case the photoelectric cross-section becomes so large that almost all the incident radiation is absorbed on the surface of the crystal. The X-ray produced then has a probability approaching 1/2 of

escaping, and a second line is obtained corresponding to the energy of the photoelectron alone.

The Compton Effect:- This interaction produces a continuous distribution of electron energies up to a maximum at about $mc^2/2$ (0.25 MeV) less than the incident γ-ray energy. The high energy end of the spectrum has a fairly well defined "edge" from which it is possible to obtain an approximate measurement of the γ-ray energy. If the crystal is a large one ($>$ 1 in^3.) of NaI(Tl), the 0.25 MeV scattered quanta associated with the highest energy electrons may be completely absorbed in the crystal. The resultant pulse will therefore represent the full γ-ray energy and will add on to the photoelectric peak.

Pair Production:- This effect only occurs if the incident γ-ray energy is greater than $2mc^2$. A positron-electron pair is then produced whose total energy is $2mc^2$ (1.02 MeV) less than the γ-ray energy. The output pulse will therefore correspond to this energy provided the annihilation quanta escape from the crystal. If the two annihilation quanta are trapped in the crystal then the full energy of the γ-ray will again be obtained. Another possibility is that only one of the two quanta escapes, in which case pulses corresponding to 0.51 MeV less than the γ-ray energy will be seen.

From a knowledge of these different processes and their

relative cross-sections it is possible to calculate the pulse-height distribution to be expected from various γ-ray energies. In Figures II.3, II.4 and II.5 are shown the distributions in NaI(Tl) corresponding to γ-ray energies of mc^2, $4mc^2$ and $10mc^2$. These have been calculated assuming primary processes only, i.e. assuming all secondary and scattered radiations escape from the crystal. With a 0.5 in. cube of NaI(Tl) this condition is fairly well realised, except for the X-rays which it is difficult to avoid absorbing.

It will be seen from these curves that where the photoelectric effect or pair production predominates, the determination of γ-ray energies is relatively easy and unambiguous. In the intermediate region where the Compton effect predominates, each γ-ray produces a distribution curve which may consist of up to three peaks. The interpretation of this curve may be possible if only one or two γ-rays are present, but if the γ-ray spectrum is at all complex the resultant distribution will become very confused. It is true that for anthracene there is a wide energy region in which both the photoelectric effect and pair production are completely negligible, but the determination of γ-ray energies from a number of superimposed Compton distributions is not a very reliable and accurate method.

To sum up then, we can say that techniques making use of the photoelectric effect or pair production are to be

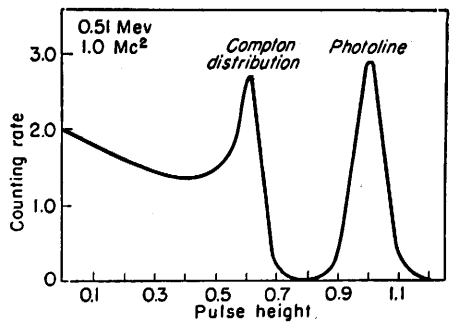

Approximate theoretical pulse distribution for 0.51 Mev assuming primary process only

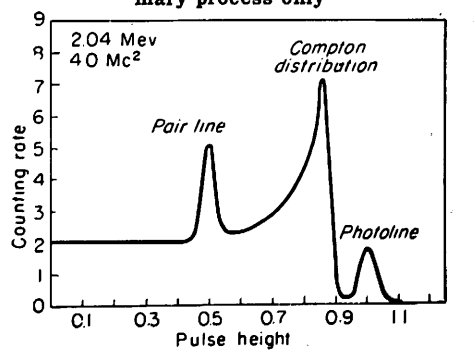

Approximate theoretical pulse distribution for 2.04 Mev assuming primary process only

Figures II.3 and II.4.

Taken from an article by Hofstadter and McIntyre (1950a).

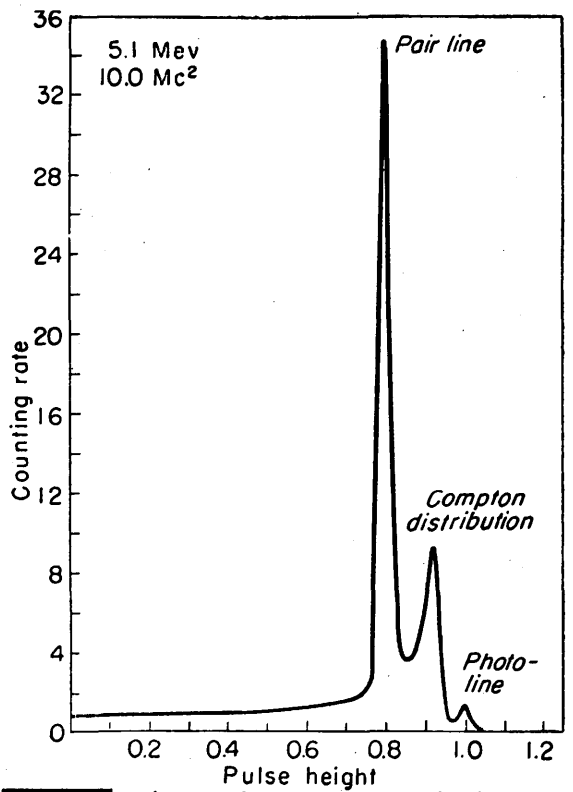

Approximate theoretical pulse distribution for 5.1 Mev assuming primary process only

Figure II.5.

Taken from an article by Hofstadter and McIntyre (1950a).

preferred in γ-ray spectroscopy with single crystals. In this respect NaI(Tl) is superior to anthracene, because its high iodine content (85% by weight) allows it to make use of these effects over a wider energy range. A description of a coincidence method which makes use of the Compton effect and is designed to cover the intermediate energy range is given later in this thesis in Part IV.

Part III. The Scintillation Counter. (continued)

1. Description of Equipment.

(a) The Scintillation Counter.

When work was started on the measurement of γ-ray energies only R.C.A. 931A type photomultiplier tubes were available and the phosphors used were naphthalene crystals or polycrystalline masses of NaI(Tl). Both types of crystal were grown in this Department. In the initial stages, therefore, both the crystals and photomultiplier tubes available were unsatisfactory, the former having either a low efficiency or a non-uniform response, and the latter having a very poor geometry for light collection onto the photocathode.

Nothing could be done in this Department to improve the photomultiplier tubes, and the preparation of good crystals of say 1 cm^3. in size of either anthracene or NaI(Tl) would have entailed an unjustifiably large expenditure of effort. Progress was therefore dependent mainly on outside technical advances in both fields. However, early in the summer of 1950 both E.M.I. photomultiplier tubes with end-window photocathodes, and good quality crystals of anthracene and NaI(Tl) became readily available. Further progress was then only dependent on the development of techniques to exploit the possibilities of these materials to the full. The following paragraphs contain a description of the final

form of the scintillation counter.

Phosphor Crystals:- The phosphors which have been used almost exclusively in the work described in Parts IV and V of this thesis are thallium-activated sodium iodide, NaI(Tl), and anthracene. Silver-activated zinc sulphide, ZnS(Ag), has been used for the detection of α-particles and an account of the work done with this phosphor is given in Appendix I. Since the performance of these phosphors is strongly dependent on the optical clarity of their surfaces, an account has been included in Appendix II of the methods developed by the writer for handling and cleaning them. It is sufficient to say here that both anthracene and NaI(Tl), particularly the latter, can now be readily cleaned and surfaces of a very high degree of clarity obtained. This ensures the maximum energy response and resolution from the crystal.

Photomultiplier Tubes:- The two different types of tube which have been used are the R.C.A. 931A type and the E.M.I. 5311. The R.C.A. type of tube (931A, 1P21 and 1P28) was used only for early work, mainly of an exploratory nature, until the E.M.I. type became available. The use of an R.C.A. 1P21 photomultiplier tube in conjunction with a ZnS(Ag) phosphor to detect α-particles is described in Appendix I. An R.C.A. 931A tube has recently been used to examine the screen of a cathode ray tube, and such a use

will be mentioned in the next section in connection with the single-channel kicksorter. All the work described in Parts IV and V was carried out using E.M.I. 5311 photomultiplier tubes, with 1 in. diameter end-window photocathodes (see Figure III.1). Some of the earlier work in Part IV was done with E.M.I. VX 5031 photomultiplier tubes, which are similar to the E.M.I. 5311 type but have only 1 cm. diameter photocathodes.

Crystal Mounting:- The phosphor crystals are mounted directly opposite the photocathode on the end of the tube (E.M.I. type), usually with liquid paraffin between the crystal and the glass of the photomultiplier envelope to provide a good optical contact. The use of paraffin is essential with NaI(Tl) crystals to prevent attack by the moisture of the air. The crystal is also surrounded by a reflecting cover of aluminium foil (thicknesses of 1 and 2 thou. were found to have the highest polish) and in the case of NaI(Tl) this close-fitting reflecting cover performs the additional function of maintaining a film of paraffin round the crystal by surface tension. To hold them in position, the crystals are strapped onto the photomultiplier tubes with Scotch tape.

Photomultiplier Tube Containers:- The E.M.I. photomultiplier tubes are housed in cylindrical lightproof cans made out of the thinnest sheet brass available (1/64 in.), in order to

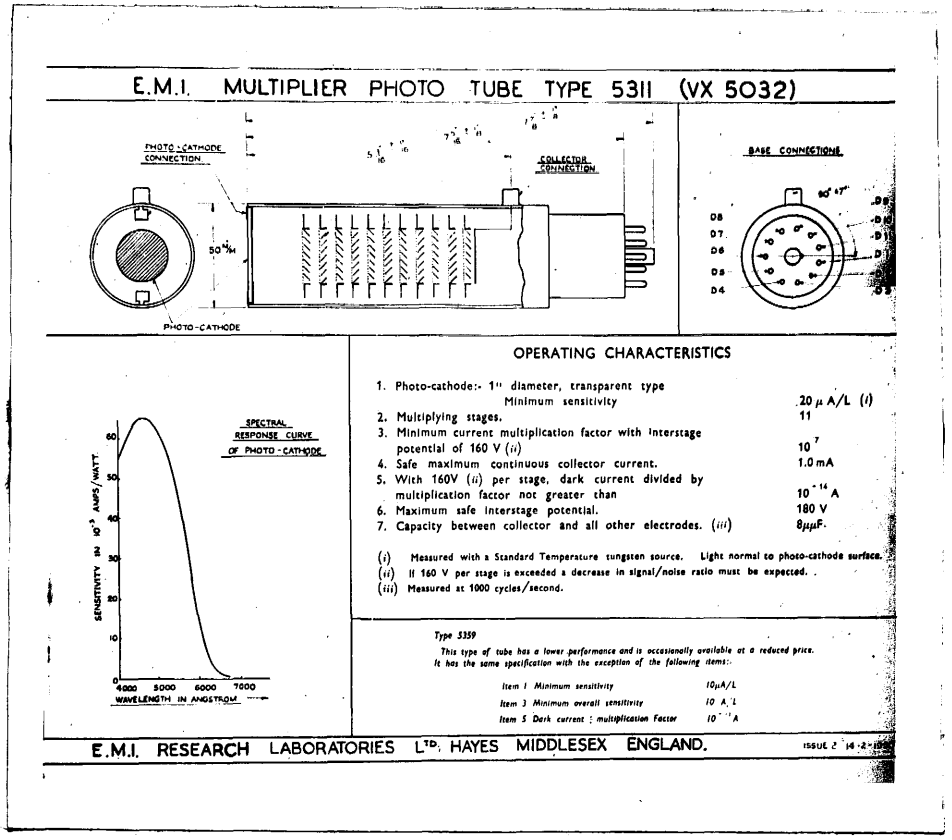

Figure III.1.

Data sheet for the E.M.I. 5311 photomultiplier tube.

minimise the scattering of γ-radiation. The dimensions of the cans are 3.5 in. internal diameter by 9.5 in. long. The tube base, similar in principle to an ordinary valve base, is supported by three lengths of 4BA studding rigidly attached at right angles to a brass end-plate, on which is also mounted the E.H.T. supply input socket and the signal output plug. The position of the tube base is fixed by clamping with 4BA nuts, and the use of the studding permits about 2 in. of movement of the photomultiplier tube along the direction of the axis of the cylinder. This allows the photocathode of the tube to be either inside or outside the limits of the opposite end of the can. The photocathode end was originally made light-proof by means of a thin cylindrical cap of aluminium foil, supported on a brass flange which was bolted onto a similar flange on the end of the can. This method, however, proved to be rather rigid and cumbersome, particularly in coincidence work involving two such counters, and it was superseded by the very flexible method used at present. Here the can is closed with a few layers of thick black cloth draped over the end and held in place by an elastic band. If the photocathode of the tube is now moved as far out from the can as possible, about 1.5 in. say, then the outline of the tube and of the phosphor mounted on it can be clearly seen and it becomes possible to obtain very close and accurately defined geometries. Indeed, in some coincidence experiments the two ends were

joined together with a piece of cloth so that the cans formed a single light-tight unit. Here, of course, it is essential to ensure that neither photomultiplier tube can see scintillations from the other phosphor.

Photomultiplier Tube Voltage Supply:- The E.H.T. voltage supply for the photomultiplier tubes is obtained from a 2 kV stabilised power pack (T.R.E. type 1007), and is continuously variable by means of a potentiometer unit from 500 V up to 2,000 V. The accelerating voltages can be distributed to the dynodes of the photomultiplier tube in either of two ways (Figure III.2a and 2b) depending on the polarity of the supply. Neither method is intrinsically superior to the other and the choice of circuit will be decided by external factors. A negative supply (Figure III.2a) was used originally, since here the collector is "earthy" and a very simple collecting system can be used to connect onto the grid of the external cathode-follower valve. (This mode of operation is essential if a D.C. measurement is being made.) The photocathode of the tube, however, is at a high negative potential and it is necessary to close the end of the can with a metal cap to provide electrostatic screening. When the change-over was made to cloth end-covers, it became necessary to reverse the polarity of the E.H.T. supply (Figure III.2b) so that the tubes could be used with their photocathodes earthed. One advantage of this is that in coincidence work the two tubes can be brought very close

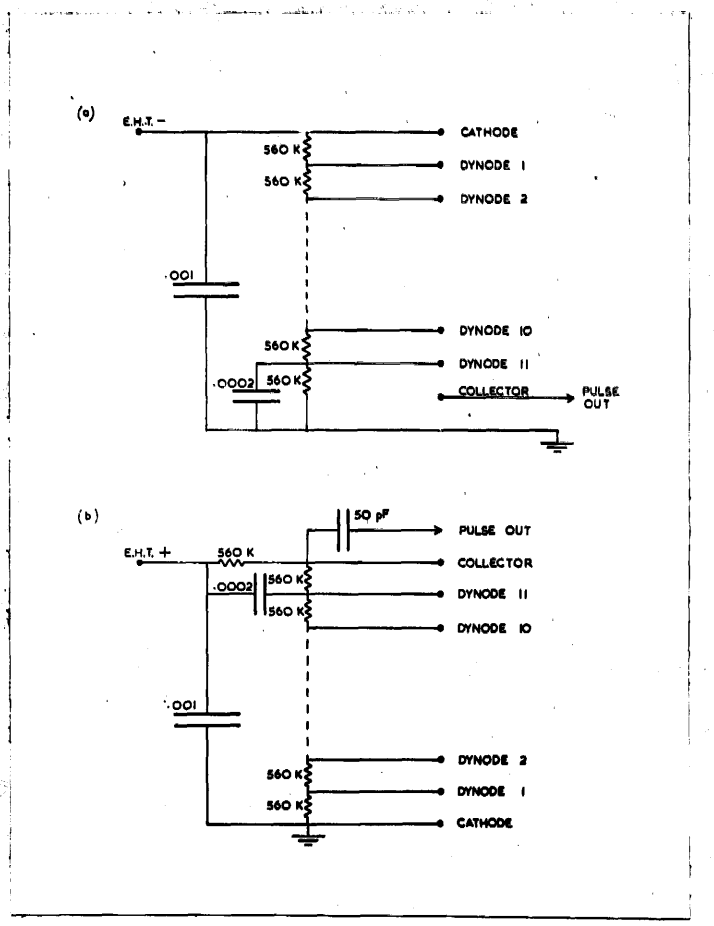

Figure III.2.

Photomultiplier tube voltage supply circuits;

(a) using a negative E.H.T. supply.

(b) using a positive E.H.T. supply.

together and even allowed to touch, which was not possible beforehand.

It will be seen from the data sheet of the E.M.I. 5311 photomultiplier tube (Figure III.1) that the electrical connections to the photocathode are made through small metal contacts on the cathode end of the tube. This feature of the photomultiplier tube has proved to be very troublesome, since any connections used interfere with the mounting of phosphor crystals. A system was devised using spring-loaded contacts which took up as little as possible of the area of the end surface of the tube. The resistor chain supplying voltages to the dynodes is wired directly onto the photomultiplier base and the remaining components are also housed inside the can. The integrating time constant at the output stage was made about 1 μsec.

(b) Electronic Equipment.

A block diagram of the electronic equipment following the scintillation counters is given in Figure III.3a. The arrangement shown is that used in coincidence work. The output pulse from the photomultiplier tube is first fed into a single valve cathode-follower which is attached rigidly to the photomultiplier can. The connection to the grid of this valve is made as short as possible to reduce to a minimum the stray capacitance of the leads. The pulse is then fed through about 3 yds. of concentric cable (characteristic

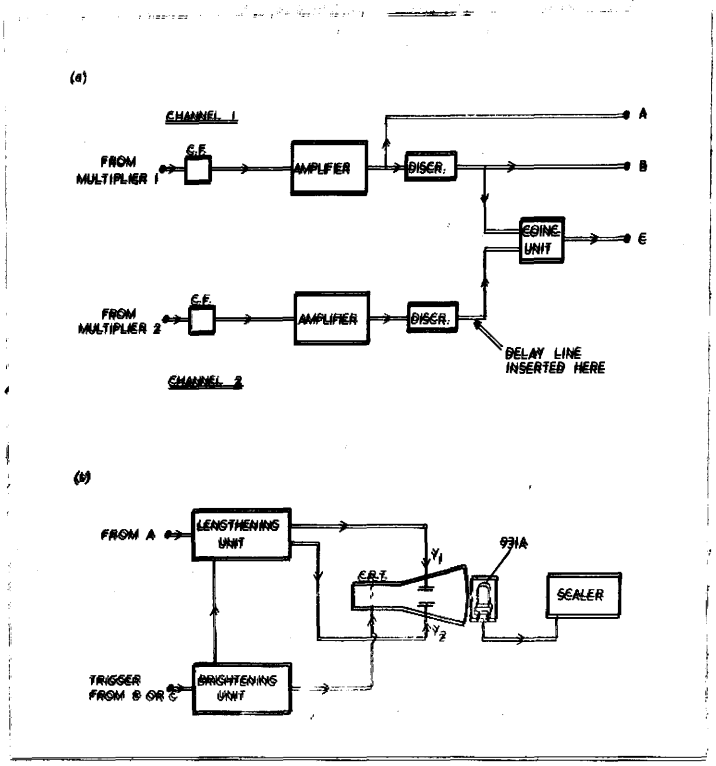

Figure III.3.

(a) Block diagram of the circuitry following the scintillation counters, showing the arrangement used in observing coincidence spectra.

(b) Block diagram of the single-channel kicksorter.

impedance = 100Ω) to the matched input of an amplifier. Since channel 1 carries the pulses whose spectrum is to be measured, a standard linear amplifier (T.R.E. type 1008) is used here. This amplifier has a linear output up to 50 V and above, a band-width of from 50 c/s to 500 kc/s with variable cuts at either limit, and a gain of 16,000 which can be attenuated by a factor of 100 in steps of 2 dB. Channel 2 provides coincidence pulses and the amplifier used here need not conform to such rigid standards as in channel 1. A simple 3-stage amplifier is used, which is linear up to 30 V output and saturates at 50 V output. It has a fixed gain of ~10,000 and a band-width of from 50 kc/s to 1 Mc/s. The gain change in channel 2 is produced by varying the E.H.T. voltage on the photomultiplier tube.

Both amplifiers feed into discriminators (T.R.E. type 1028) which provide fixed pulses of 20 V, 1 μsec. wide, for the input of the coincidence unit. This unit (for circuit see Appendix III) has a measured resolving time of 0.5 μsec. The discriminators are also used to cut out any unwanted low energy pulses, such as tube noise, etc. In coincidence experiments a 3 μsec. delay cable can be introduced in channel 2 between the discriminator and the coincidence unit in order to determine the random coincidence rate. This technique was found to be very useful when the counting rate in the two channels was too high (> 400 counts/sec.) to be measured directly on the scaler.

The power supplies for the two cathode-followers, the amplifier in channel 2 and the coincidence unit are all obtained from a 300 V valve-stabilised power pack, built to the same design as the power pack of the "1008" amplifier. All four units are decoupled to prevent interaction between them via the H.T. lines. Discriminator 1 is supplied from the "1008" amplifier and discriminator 2 from the scaler. The mains supply for these units, and also for the kick-sorter, was first hand-stabilised with a Variac transformer to compensate for wide long-term fluctuations in voltage.

The single-channel kicksorter (Figure III.3b), which has been used successfully in the work described in Parts IV and V, is based on a circuit-design by Mr. R. Giles of this Department. It consists of two main parts, the electronic circuits, and the cathode-ray tube plus photomultiplier tube. The operation of the kicksorter is as follows.

The spectrum of pulses to be analysed is fed from the output of the "1008" amplifier into the Pulse Lengthening Unit. Trigger pulses are obtained either directly from discriminator 1 (point B) or from the coincidence unit (point C) and fed into the Pulse Brightening Unit. The push-pull output of the pulse lengthening unit is A.C. coupled to the Y-plates of the cathode-ray tube, and the pulse brightening unit supplies a lengthening signal to the pulse lengthening unit and also puts a positive brightening signal onto the grid of the cathode-ray tube. The brilliance

control of the cathode-ray tube is turned down so that pulses are not normally visible unless an external brightening signal is applied to the grid.

If we now consider a signal pulse of width ~ 1 μsec., then this is lengthened into a flat-topped pulse about 10 μsec. long before being applied to the Y-plates. During this flat portion of the signal a brightening pulse is applied to the grid of the cathode-ray tube, and a spot of light is therefore seen at the point of maximum deflection produced by the signal pulse. A spectrum of pulses will appear as a series of spots of light spread out along the Y-axis of the cathode-ray screen, each spot marking the maximum height of a signal pulse. The pulse-height distribution can then be obtained if we count the number of spots observed in a given time at each point on the Y-axis. This is achieved by looking at the screen through a narrow slit, 1 mm. wide, with an R.C.A. 931A photomultiplier tube mounted in a light-tight box. The spectrum is scanned by moving it past the slit by means of a variable D.C. bias applied to the Y-plates. The value of this bias is then a measure of the pulse-height under observation.

The amplitude of the brightening pulse is used as a control of the channel-width. In normal operation a 2 V channel is used over a range of 100 V. The output of the 931A is recorded on a scaler (T.R.E. type 200). It was found that if the 931A was run at 1100 V, the output was

sufficiently large to operate the scaler without the necessity of any further amplification.

If the spectrum to be studied is a single crystal one, involving the use of channel 1 only, the triggering pulse for the kicksorter is taken from the point B (Figure III.3a). If, on the other hand, it is desired to observe the spectrum which is in coincidence with some second event recorded in channel 2, the triggering pulse is taken from point C, and those pulses from channel 1 which do not produce coincidences remain unlengthened and unbrightened and so are not recorded.

The maximum counting rate which the kicksorter was found capable of handling is about 400 counts/sec. This refers to the number of brightened pulses, i.e. to the number of trigger pulses from B or C. In a coincidence experiment the total number of pulses entering the pulse lengthening unit may be several thousand per second.

In coincidence experiments with weak sources it becomes tedious and inaccurate to examine a spectrum with a coincidence counting rate of less than about 500 counts/min.; tedious because of the time involved in covering the spectrum and inaccurate because of the poor statistics obtained on each reading. In such a case it has been the practice to remove the photomultiplier attachment and photograph the whole spectrum on slow-moving film. The film is afterwards analysed into a pulse-height distribution by projecting onto a screen ruled off in equally spaced horizontal strips.

This gives, in effect, all the advantages of a multi-channel kicksorter. The total time involved in exposing, developing and analysing the film is much less than would be required to obtain the same amount of information by the single-channel method. A coincidence rate of as low as 4 counts/min. has been successfully dealt with by this technique.

A more detailed account of some of the above apparatus, including the kicksorter, is given at the end of this thesis in Appendix III.

2. Performance of the Scintillation Counter.

As soon as the complete counting system, in particular the scintillation counter and the kicksorter, was working sufficiently well to undertake energy measurements, the study of radioactive sources was begun. No time was spent in making a systematic study of the performance of the instrument. However, an idea of its capabilities and limitations was built up as experimental work progressed and these findings are summarised below. Since the data is collected from many different experiments, the results are not as accurate as would be obtained from a direct study of the performance characteristics.

(a) Energy Response and Resolution.

NaI(Tl):- Data on the energy response of this phosphor has been obtained over a wide range of energies from 9.3 keV up to ~~2.42~~ 2.39 MeV. In all cases the crystal was mounted on the cathode of the photomultiplier tube, surrounded by a film of liquid paraffin and a reflecting cover of Al foil. The E.M.I. 5311 tube was run at 1000 V, although for the higher energies this was reduced to 900 V to avoid saturation in the cathode-follower. The low energy region of the response curve is shown in Figure III.4. This is obtained by measuring the pulse-height of photoelectric peaks produced in the NaI(Tl) crystal by various radiations. A list of the energies used, together with the sources of the radiations

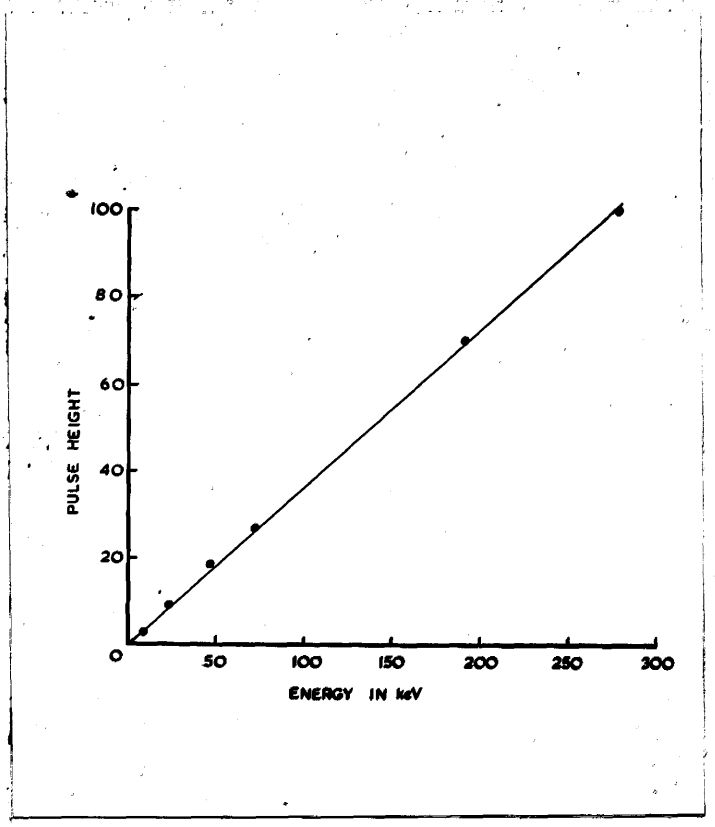

Figure III.4.

NaI(Tl) response curve - Low energy region.

is given in Table III.1.

Table III.1.

Source of Radiation	Energy	Pulse Height
Ga K X-rays from Ge^{71}.	9.3 keV	3.4 (Arbitrary Units)
In K X-rays from In^{114}.	24.1	9.5
γ-rays from RaD.	46.7	18.7
Tl K X-rays from Hg^{203}.	73	27.2
γ-rays from In^{114}.	192	70.5
γ-rays from Hg^{203}.	279	100

The high energy region of the response curve is shown in Figure III.5. Here the pulse height is obtained from the peaks produced by the Compton coincidence spectrometer and the energies are therefore those of the Compton electrons and not of the γ-rays. A list of the electron energies and the associated γ-rays is given in Table III.2.

Table III.2.

Source of Radiation	Electron Energy	Pulse Height
0.335 MeV γ-rays from La^{140}.	0.19 MeV	7.0 (Arbitrary Units)
0.49 MeV γ-rays from La^{140}.	0.32	12.7
0.82 MeV γ-rays from La^{140}.	0.62	26.0
1.25 MeV γ-rays from Co^{60}.	1.04	42.9
1.62 MeV γ-rays from La^{140}.	1.40	57.1
2.62 MeV γ-rays from ThC".	~~2.42~~ 2.39	100

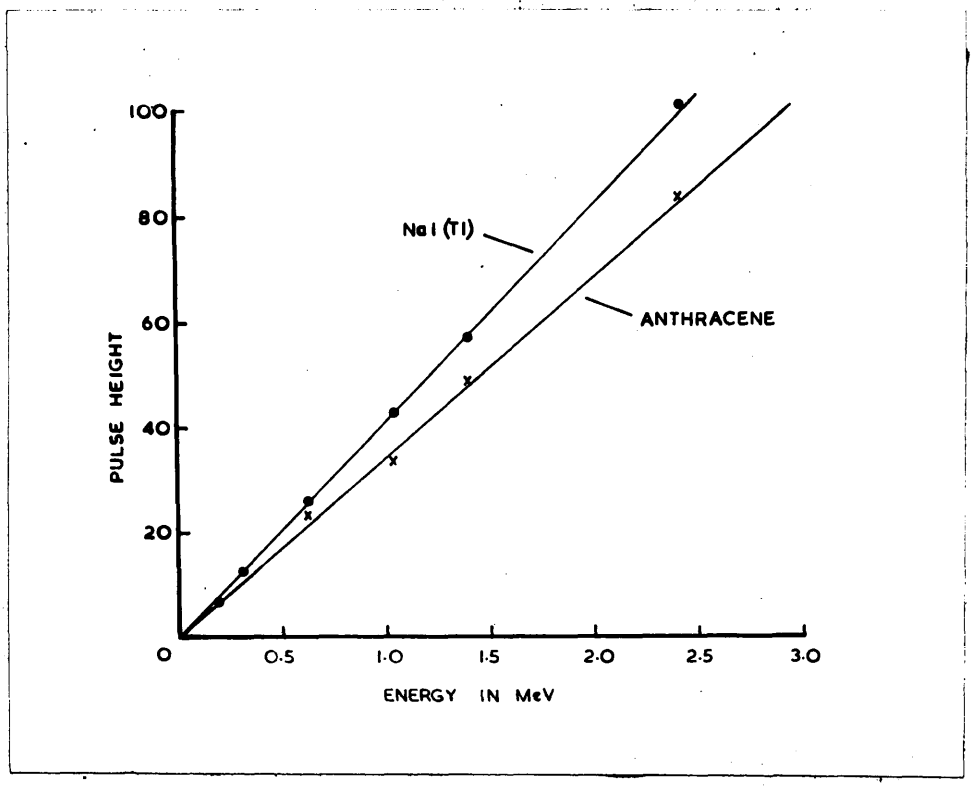

Figure III.5.

NaI(Tl) and anthracene response curves - High energy region. Both curves are drawn to the same scale.

All the X-ray energies in Table III.1 are taken from Compton and Allison (1935), and the γ-ray energies in Tables III.1 and III.2 are taken from Nuclear Data (1950). The pulse heights are corrected for non-linearity in the kicksorter using the calibration curve of Figure 4, Appendix III.

The two curves are seen to be linear to within 2 or 3%, which is the magnitude of the experimental error. The response of NaI(Tl) to electrons is therefore linear over the complete range 9.3 keV to ~~2.42~~ 2.39 MeV. This is in agreement with the work of Taylor et al. (1951) and many others. Taylor et al. report a linear response from 1 keV upwards, with a non-linear response below 1 keV.

A measure of the energy resolution of the counter is obtained from the percentage width at half-height of photo-electric peaks produced in the NaI(Tl) crystal. These peaks are of an approximately Gaussian shape. Theoretically the peak width should arise from statistical fluctuations in the number of electrons produced at the photocathode, plus a small additional spread caused by the multiplier tube. The resolution R should therefore vary as the reciprocal of the square root of the incident γ-ray energy E, i.e.

$$R \propto E^{-0.5}.$$

The peaks obtained with the Compton coincidence spectrometer have an additional spread due to the geometry of the experiment,

and are therefore not suitable for a direct measurement of the resolution of the crystal.

A series of measured values for the percentage width R of a number of photoelectric peaks is given in Table III.3.

Table III.3.

Energy E	Resolution R
9.3 keV	65 %
24.1	49
41.5	33
46.7	32
73	35
101	22
192	20
279	19
1,110	10

Log R is plotted against log E in Figure III.6, and for comparison a line is shown drawn with a gradient of -0.5. The agreement is reasonably good when we consider that these results are derived from a number of experiments carried out with different sizes of crystals. The resolution is therefore proportional to $E^{-0.5}$, demonstrating that the peak width is statistical in origin.

A short calculation will confirm that this is so. Consider a 1 MeV γ-ray producing a photoelectron inside a

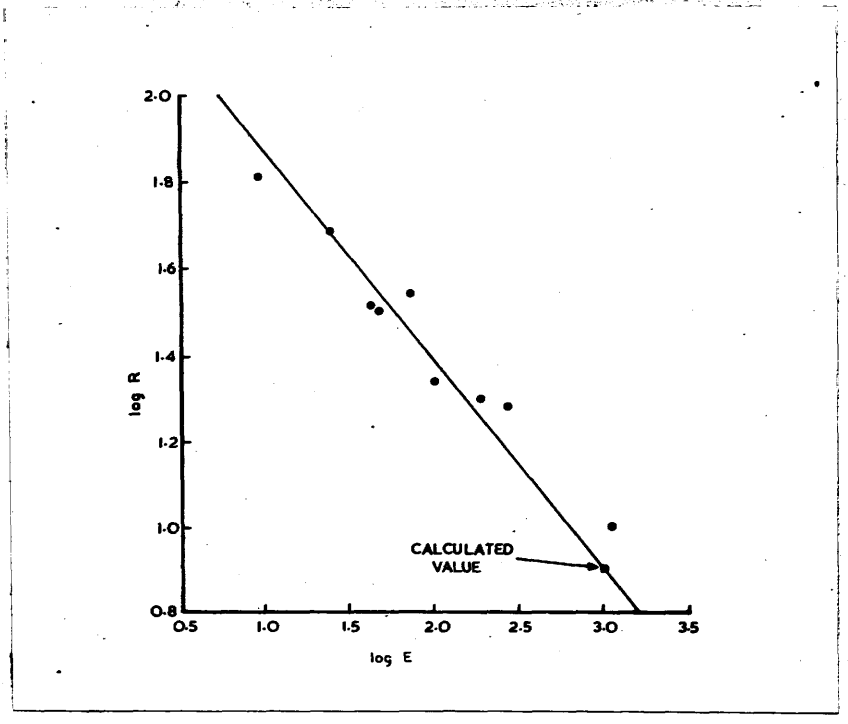

Figure III.6.

Plot of percentage line width R against energy E for photoelectric peaks in NaI(Tl). The line shown has a gradient of -0.5 and is drawn through a calculated value for R of 8% at 1 MeV.

NaI(Tl) crystal. The phosphor is 6% efficient for electrons, so 60 keV of the energy expended in the crystal appears as light. If we take a figure of 3 eV per photon (λ = 4130 Å), this gives a pulse of 20,000 photons. This is reduced by a factor of ~ 2 for light collection onto the photocathode, and by a further factor of ~ 10 for conversion into an electron pulse. This pulse therefore consists of about 1000 electrons and the statistical spread is 6.4%, since for a Gaussian distribution the half-width at half-height is approximately equal to the standard deviation ($\pm$3.2%). The process of multiplication in the photomultiplier produces an increase in the spread of the pulse by a factor $[G/(G-1)]^{1/2}$, where G is the gain per stage (Morton 1948). The value of G is ~ 3.2 with 1000 V on the photomultiplier tube, so the resultant spread in pulse height is $\sim$8%. This is in close agreement with the observed value of 10%. The line of gradient -0.5 shown in Figure III.6 is drawn through a point representing this calculated value.

Some results have been published recently by Schardt and Bernstein (1951) on the resolution of a scintillation counter composed of a NaI(Tl) crystal mounted on an R.C.A. 5819 photomultiplier tube. They also obtain an $E^{-0.5}$ variation for the percentage resolution, but only in the range 10 - 35 keV. Poorer resolution than expected above this energy is attributed to non-uniformity in the photocathode surface.

Anthracene:- Data on the energy response of anthracene is not available over such a wide range as for NaI(Tl). In the high energy region results are available from 0.62 MeV up to 2.42 MeV. These are obtained from Compton coincidence spectrometer peaks in the same manner as for the high energy NaI(Tl) response. The results are listed in Table III.4 and shown graphically in Figure III.5. The anthracene and NaI(Tl) responses are both drawn to the same scale.

Table III.4.

Source of Radiation	Electron Energy	Pulse Height
0.82 MeV γ-rays from La^{140}.	0.62 MeV	23.4 (Arbitrary Units)
1.25 MeV γ-rays from Co^{60}.	1.04	33.8
1.62 MeV γ-rays from La^{140}.	1.40	48.6
2.62 MeV γ-rays from ThC".	~~2.42~~ 2.39	83

Anthracene therefore shows a linear response to electrons in the region 0.62 - ~~2.42~~ 2.39 MeV. Results in the low energy region are more difficult to obtain with γ-rays, since the Compton effect is not very suitable and the photoelectric effect does not become evident until below about 25 keV. Two points on the anthracene response curve were obtained at 9.3 keV and 24.1 keV from photoelectron peaks. These points show a departure from linearity, the observed pulse height of the 9.3 keV peak being 30% lower than the pulse

height calculated from the position of the 24.1 keV peak. This degree of non-linearity is in agreement with the results published by Hopkins (1951) and Taylor et al. (1951), who both obtain a linear response above about 100 keV with a non-linearity below this point due to a drop in efficiency with decreasing energy.

Because of the low photoelectric cross-section of anthracene in the energy range studied (~ 10 keV to 1 MeV), data on the energy resolution of the crystal similar to that given for NaI(Tl) is not available. In general the resolution is inferior, due to the poorer energy efficiency of the anthracene.

From the two curves in Figure III.5 it is seen that the response of NaI(Tl) is greater than that of anthracene by a factor 1.2/1. This may be an underestimate of the ratio, since when these measurements were carried out a proper cleaning technique for NaI(Tl) had not been found.

Scheelite:- The performance of this phosphor in the low energy region was investigated with a view to using it in place of NaI(Tl). Its advantages are that it has a higher atomic number and that it can be used without any surrounding film of liquid paraffin. Its response was found to be linear between 24.1 keV and 46.7 keV, although the pulse height was down by ~6 on that of NaI(Tl). The increase in the spread of the photoelectric peaks, over those observed in NaI(Tl) at the same energies, was found to be consistent

statistically with the observed drop in response. In addition, each pulse from the scheelite was seen on an oscilloscope screen to be made up of a number of sharp pulses about 1 μsec. long extending over a period of ~ 20 μsec.

Scheelite is thus seen to have a long decay time and a poor response, with a resultant poor energy resolution. It was therefore concluded that this phosphor was unsuitable for use in a scintillation spectrometer.

(b) The Photomultiplier Tubes.

It is a property of the photomultiplier tube that for a given increase in voltage, the noise level of the tube increases more rapidly than the gain. This is of great importance if the scintillation counter is used to examine low energy radiations, and it may limit the operating voltage, and hence also the gain, to a value much less than the maximum. For an E.M.I. VX 5031 (1 cm. cathode) tube it was found that the gain varied approximately as $V^{7.5}$ and the noise level as V^{10} over a range of V from 1000 to 1500 volts. A similar variation ($\propto V^{7.7}$) was found for the gain of an E.M.I. 5311 (1 in. cathode) tube over the range 900 to 1500 volts, but no information is in this case available on the change in noise level. A similar change in both gain and noise level was also observed for an R.C.A. 931A and an R.C.A. 1P28 tube in the region 800 to 900 volts.

The noise levels of a number of different photomultiplier tubes are shown in Table III.5 below. The noise level is expressed in terms of the energy of an electron which would produce a pulse in the phosphor of the scintillation counter of the same height as noise. The phosphors in each case are listed in column 2 of the Table. The figures quoted are the noise levels at normal operating voltages, i.e. 800 V on the R.C.A. type tubes and 1000 V on the E.M.I. type tubes. The results for the first three tubes indicate orders of magnitude only, whereas those for the E.M.I. 5311 tube are more accurate.

Table III.5.

P-M. Tube	Phosphor	Noise Level
R.C.A. 931A	Anthracene	400 keV
R.C.A. 1P28	Anthracene	100
E.M.I. VX 5031	Anthracene	20
E.M.I. 5311	Anthracene	6
E.M.I. 5311	NaI(Tl)	3
E.M.I. 5311	Scheelite	20

Another important criterion in the choice of a photomultiplier tube for work involving energy measurement is stability of gain and of noise level. Both types of instability were encountered in some of the early E.M.I.

VX 5031 tubes, but the more recent E.M.I. 5311 tubes have proved very satisfactory. With the latter type of tube it has been found, from repeated observations on the same γ-ray line, that the whole counting system is stable to within the limits of the accuracy of measurement ($\pm 2\%$) over a period of several days. The E.M.I. 5311 tube, as well as the cathode-follower, the amplifier and the kicksorter, plus the associated power packs, must therefore be stable to much better than $\pm 2\%$. Repeated and accurate calibration is thus not necessary from day to day during the examination of radioactive sources, although it is still desirable.

(c) Merits and Demerits as a Spectrometer.

The most favoured crystal for use in γ-ray detection has been NaI(Tl). At high energies where the Compton effect predominates this is due to its increased stopping power over anthracene, but it is in the lower energy region, below about 500 keV, that its advantages due to the photo-electric effect in the iodine become fully apparent. The whole tendency of the work on the study of radioactive sources shows a movement towards lower γ-ray energies in order to exploit this effect to the full. In this region it becomes possible to use the scintillation counter in a manner similar to the gas-filled proportional counter. In both types of counter a monoenergetic γ-ray produces a well-defined peak, but the scintillation counter has the advantage of a much greater stopping power. The photoelectric

cross-section ranges from ~10% in a 1 cm. thickness at 500 keV up to ~100% at energies of 100 keV and below. It is true that the energy resolution is inferior to that of a proportional counter, but in most cases, unless the γ-ray spectrum is very complex, this disadvantage is far outweighed by the increased stopping power. It is this latter quality which makes the scintillation counter ideal for γ-γ and β-γ coincidence work, particularly below 100 keV. The scintillation counter can never compete with magnetic spectrometers or proportional counters as far as a high energy resolution is concerned, unless it be at very high energies (see below) where the statistical spread is considerably reduced due to the increased number of photons per pulse. It can however be used to study very weak sources ($\sim 10^{-9}$ Curies) and where convenient calibration sources are available, energies can usually be determined to an accuracy of a few percent.

For the detection of γ-rays, then, the region in which the scintillation counter is most powerful is from about 500 keV down to tube noise (~ 10 keV) using NaI(Tl) as a phosphor. From 500 keV upwards to about 2 MeV the scintillation counter, using either NaI(Tl) or anthracene, still has the advantage of a relatively high stopping power, although the predominance of the Compton effect makes energy measurement difficult. Moderately good resolution (10% -20%) can be obtained using the Compton coincidence technique but only

at the expense of an additional reduction in solid angle of about 100. This however is still superior in solid angle to the conventional magnetic spectrometer which examines photoelectric peaks produced in a "radiator". No work has been done using the pair-production effect in the region 2 MeV and above, but it can be mentioned briefly here that the scintillation pair spectrometer using NaI(Tl) crystals (Johansson 1952) has a superior stopping power to the pair spectrometer of Walker and McDaniel (1948), and at high energies (>10 MeV) has a comparable resolution of $\sim 4\%$.

The main advantage of a high stopping power no longer holds in the study of β-rays since all counters are practically 100% efficient in detecting electrons. Because of the scintillation counter's poor resolution at low energies it is doubtful if anything is to be gained in using it in preference to a magnetic spectrometer or a proportional counter, since the only possible advantage of a large solid angle is also possessed by the latter. Its main strength lies in the study of weak, high energy sources, where the counter's large solid angle and now tolerable resolution make it superior in many respects to the magnetic spectrometer. Also, since the path length of a 1 MeV electron in anthracene is only 0.5 cm., no elaborate techniques such as the use of magnetic fields with proportional counters (Rothwell and West 1950; Curran, Cockroft and Insch 1950) are required to keep the electrons within the counting medium.

Part IV. The Compton Coincidence Spectrometer.

This is an energy measuring device which is designed to cover the gap ($\sim$0.25 to 2 MeV) between the two energy regions in which the photoelectric effect and the pair-production effect can be employed. It makes use of the Compton effect which predominates in this energy interval. The basic idea of the spectrometer was suggested by Dr. S.C. Curran, and the theory of the instrument was developed and the experimental work carried out by the writer. The first results using this method were obtained independently by Hofstadter and McIntyre (1950b), who succeeded in resolving the two γ-rays from Co^{60} of energy 1.17 and 1.33 MeV. The writer obtained a similar result shortly afterwards, and the spectrometer has since been used in the study of the decay schemes of radioactive isotopes (Bannerman, Lewis and Curran 1951).

1. The Theory of the Spectrometer.

The Compton effect is the term used to describe the elastic collision of a γ-ray quantum with a free electron. In practice the electron is usually bound in an atomic level, but can be considered as free if the incident quantum energy is much greater than the binding energy of the electron. The interaction is illustrated diagramatically in Figure IV.1. The incident quantum (energy k_o) knocks forward an electron

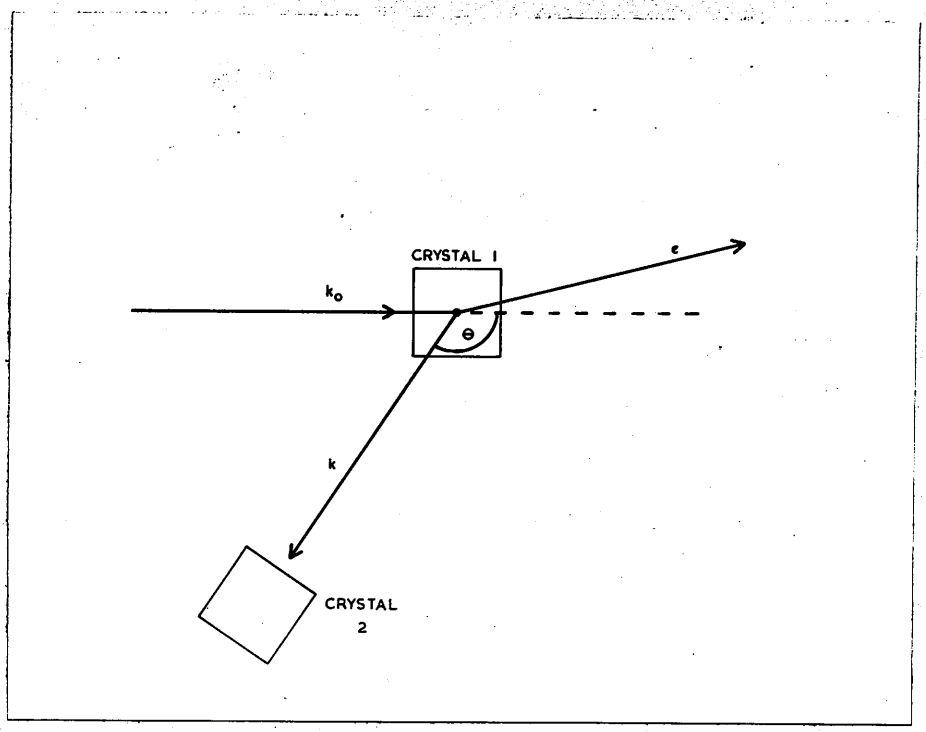

Figure IV.1.

Schematic diagram of the Compton effect.

k_o - energy of incident quantum: e - energy of Compton electron produced by collision with k_o: k - energy of scattered quantum ($< k_o$): θ - angle of scatter of quantum k relative to incident quantum k_o.

with kinetic energy e and at the same time is scattered with a reduced energy k at an angle θ to its original direction. The energy k is given by

$$k = \frac{k_0 \mu}{\mu + k_0 (1 - \cos\theta)} \quad \text{---------- (1)}$$

where $\mu = mc^2$ is the rest energy of the electron (Heitler 1944, p.146, equ.4). The kinetic energy of the electron is given by

$$e = k_0 - k \quad \text{..... (2)}$$

Further, the probability of the quantum k_0 being scattered at an angle θ with an energy k is given by a modified form of the Klein-Nishina formula (Heitler 1944, p.155, equ.51),

$$d\phi = \frac{r_0^2 d\Omega}{2} \frac{k^2}{k_0^2} \left(\frac{k_0}{k} + \frac{k}{k_0} - \sin^2\theta \right) \quad \text{---(3)}$$

where $d\phi$ is the differential cross-section per electron, r_0 is the classical electronic radius, and $d\Omega$ is the element of solid angle into which the quantum k is scattered.

From Equations 1, 2 and 3 the distribution of electrons with energy, for a given incident energy k_0, can be calculated. This will be the shape of the spectrum observed in a single phosphor crystal, and examples of some Compton distributions are shown in Figures II.3, II.4 and II.5 for incident γ-ray energies of mc^2, $4mc^2$ and $10mc^2$.

The variation of electron energy e as a function of θ for various values of k_0 was calculated, and e/k_0 is shown

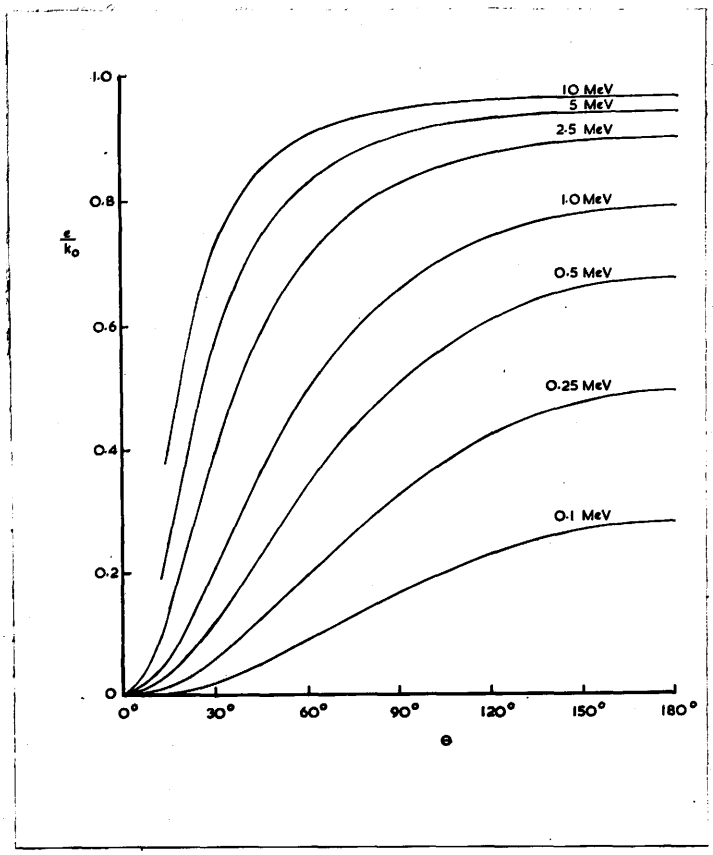

Figure IV.2.

Energy of recoil electron e as a function of angle θ for different incident quantum energies k_0.

plotted against θ in Figure IV.2. It will be seen that as k_o increases in value a considerable "flattening" of the curves occurs ~~at the maximum electron energy~~ for $\theta > 90°$. This is another way of saying that the energy k of the back-scattered quantum is appreciably constant ($\sim \mu/2$) for values of $k_o > \mu$. It is this behaviour of the Compton effect which forms the basis of the coincidence spectrometer. For, if we can detect these back-scattered quanta and use them in a coincidence technique to "gate" the single crystal spectrum, the pulses passed by the gate will correspond only to the almost homogeneous maximum energy electrons. Each γ-ray should therefore produce a single line in the spectrum, instead of a continuous Compton distribution. We shall now consider the resolving power and effective solid angle of such an instrument.

Due to the finite solid angle of the detecting crystal 2 (Figure IV.1), scattered quanta will be counted within an angular range $\theta - d\theta$ to $\theta + d\theta$. Corresponding to this range, the recoil electrons in the first crystal will have energies from e-de to e+de, provided that the γ-ray beam incident on crystal 1 is well collimated so that the angular spread at this point can be considered as negligible. The γ-ray line will therefore appear as a peak of width 2de, and we can write the percentage width D as (2de/e) x 100. This is the inverse of the resolving power P. D will vary with $d\theta$ and e, and so is a function of k_o, θ and $d\theta$.

The number of quanta dN scattered in the direction of the detector crystal 2 will be proportional to the source strength N_0 and the differential Compton cross-section $d\sigma$ for the particular solid angle of collection $d\Omega$. dN is therefore again a function of k_0, θ and $d\theta$, since $d\Omega \cong (d\theta)^2$.

We have therefore the following six variables to consider:-

N_0 - the strength of the source.

k_0 - the energy of the γ-quanta emitted by the source.

θ - the angle at which scattered quanta are detected.

$d\theta$ - the angular spread about the mean angle θ.

D - the corresponding percentage spread in electron energy.

dN - the flux of scattered quanta through the detector crystal.

Of these, N_0 and k_0 are independent variables determined by choice of a specific radioactive source; θ and $d\theta$ are independent variables decided by geometry; and D and dN are the two dependent variables which determine the performance of the instrument.

D:- From Equation 2 we have $e = k_0 - k$, therefore

$$e = \frac{k_0^2 (1 - \cos\theta)}{\mu + k_0 (1 - \cos\theta)} \quad - - - - \quad (4)$$

and so since $D = 2de/e$, we have

$$D = \frac{2k \sin\theta . d\theta}{k_0 (1 - \cos\theta)} \quad - - - - - - - - \quad (5)$$

The variation of D with k_o is shown graphically in Figure IV.3a, for several different values of θ and for $d\theta = 10°$. As we would expect from the results shown in Figure IV.2, the resolution of the instrument increases with both increasing quantum energy and angle of scatter. We find that $D \propto 1/k_o$ for a given angle θ; and that for a given energy k_o, $D \rightarrow 0$ as $\theta \rightarrow 180°$.

dN:- The differential Compton cross-section $d\phi$ is given in Equation 3 as

$$d\phi = \frac{r_o^2 d\Omega}{2} \frac{k^2}{k_o^2}\left(\frac{k_o}{k} + \frac{k}{k_o} - \sin^2\theta\right)$$

If we write

$$\epsilon = \frac{1}{2}\frac{k^2}{k_o^2}\left(\frac{k_o}{k} + \frac{k}{k_o} - \sin^2\theta\right) \quad \text{---- (6)}$$

then $$d\phi = \epsilon r_o^2 . d\Omega \quad \text{------- (7)}$$

Now $d\phi$ is the differential cross-section per electron of the scattering material, so the differential cross-section per cc. will be given by

$$d\sigma = nZ . d\phi \quad \text{..... (8)}$$

where nZ is the total number of electrons per cc. For an element n is the number of atoms per cc. and Z is the atomic number. For a compound, e.g. NaI(Tl), n is the number of molecules per cc. and Z becomes ΣZ for each molecule. Values of nZ and $d\sigma$ for some typical phosphors are listed in Table IV.1.

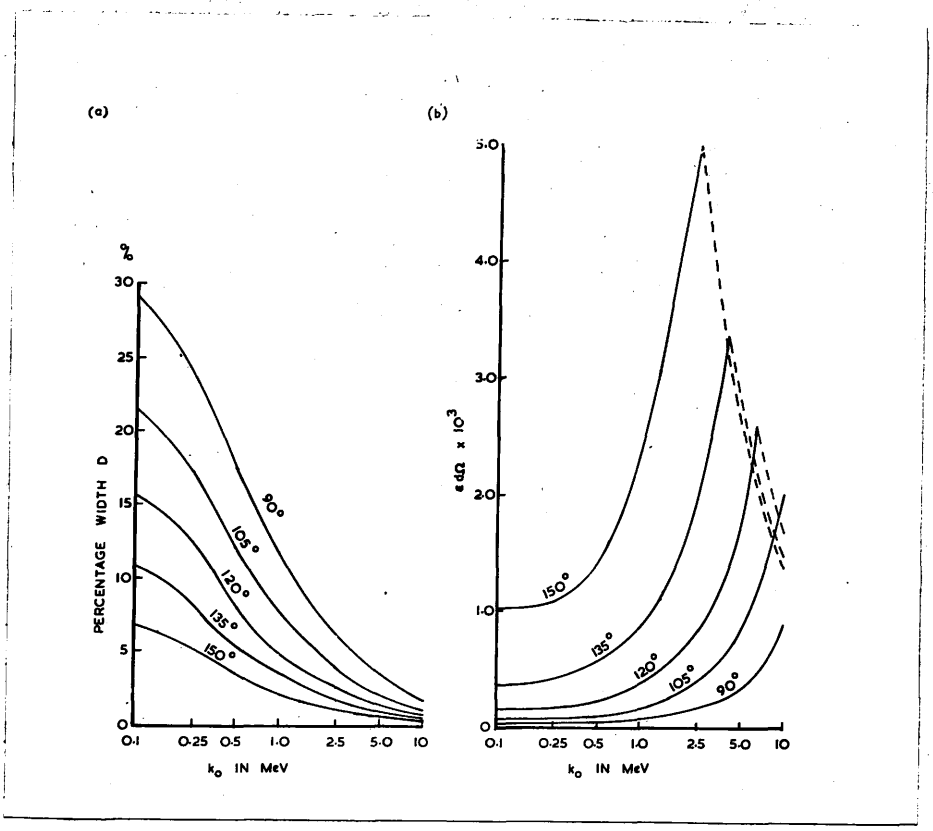

Figure IV.3.

(a) Percentage line-width D as a function of energy k_0 for different values of angle θ, and for $d\theta = 10°$.

(b) Counting rate dN ($\propto \varepsilon d\Omega$) as a function of energy for different values of angle θ, and with the percentage line-width constant at D = 2%.

Table IV.1.

Phosphor	nZ	dσ
Anthracene	3.35×10^{23} per cc.	$2.62 \times 10^{-2}.\varepsilon d\Omega$ per cc.
NaI(Tl)	9.45	7.4
Scheelite	15.8	12.3

If N quanta per second is the fraction of the total N_0 reaching crystal 1 due to collimation, and if V cc. is the volume of crystal 1 traversed by the collimated beam, then the number of quanta scattered in the direction of crystal 2 will be

$$dN = NV.d\sigma \quad \ldots\ldots\ldots\ldots\ldots\ldots \quad (9)$$

Therefore, for a given set of conditions; collimation, phosphor, etc. we have as previously stated

$$dN \propto N_0 \varepsilon d\Omega \quad \ldots\ldots\ldots\ldots\ldots\ldots \quad (10)$$

Values of ε as a function of angle θ have been calculated for different incident quantum energies, and these are shown graphically in Figure IV.4. For low energies ($k_0 < \mu$) the curve tends towards the classical $(1 + \cos^2\theta)$ variation; while for high energies ($k_0 > \mu$) and for $\theta > 90°$, ε tends to a ~~constant~~ value which is inversely proportional to $\frac{K_0(1-\cos\theta)}{K_0}$. If $d\Omega$ is kept constant, then dN will vary in a similar manner to ε.

The relationship between dN and D can be established

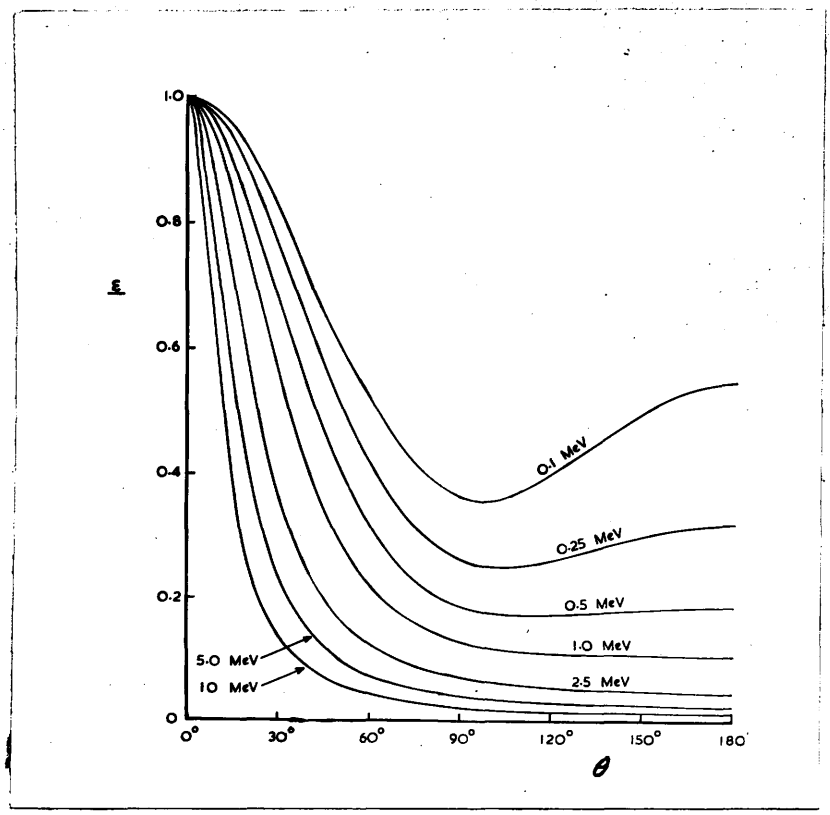

Figure IV.4.

The differential Compton cross-section $d\phi$ ($\propto \varepsilon$) as a function of angle θ, for different incident quantum energies k_0.

as follows. From Equation 5 we have

$$d\theta = \frac{D k_0 (1-\cos\theta)}{2k \sin\theta} \quad \text{- - - - - - - - (11)}$$

Therefore since $d\Omega \cong (d\theta)^2$, we have

$$\varepsilon d\Omega = \frac{D^2}{8}\left(\frac{k_0}{k} + \frac{k}{k_0} - \sin^2\theta\right)\frac{(1-\cos\theta)^2}{\sin^2\theta} \quad \text{- - - - - (12)}$$

In Figure IV.3b, $\varepsilon\, d\Omega$ is plotted against k_0 for a constant value of D (2%) and for various values of θ. For low energies ($k_0 < \mu$) we find that dN ($\propto \varepsilon d\Omega$) tends to a constant value which is larger the greater the value of θ; and at higher energies ($k_0 > \mu$) we obtain the rather surprising result that dN is proportional to k_0, although the differential cross-section $d\phi$ varies as $1/k_0$. This increase, however, is limited by practical considerations. Due to the finite size of the crystals there will be a minimum value for the distance between their centres, and therefore a maximum value for dθ and $d\Omega$. After this point has been reached, both dN and D will decrease as $1/k_0$. This is shown by the dotted portions of the curves in Figure IV.3b, which have been calculated assuming a maximum value of 20° for dθ.

Returning to Equation 12, if k_0 and θ are kept constant we find that $dN \propto D^2$, i.e.

$$dN \propto P^{-2} \quad \text{..... (13)}$$

where P is the resolving power. The Compton coincidence spectrometer is therefore superior to the magnetic resolver,

most types of which are governed by the relationship

$$F \propto P^{-5/2} \quad \ldots\ldots\ldots\ldots\ldots\ldots \quad (14)$$

where F, the analogue of dN, is the intensity factor and is given by the product (source area x solid angle) (Persico and Geoffrion 1950).

The performance of the Compton coincidence spectrometer can be summarised as follows:-

(1) If it is used as a constant resolution instrument, then for a given angle θ we find

$$dN \rightarrow \text{constant} \quad \text{for } k_o < \mu.$$

$$dN \propto k_o \quad \text{for } k_o > \mu.$$

(see Figure IV.3b)

(2) For the examination of any given energy k_o at a constant angle θ we have

$$dN \propto D^2 \propto P^{-2}.$$

(3) The most usual practice is to use the spectrometer with a fixed geometry at the maximum possible value of θ. In this case θ and $d\theta$ are constant and so we have

$$\left.\begin{array}{l} dN \rightarrow \text{constant} \\ D \rightarrow \text{constant} \end{array}\right\} \quad \text{for } k_o < \mu.$$

$$\left.\begin{array}{l} dN \propto 1/k_o \\ D \propto 1/k_o \end{array}\right\} \quad \text{for } k_o > \mu.$$

(see Figures IV.3a and IV.4)

2. Description and Performance of the Spectrometer.

The geometry normally used is illustrated in Figure IV.5. Crystal 1 is a 1 cm. cube of anthracene or NaI(Tl). This is about the optimum size, since it allows secondary electrons of up to several MeV to be confined within the crystal without absorbing the 0.25 MeV scattered quanta to any appreciable extent. Crystal 2 consists of a 3/4 in. dia. by 3/4 in. cylinder of NaI(Tl), which detects about 75% of the scattered quanta incident upon it. For maximum sensitivity crystal 2 should be toroidal in shape, since this does not interfere with the resolving power. Both crystals are mounted on E.M.I. 5311 photomultiplier tubes. The lead collimator, which also shields crystal 2 from the source, is 4 in. in length and 0.2 in. in diameter so that the radiation incident on crystal 1 lies in a cone of semi-vertical angle 5°. The detecting angle used is 140° ± 20°, therefore at 1 MeV the energy spread D should be about 6% (see Figure IV.3a). If the statistical spread at this energy (~ 10%) is also taken into account, then the observed peak widths at half-height (see Figures V.5 and V.6) are in good agreement with the theoretical estimate.

The circuitry following the two scintillation counters, which detects the coincidences and analyses the coincidence spectrum from crystal 1, has already been described in detail in Part III.1b.

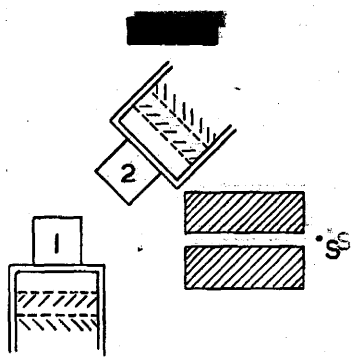

Two-crystal Compton method of γ-ray analysis.

Figure IV.5.

The geometrical arrangement of the two scintillation counters in the Compton coincidence spectrometer.

In this type of coincidence experiment there exists no definite relationship between the source strength N_0 and the resolving time τ of the coincidence unit as is the case, say, in β-γ or γ-γ coincidence measurements, where the ratio of the number of real coincidences to random coincidences is given by the expression $1/2N_0\tau$. For a given resolving time and source strength, it is possible to obtain any chosen value for the real-to-random ratio merely by altering the geometry and the thickness of lead between the source and crystal 2. However, if the absolute value of the real coincidence rate is at the same time to be kept high, then the source must be fairly strong. For the satisfactory operation of the spectrometer it is desirable to have a source strength of ≥ 1 mCurie, although weaker sources can be handled. The effective solid angle of the spectrometer as used here is $\sim 10^{-6}$ of 4π.

An imperfection in the spectrometer will arise from the escape of the forward scattered electrons produced near the face of the crystal furthest from the source. These tend to produce a low energy "tail" on the coincidence peaks. However, the associated 0.25 MeV back-scattered quanta have to traverse the whole of crystal 1 before escaping, and some will be absorbed and not produce coincidences. This second effect therefore tends to cancel out the first, and for a 1 cm. cube of NaI(Tl) the "edge effect" is reduced by $\sim$ 50% by this means.

The application of this method to the measurement of γ-ray energies is considered in the next part of the thesis. The radiations from several sources, including Co^{60}, ThC" and La^{140}, have been examined and typical curves obtained with the γ-rays of La^{140} are illustrated in Figures V.5 and V.6. The range of energies covered by these radiations was from 0.335 MeV to 2.62 MeV.

Part V. The Study of Decay Schemes.

1. The Techniques Employed.

The techniques employed in examining the decay scheme of a radioactive isotope depend to a great extent on the energy and complexity of the emitted radiations. In particular instances special techniques may have to be used, but experience has shown that in general five main methods of approach can be adopted. These will now be described in detail.

(a) The γ-Ray Spectrum.

This method involves a straightforward examination of the quanta (γ-rays and X-rays) emitted by the source. If the energy is low (< 250 keV) a single crystal spectrum can be taken using a NaI(Tl) crystal. Otherwise the Compton coincidence spectrometer has to be employed. With the single crystal method no collimation is necessary, so that large solid angles can be used here. This allows very weak sources ($\sim 10^{-9}$ Curies) to be examined, although care must be taken to ensure that, if there are cascade γ-rays present, the number of coincidences in the crystal due to the large solid angle is kept small. With the Compton coincidence method, on the other hand, sources of ~ 1 mCurie are required, although source strengths down to ~ 10 μCuries can be handled if the spectrum is photographed. The relative

intensities, as well as the γ-ray energies, are also determined from these measurements.

(b) The γ-γ Coincidence Spectrum.

This involves the measurement of γ-γ coincidences and also, if one or more of the transitions is internally converted, of γ-X and X-X coincidences. At the moment two techniques are employed. In the first case two counters with NaI(Tl) crystals are arranged symmetrically with respect to the source so that the complete γ-ray spectrum is observed in each counter. These pulses are passed to the coincidence unit and the output is used to gate one of the channels. The resultant spectrum should show all the γ-rays which produce coincidences. If coincidences are obtained, then the minimum number of γ-rays which can appear in the coincidence spectrum is two, and these must obviously be in cascade. If more than two γ-rays appear, the correlation between them cannot be stated with certainty. The relative intensities of the γ-rays in the coincidence spectrum should afford some indication of the decay scheme, but in general this method is not sufficiently sensitive to distinguish between possible alternatives.

The second method of approach is next employed. Here the γ-ray spectrum in coincidence with each individual γ-ray is determined and the γ-ray decay scheme should be established without any ambiguity. At present, due to restrictions of

circuitry, it is only possible to isolate the highest energy γ-ray by means of the discriminator in one of the channels (see Figure III.3a). If the source is not too complex, however, this may be sufficient to establish a decay scheme in conjunction with the first result. Steps are being taken to modify the circuitry so that the spectrum in coincidence with γ-rays of intermediate energy can also be determined.

Since this coincidence technique involves the use of two single crystal spectrometers, it operates best with NaI(Tl) crystals in the low energy region below ~ 250 keV.

(c) The β-Ray Spectrum.

The β-ray spectrum is examined in a single crystal of anthracene or NaI(Tl), using a specially prepared thin source and the minimum of absorber between the source and the crystal. Anthracene has a greater transparency to γ-rays, but if it is possible to use NaI(Tl) this has the advantage of being much easier to calibrate with γ-rays of known energy. In addition, the non-linearity of anthracene below ~100 keV must be borne in mind. If the solid angle is kept small (~ 1% of 4π) to keep down the number of coincidences in the crystal, then the end-point of the observed β-spectrum will give the energy of the most energetic β-ray transition. If the shape of the spectrum is recorded accurately, a Kurie plot should indicate the presence of any other β-rays. However these can also be detected by coincidence techniques, and the main emphasis of the β-ray work up to the present

has been on the determination of end-point energies.

(d) The β-γ Coincidence Spectrum.

This method is similar in principle to the γ-γ coincidence technique, and the β-spectrum in coincidence with a given γ-ray is isolated and examined. Due to the circuitry limitations already mentioned, it is only possible at the moment to isolate the β-spectrum in coincidence with the highest energy γ-ray. Here again the main emphasis has been on end-point measurements. A typical example of the geometry employed is shown in Figure V.13, inset. If the geometry of counter M_1 is made the same as that of M_2, then the arrangement used in detecting γ-γ coincidences is obtained.

(e) The Integrated Spectrum.

This method is the development of a technique which was originally used by Wilson and Curran (1951) in the study of β-spectrum shapes with proportional counters. These authors mounted a thin source of Hg^{203} (see Figure V.1 for decay scheme) inside the counter and examined the radiations with a 4π geometry. Due to the low stopping power of the gas most γ-ray and X-ray quanta escaped, but the coincident emission of a β-particle and a conversion electron was recorded as a single pulse. The spectrum obtained was not therefore a true integrated spectrum but consisted of a series of β-spectra, each displaced by an amount equal to the energy of the K, L, M .... conversion electrons.

In the application of this method to scintillation counters a 4π geometry is achieved by splitting a cube of NaI(Tl) and clamping a thin source mounted on a light backing between the two halves (Figure V.1). This method is most useful in the study of sources with γ-rays $\leq$ 100 keV, since at these energies the absorption of quanta in 1 cm. of NaI(Tl) is approximately 100%, and so all radiations will be trapped within the crystal. All time-coincident β-particle and γ-ray pulses will therefore add up, and the resultant pulse-height distribution will be the "integrated spectrum" from the source. To illustrate the method we shall consider the application of it to the radiations of Hg^{203} (Bannerman, Lewis and Curran 1951).

The decay scheme of Hg^{203} (Slätis and Siegbahn 1949) is shown in Figure V.1. Hg^{203} decays to the ground state of Tl^{203} by the emission of a β-particle of energy 208 keV and a γ-ray of energy 280 keV. This γ-ray is internally converted in the K- and L-shells ($\sim$ 20% and 5% respectively), giving rise to photoelectrons of energy $\sim$ 200 keV and $\sim$ 270 keV respectively. A thin source ($\sim$ 1 $\mu g/cm^2$.) of HgS was evaporated on to an aluminium foil of thickness 1.8 mg/cm^2., and this was clamped between two blocks of NaI(Tl), each 1 x 1 x 0.5 cm^3. The assembly was surrounded with paraffin and an aluminium foil reflector and mounted on an E.M.I. 5311 photomultiplier tube (Figure V.1).

About 25% of the γ-rays are absorbed in the crystal by

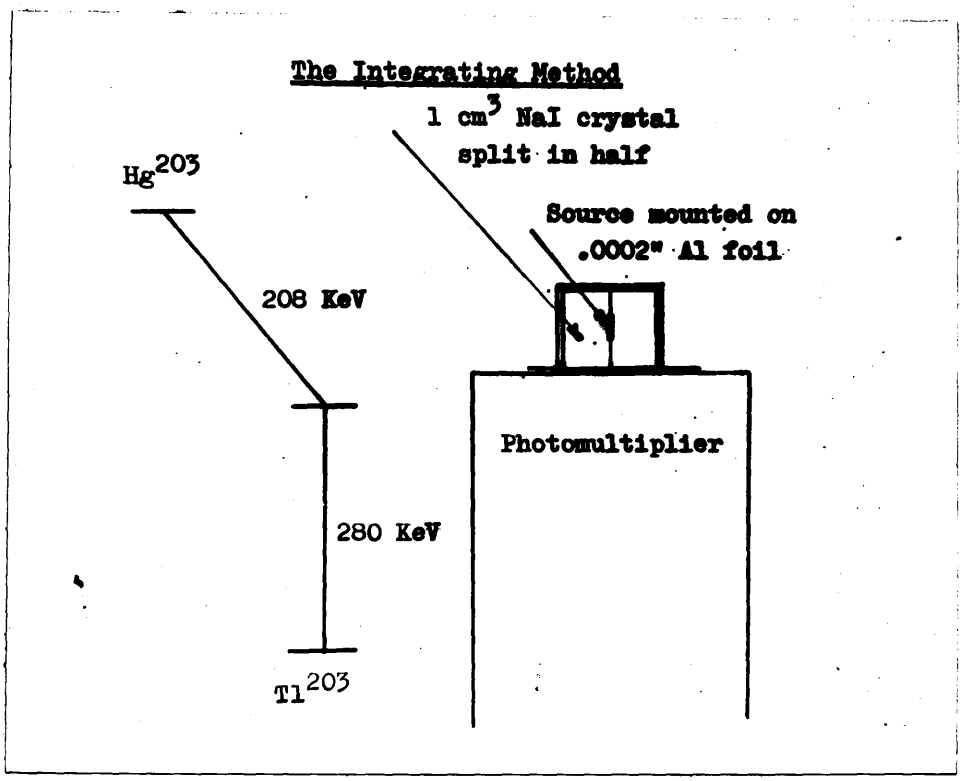

Figure V.1.

The integrating method, showing the source clamped between the two halves of a cube of NaI(Tl), and the position of the crystal with respect to the photomultiplier tube. Also illustrated is the decay scheme of Hg^{203}.

the photoelectric effect and another 25% suffer Compton scattering. We therefore expect three types of pulses:-

(1) β-rays accompanied by ϒ-rays which escape from the crystal and are not counted.

(2) β-rays accompanied by ϒ-rays which produce Compton electrons in the crystal.

(3) β-rays accompanied by ϒ-rays whose full energy is absorbed in the crystal. This can occur in several ways.

(a) β-particles + K conversion electrons + Tl K X-rays, from internal conversion.
(b) β-particles + L conversion electrons + Tl L X-rays, from internal conversion.
(c) β-particles + K conversion electrons + I K X-rays, from photoelectric absorption in the crystal.

Neglecting group (2) for the moment, groups (1) and (3) should result in two spectra being produced; one due to particles of the normal β-spectrum ending at 208 keV, and the other due to particles of the β-spectrum carried forward by 280 keV. This second group should therefore extend from 280 keV up to 280 + 208 = 488 keV, which is the total disintegration energy of the decay. These two groups are clearly separated, and the second will display the form of the β-spectrum from zero up to the end-point. The experimental distribution obtained is shown in Figure V.2. This agrees closely with the predicted result, but unfortunately the Compton effect (group (2) particles) has resulted in a filling in of the gap between group (1) and group (3) particles. If 100% absorption had been obtained for the ϒ-rays, then all pulses would contribute to group (3), and

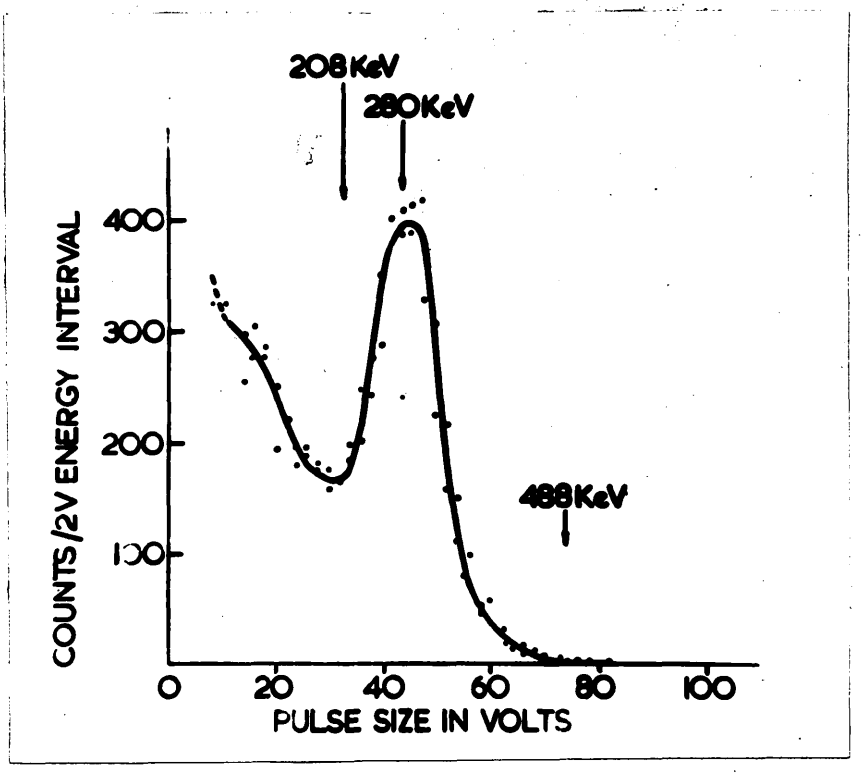

Figure V.2.

The integrated spectrum of the radiations from Hg^{203}.

no pulses would be observed below 280 keV.

Again, if we consider a more complex decay scheme of the form shown in Figure V.3 and assume 100% absorption for all γ-rays, we will obtain the following results. The β-spectrum β_2 will be displaced by an amount $h\nu_2$, so that it will extend from a "zero" value of $h\nu_2$ up to an end-point at an energy $h\nu_2 + \beta_2$. Similarly the spectrum β_1 will be displaced by an amount $h\nu_3$, whatever the mode of de-excitation to the ground state from the level at energy $h\nu_3$. This second spectrum will therefore have a displaced "zero" at $h\nu_3$ and will extend up to an energy $h\nu_3 + \beta_1$, which is the same end-point as for the first displaced spectrum.

In general, therefore, we can say that the end-point of the integrated spectrum represents the total disintegration energy of the decay, and that the "zeros" of the displaced β-spectra occur at values which correspond to energy levels in the product nucleus to which β-ray transitions take place. This result should thus provide the framework into which the transitions found by other methods can be fitted.

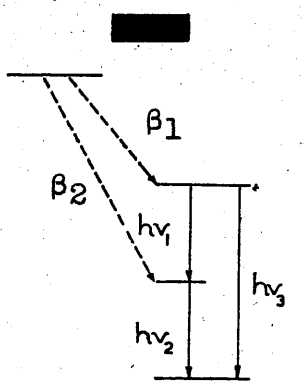

De-excitation process from two excited states.

Figure V.3.

Example of complex β-decay.

2. The Decay Scheme of La^{140}.

La^{140} was originally chosen as a suitable source for use in testing the performance of the Compton coincidence spectrometer, since it emits a number of γ-rays which cover almost the complete working range of this device. This test led to a more detailed examination of the source, in the course of which some new information was found concerning the decay scheme. The writer was assisted in the approach to the problem and in the interpretation of results by Mr. G.M. Lewis and Dr. S.C. Curran. All the experimental work described here was carried out by the writer. The results on La^{140}, and those on Hg^{203} described in the previous section, have been published as part of a general article on electron and γ-ray spectroscopy with scintillation counters (Bannerman, Lewis and Curran 1951).

Introduction.

Of the many previous workers on the 40-hour La^{140} isotope (Nuclear Data 1950), Beach, Peacock and Wilkinson (1949) have obtained the most detailed results. The β-spectrum and the photoelectrons from a lead radiator were both studied in a small 180° spectrometer. The β-spectrum showed K and L conversion lines from two γ-rays of energy 0.335 and 0.49 MeV, and a Kurie plot of the β-spectrum indicated three end-points at 1.32, 1.67 and 2.62 MeV. Three low energy lines were also observed, the lowest of

which was probably an Auger line associated with internal conversion of the γ-rays. The other two were weak and their identification uncertain but as K and L components corresponded to a γ-ray of energy 0.093 MeV.

From the photoelectron spectrum evidence was found of γ-rays at 0.335, 0.49, 0.82 and 1.62 MeV. No trace of a 0.093 MeV γ-ray was found by this method. At the high energy end of the spectrum a weak Compton distribution extending beyond the strong 1.62 MeV line was observed, which finally came to zero in the region of 2.5 MeV. No trace of a photoelectric peak corresponding to a γ-ray of energy $\sim$2.5 MeV was found. Evidence of a high energy γ-ray of this energy has also been obtained from the nuclear photo-effect by Wattenberg (1947), Hanson (1949), and Bishop, Wilson and Halban (1950).

The decay scheme proposed by Beach et al. is shown in Figure V.4.

The γ-Ray Spectrum.

The γ-ray spectrum of La^{140} was examined with the Compton coincidence spectrometer, using the standard geometry already described. A source of initial strength $\sim$15 mCuries was used, and the β-particles from it were screened off with Al absorbers. Some of the results are shown in Figures V.5 and V.6, which were taken using crystals of anthracene and NaI(Tl) respectively as the scattering crystal. The

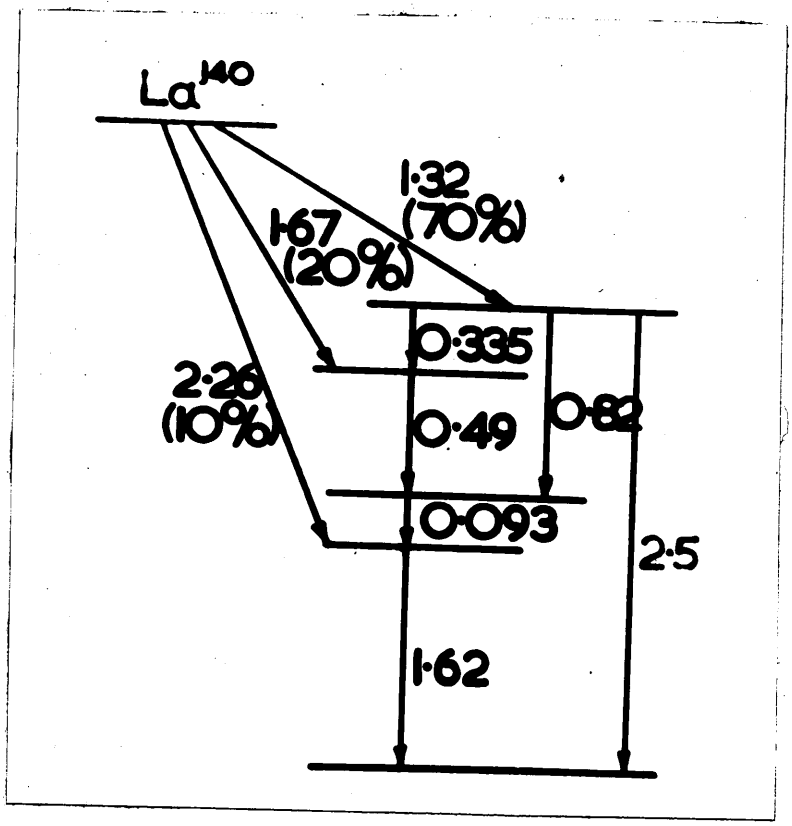

Figure V.4.

The decay scheme of La^{140}.

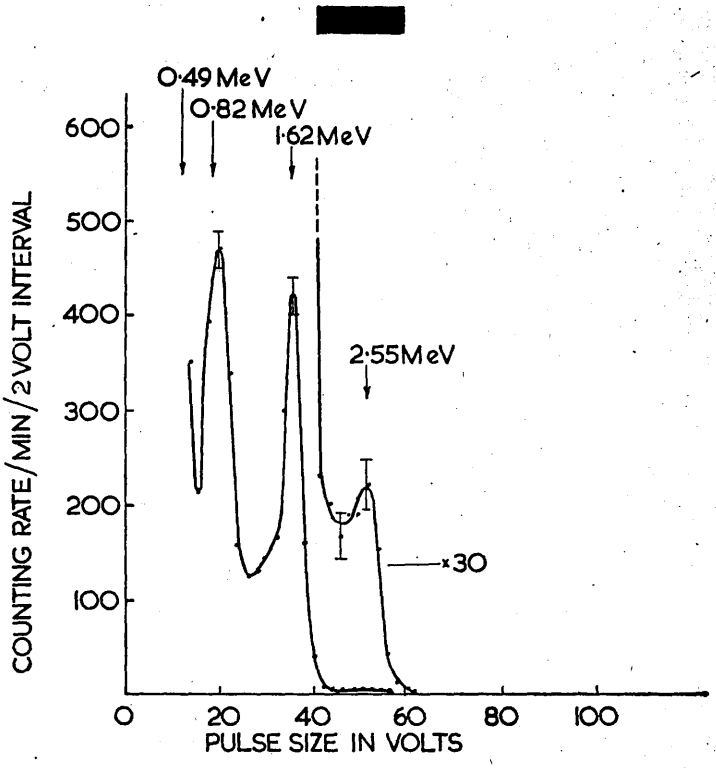

Gamma ray spectrum for La^{140} with 1 cm.^{3} of [redacted] (anthracene) as scattering crystal.

Figure V.5.

Higher energy region of the Υ-ray spectrum from La^{140}, observed by the Compton coincidence method using a 1 cm^3. crystal of anthracene as the scatterer (crystal 1 in Figure IV.5).

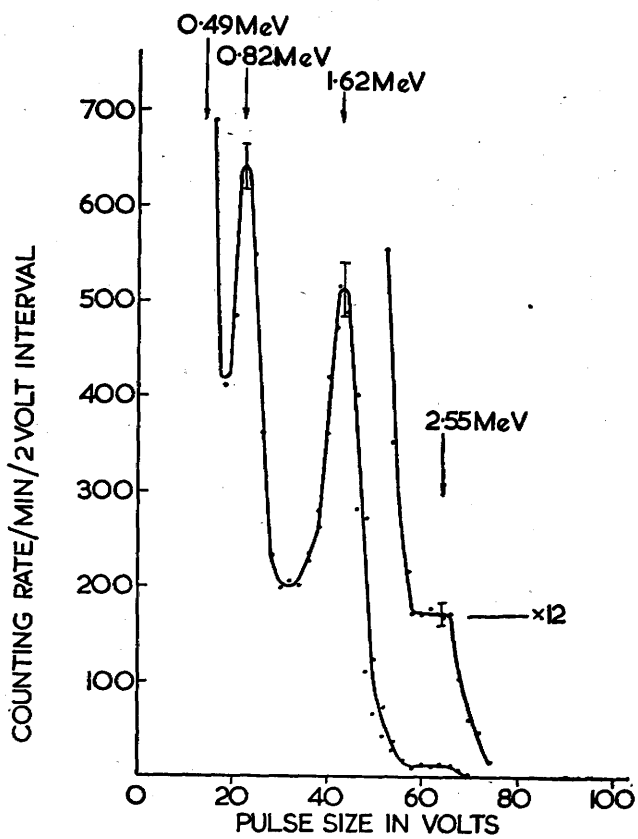

Gamma ray spectrum for La^{140} with 1 cm.^{3} of [redacted] as scattering crystal.
NaI (Tl)

Figure V.6.

Higher energy region of the γ-ray spectrum from La^{140}, observed by the Compton coincidence method using a 1 cm^3. crystal of NaI(Tl) as the scatterer (crystal 1 in Figure IV.5).

γ-rays from Co^{60} (1.17 and 1.33 MeV) and ThC" (2.62 MeV) were used to calibrate the spectrometer. The peaks obtained correspond to γ-rays of energy 0.335, 0.49, 0.82 and 1.62 MeV within the limits of experimental accuracy ($\pm$2%). The weak high energy line was also found (see Figures V.5 and V.6), and by comparison with the ThC" line had an energy of 2.55 $\pm$ 0.05 MeV. No trace was found by this method of a γ-ray of energy 0.093 MeV.

An examination of the γ-ray spectrum was carried out in the region of 90 keV with a NaI(Tl) single crystal spectrometer. No sign of a photoelectric peak was found above the Compton distributions produced by the higher energy radiations, even though the crystal has almost 100% efficiency at this energy. From this result it was estimated that the intensity of the 93 keV γ-ray must be less than 1% of the total γ-ray intensity. This agrees with the findings of Beach et al. regarding the intensity of the γ-radiation from this transition.

An assessment of the relative intensities of the γ-rays emitted by La^{140} can be made from the Compton coincidence measurements. These are listed below in Table V.1, and agree in general trend with the results quoted by Rall and Wilkinson (1947).

Table V.1.

γ-Ray Energy	Relative Intensity
0.093 MeV	$\ll 1$ %
0.335	3
0.49	22
0.82	16
1.62	56
2.55	3

The β-Ray Spectrum.

If we examine the decay scheme of Figure V.4, we see that almost 90% of the disintegrations should result in transitions of energy 93 keV. This suggests that the 93 keV γ-ray may be very strongly converted, although Beach et al. found little trace of internal conversion lines. To decide this point the electrons from a thin source of La^{140} (~ 1 $\mu g/cm^2$.) were examined with a 1 mm. thick crystal of anthracene. The crystal was calibrated by photoelectric peaks from the 24.1 keV X-rays of In^{114} and the 46.7 keV γ-rays of RaD. A peak of very low intensity, superimposed upon the main β-spectrum, was observed (Figure V.7) of energy 55 $\pm$ 5 keV, presumably corresponding to internal conversion in the K shell of a γ-ray of energy 95 $\pm$ 5 keV. The intensity was found to correspond to about 1 per 100 disintegrations and seems to establish the necessity of

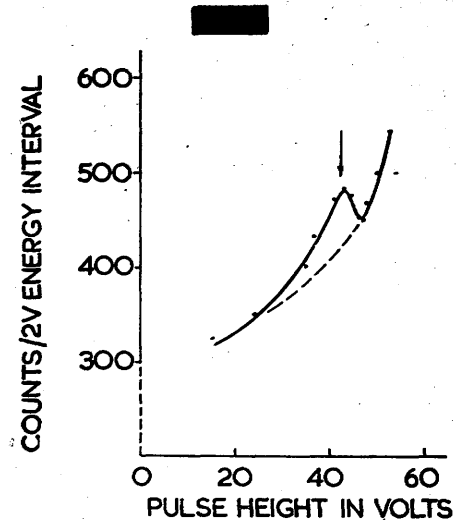

Conversion electrons, energy ~55 KeV., due to weak γ-ray, energy 90–95 KeV., as observed in thin anthracene exposed to electrons from La^{140}.

Figure V.7.

Internal conversion electron peak from La^{140}.

modifying the existing decay scheme.

With a 1 cm^3. crystal of anthracene the high energy region of the β-spectrum was examined and found to extend up to ~2.26 MeV. The K conversion peak from the 0.335 MeV γ-ray was detected, but that from the 0.49 MeV γ-ray was not strong enough to be observed.

The γ-γ Coincidence Spectrum.

β-γ and γ-γ coincidences have been reported by Osborne and Peacock (1946), Mitchell, Langer and Brown (1947), and Mandeville and Scherb (1948), but without any direct evidence being obtained for the energies of the radiations in coincidence.

γ-γ coincidences were therefore investigated using anthracene as the phosphor crystal in both counters. The spectrum observed in each counter, a series of superimposed Compton distributions, is shown in curve (b) of Figure V.8. When coincidences were used to gate the output of one counter, the curve of Figure V.8a was obtained, showing the presence of the 1.62, 0.82 and 0.49 MeV γ-rays. These γ-rays are therefore in coincidence with one another.

The discriminator bias in the second channel was then increased so that only pulses greater than 0.8 MeV were allowed to pass on to the coincidence unit. These pulses arise solely from the 1.62 MeV γ-ray. The coincidence curve obtained from the gated first channel is shown in Figure V.9a,

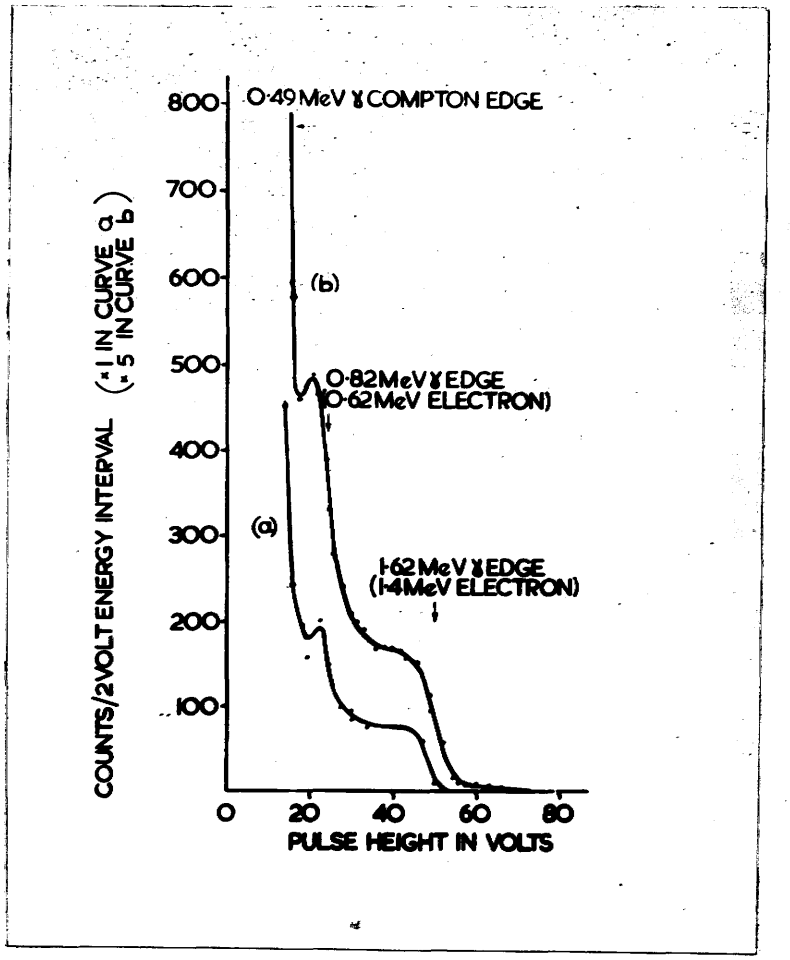

Figure V.8.

(a) Part of the γ-γ coincidence spectrum of La^{140}, showing all γ-rays which produce coincidences; obtained by detecting all γ-rays in both counters.

(b) The γ-ray spectrum of La^{140} as observed in the anthracene crystal of each counter of the coincidence arrangement.

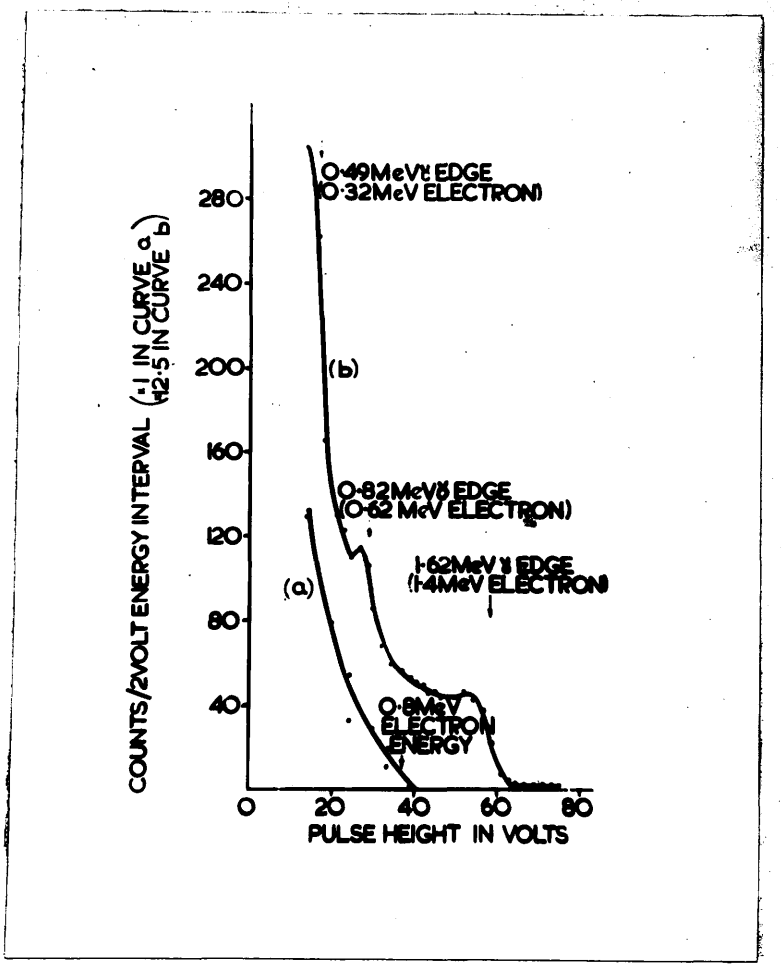

Figure V.9.

(a) Part of the γ-γ coincidence spectrum of La^{140}, showing γ-rays in coincidence with the 1.62 MeV γ-ray.

(b) The same part of the ungated γ-ray spectrum shown for comparison.

and the ordinary single crystal spectrum is shown in curve (b) for comparison. No counts are observed in the coincidence spectrum above 0.8 MeV, while below this point the curve follows the same trend as curve (b), although the counting rate is too low to distinguish the peak of the 0.82 MeV γ-ray Compton edge. The 0.49 and 0.82 MeV γ-rays are therefore in coincidence with the 1.62 MeV γ-ray. It was similarly shown that the 0.335 MeV γ-ray is also in coincidence with the 1.62 MeV γ-ray. These results are in agreement with the decay scheme of Figure V.4.

Conclusion.

The above results show a considerable measure of agreement with those obtained by Beach et al. The energies of the more intense γ-rays have been verified, while the presence of a weak high energy γ-ray at 2.55 MeV has been confirmed. The 0.093 MeV transition has been observed as a low intensity conversion electron peak, but no evidence has been found for the direct emission of γ-rays. The intensity of this transition, therefore, makes it impossible to retain it in the position assigned to it in the decay scheme of Figure V.4, where it is shown as a member of the main cascade. The γ-γ coincidence results lend strong support to the structure of the remainder of the decay scheme.

Since this work was completed results obtained by Robinson and Madansky (1951) with scintillation counters

have confirmed some of the above coincidence measurements, and have also indicated uncertainty as regards the assignment of the 0.093 MeV transition.

3. The Decay Scheme of RaD.

In the investigation of the radiations from this source, the approach to the problem and the interpretation of results was carried out jointly with Dr. S.C. Curran, although the application of the experimental methods was solely the work of the writer. An abbreviated account of the work described below has appeared in the Physical Review (Bannerman and Curran 1952).

Introduction.

The disintegration of RaD has been the subject of much research and a recent summary due to Feather (1949) indicates the present uncertainty as to the mode of decay. Most workers in the past have used magnetic spectrographs, as for example in the recent work of Cranberg (1950), or bent crystal spectrometers (Frilley et al. 1951). The former method has yielded very definite information on conversion lines down to an energy of about 15 keV for the electrons (about 31 keV for the γ-rays) and has shown that the main electron peaks above 15 keV arise from the conversion of a γ-ray of energy 46.7 keV. The latter method has yielded data on quanta between the upper limit definitely detected (46.7 keV) and a lower limit of about 7 keV. The L X-rays of Bi constitute the most intense of the electromagnetic radiations and there has been much difficulty in reconciling the number of L X-rays with the intensity of the conversion

electrons. Kinsey (1948) and Cranberg (1950) conclude that about 75% of the disintegrations of RaD can be explained in terms of β-emission followed by de-excitation from the excited level at 46.7 keV, this de-excitation corresponding to conversion with an extra 3% taking place by direct emission of γ-radiation. The position is thus complicated, suggesting a complex β-spectrum. Feather stresses the complexity of the γ-spectrum, pointing out however some suggestive combinations. The well-confirmed radiations are as shown in Table V.2 and the combinations noted are $16.1 + 31.3 \cong 46.7$ and $16.1 + 7.3 + 23.2 \cong 46.7$.

Table V.2.

hν in keV	46.7	42.6	37 ±0.5	31.3 ±0.8	23.2 ±0.6	16.1 ±0.4	7.3 ±0.7
%	2.8 ±0.6	0.2 ±0.1	0.2 ±0.1	0.4 ±0.2	~1	~0	~10

The results described in previous sections of this thesis, in which various techniques employing scintillation detectors have been exploited, suggest that the problem of the disintegration scheme of RaD might be examined advantageously with the scintillation spectrometer. The scintillation method is similar in principle to the gas-filled proportional counter, which has already been used in the study of the soft γ-rays and X-rays from this source

(Curran, Angus and Cockroft 1949). It has certain very definite advantages to offer, particularly its 100% efficiency for detecting the harder radiations of RaD (37, 42.6 and 46.7 keV). Thus, assuming that the main mode of decay consists in the emission of soft β-rays followed by de-excitation from the excited level at 46.7 keV, it is reasonable to conclude that a coincidence counting system, 100% efficient for the γ-rays, would permit isolation and examination of the β-spectrum when the control impulses from one crystal were due to the 46.7 keV quanta. The high efficiency is very desirable on account of the low intensity of these quanta (~ 3 per 100 disintegrations). The limiting energy of the primary β-spectrum has been variously estimated as between about 10 and 40 keV. In the past much confusion has arisen from the softness of the spectrum itself, and also from the relatively high intensity of the conversion lines, Auger electrons and to some extent the continuum of β-rays from RaE when imperfect separation of RaD was involved.

It was further expected that the integrated spectrum technique would help to elucidate the scheme. Thus particles (conversion and Auger electrons), X-rays (L and M of Bi) and γ-rays could all be detected and they might add up to a common sum if time-coincident. It was tentatively expected that if de-excitation, whatever the means, occurred mainly from the level at 46.7 keV the spectrum of pulses from the integrating crystal would show a negligible intensity from

0 to 46.7 keV and the β-spectrum would lie beyond, reaching its upper limit E_0 at (46.7 + E_0) keV on the energy scale.

The Υ-Ray Spectrum.

A thin crystal of NaI(Tl) (1 x 8 x 8 mm^3.) surrounded by paraffin and covered with an Al foil reflector was used as the detector. Both for this work and that on Υ-Υ coincidences the source was essentially RaD+E+F in near equilibrium, since at this earlier stage of the work the separation technique had not been perfected. The crystal was shielded with an 1/8 in. thick sheet of polythene from the β-rays of RaD and RaE, and a 2 thou. sheet of copper could be inserted between the crystal and the polythene to reduce the flux of the softer radiations, particularly the L X-rays of Bi.

A typical spectrum, obtained without the Cu foil, is shown in Figure V.10a. As well as the Υ-ray of energy 46.7 keV and the L X-ray peak at ~13 keV we see some indication of the presence of 37 and 42.6 keV Υ-rays on the low energy side of the 46.7 keV peak. The resolution of the counter is not sufficiently high to distinguish the presence of any other Υ-rays. These energy values were confirmed by calibrating the NaI(Tl) crystal with known radiations such as the 9.3 keV X-rays from Ge^{71}, the 24.1 keV X-rays from In^{114} and the 73 keV X-rays from Hg^{203}.

In view of past uncertainties regarding the possible

existence of harder radiations from RaD the range up to about 140 keV was searched carefully. No appreciable amount of harder radiation was detected, but a long tail of low intensity which was observed probably arose from bremsstrahlung produced by the 1.17 MeV β-rays of RaE in the polythene absorber.

The γ-γ Coincidence Spectrum.

Two crystals of NaI(Tl) each 0.5 x 1 x 1 cm^3. were used and in Figure V.10a the form of γ-spectrum observed in each when the source was placed between them is shown. It was noted that the ratio of true coincidences to random coincidences was 8/1 when the threshold in both counters was ~7 keV. This fell to 2.5/1 when the channel attached to one of the crystals was biased by means of its discriminator so that only pulses greater than 40 keV were passed. This same bias however reduced the actual number of real coincidences by a factor of 13, and this seems to establish satisfactorily that there is no appreciable number of real coincidences between γ-rays of energy > 40 keV and any other γ-rays of energy > 7 keV. Separate examination of the spectrum in coincidence with γ-rays of energy > 40 keV indicated that the remaining coincidences were largely spurious. This implies again that the 46.7 keV level is probably the highest excitation level of the product nucleus RaE.

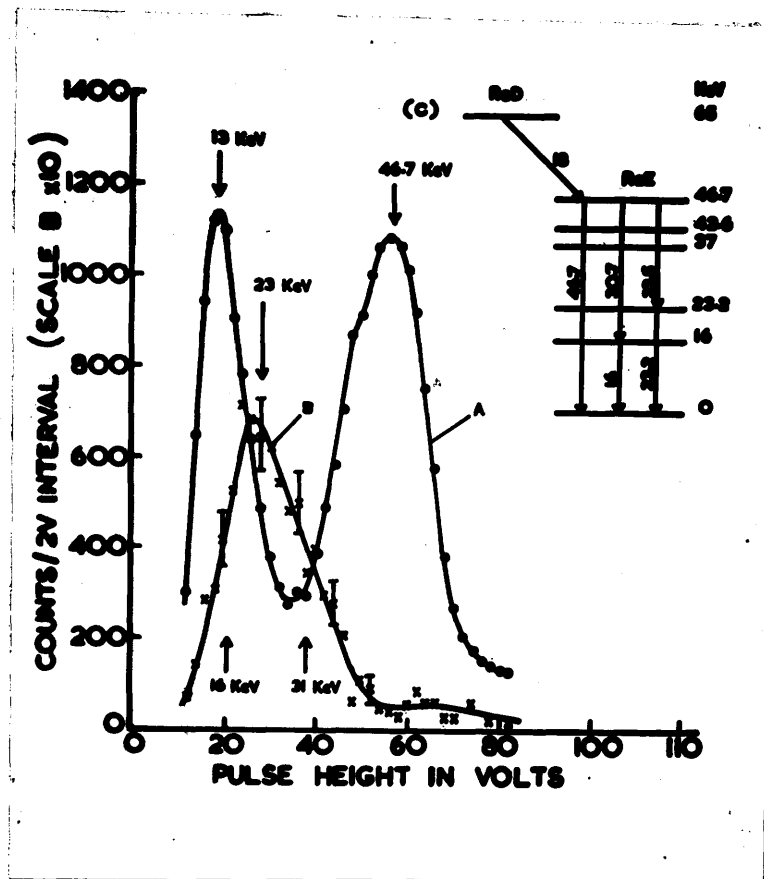

Figure V.10.

(a) The γ-ray distribution from RaD as observed in either counter of the γ-γ coincidence arrangement, showing the main γ-ray peak at 46.7 keV and the X-ray peak at $\sim$ 13 keV.

(b) The spectrum of γ-rays producing γ-γ coincidences.

(c) The suggested decay scheme for RaD, showing the main transitions involved in β-γ and γ-γ coincidences.

The spectrum of coincidences as observed for the case of minimum bias on both channels ($\sim$ 7 keV) is shown in Figure V.10b, and the γ-spectrum observed in each counter is shown on the same energy scale for comparison. We see that the distribution centres round about 23 keV and the "wings" extend to about 16 keV and 31 keV. With these facts in mind and following the sum rules noted by Feather we have tried in Figure V.11 to set forth a possible level scheme. It is difficult to avoid putting in the three top levels at 46.7, 42.6 and 37 keV. Then with two more, and here the choice is rather arbitrary, we can fit all the observed data on γ-radiation as shown. The value 23.2 keV has been chosen as a level since this gives a very close doublet (23.2 + 23.5 = 46.7) and would if necessary almost entirely explain the form of the γ-γ spectrum. Actually coincidences of the type 30.6 + 16.1 would fit well with the wings on the γ-γ curve.

The Integrated Spectrum.

The 4π integrated spectrum was taken with a source clamped between two rectangular blocks (1 x 1 x 0.5 cm^3.) of NaI(Tl) as described previously (see Figure V.1). The source of RaD was prepared by the method described by Cranberg (1950). RaD in the form of $PbCl_2$ is dissolved in doubly distilled water and about 1 cc. is allowed to stand in a small test-tube for 24 hours. A few drops are then

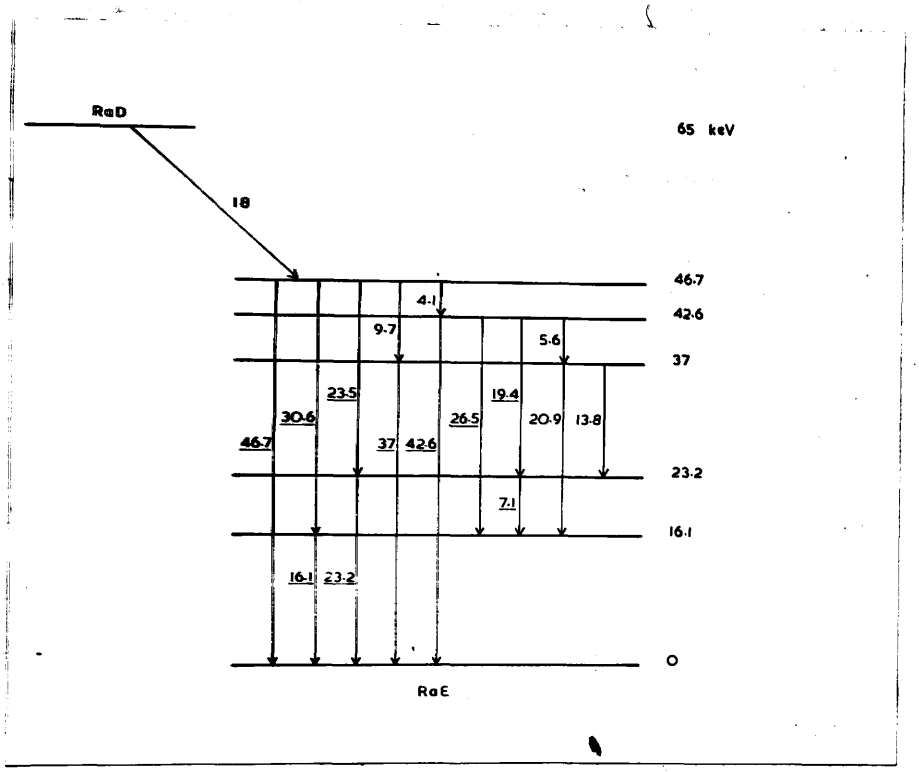

Figure V.11.

The proposed decay scheme of RaD, showing all possible Υ-ray transitions. All previously observed Υ-rays can be fitted into this scheme and are shown underlined.

taken from the surface with a micro-pipette. Sources prepared in this way were found to contain less than 5% of RaE+F. The source was spread onto a thin film of nylon with 10% insulin solution and had a thickness of less than 0.1 mg/cm^2.

In the absence of any time lags greater than the resolving time of the amplifier system ($\sim$ 1 μsec.) we would expect practically no pulses in the spectrum till we reached an energy of about 47 keV, since the various radiations from the different excited levels of Figure V.11 would produce effectively coincident light emission in the NaI(Tl) and would add up. It is hence revealing to find that the spectrum takes the remarkable form shown by the curves of Figure V.12, where the expected hollow at the low energy end is entirely absent. The form down to the lowest energies that could be examined is shown in Figure V.12b, where it is seen that the final sharp rise at $\sim$ 4 keV is only partly due to photomultiplier noise. Detailed examination of the higher energy region showed the end-point to occur at about 78 keV. This, when corrected for the resolution of the counter at this energy ($\sim$ 25%), gives a true end-point at 65 $\pm$ 3 keV. This is therefore the total disintegration energy and it would indicate a β-transition of $\sim$ 18 keV leading to the 46.7 keV excited level.

The shape of the integrated spectrum seems to force the conclusion that at least one of the excited levels shown

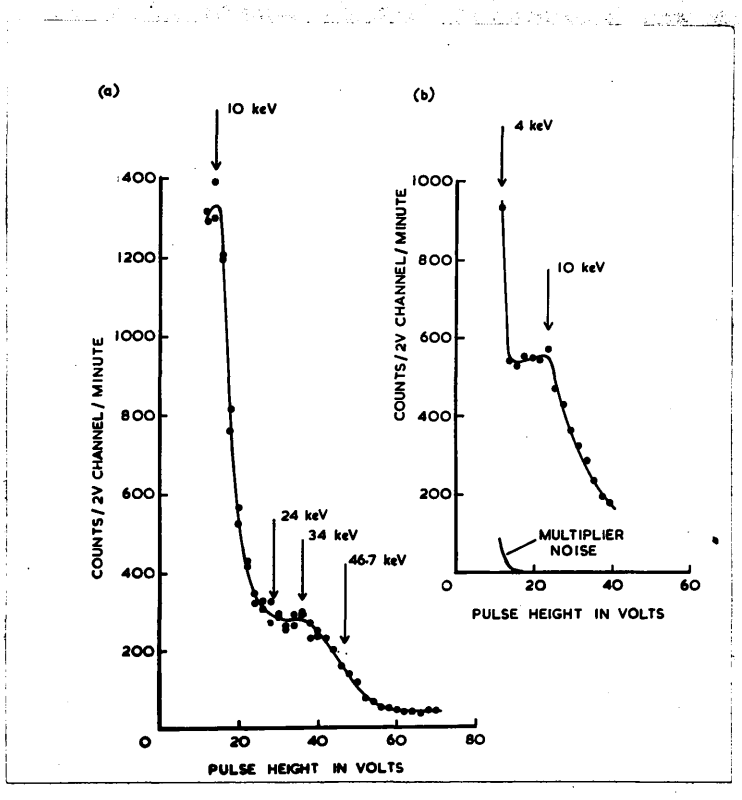

Figure V.12.

(a) The RaD integrated spectrum, showing the form of the curve below ~ 47 keV.

(b) The form of the integrated spectrum down to photo-multiplier noise level at ~ 4 keV.

in Figure V.11 is metastable, with a life-time exceeding 1 μsec. It is of course possible that all, except that at 46.7 keV for which separate evidence is given later, have life-times of this order or greater. There would be nothing remarkable in this since at the extremely low energies involved (~ 20 keV) a life-time exceeding 1 μsec. is expected theoretically for spin changes $\Delta L \geq 2$. If we proceed with the simplest interpretation of the results assuming only one level with life-time > 1 μsec. the form of the curve suggests that the level at 37 keV is metastable. The spectrum of β-rays would in this case be carried forward as indicated by about 10 or 11 keV and would terminate in the region of 30 keV. This is indeed more or less compatible with the curves but it leaves the sharp rise at very low energies to be explained. If the 42.6 keV level is likewise metastable with a life-time > 1 μsec., we would have the explanation of this final rise on the curve. This second metastability, like the first for the 37 keV level, is not incompatible with the results on the γ-γ coincidences. These γ-γ results are a useful guide in allocating the metastability as they make it unlikely that the 16.1 and 23.2 keV levels are involved.

The β-γ Coincidence Spectrum.

A separated source S of RaD, like that described above, was placed against a thin crystal A of anthracene (Figure V.13,

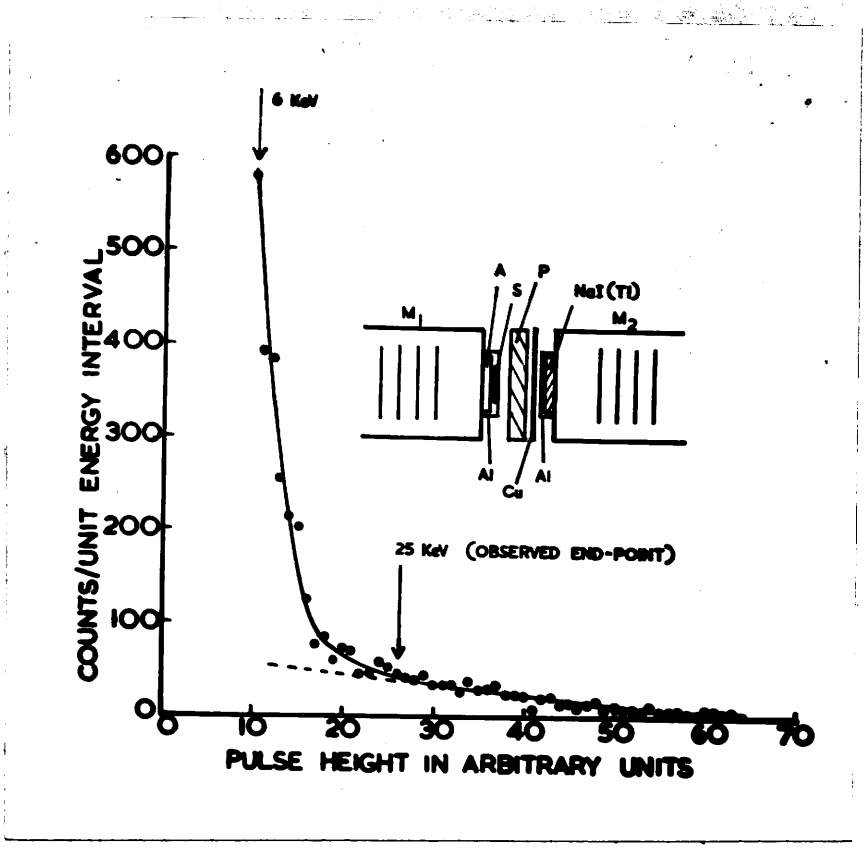

Figure V.13.

The primary β-spectrum of RaD, isolated by coincidence with γ-rays of energy > 40 keV. Inset:- The coincidence arrangement employed in obtaining the primary β-spectrum.

inset) and separated from a second crystal of NaI(Tl) by the aluminium reflector Al, an 1/8 in. sheet of polythene P and a 2 thou. foil of copper Cu. This second crystal was used to detect the harder Υ-radiations (> 40 keV) of RaD. The first accepted all particles and radiations but was relatively transparent to most of the X- and Υ-radiation. The coincidences of the pulses in the two counters were used to control the kicksorting system. The spectrum of pulses from the anthracene crystal thus selected is shown in Figure V.13. The curve covers the energy range 6 to 60 keV and shows an end-point at 25 $\pm$ 2 keV. This value, when corrected for the resolution of the counter in this energy region ($\sim$ 50%), yields a true end-point of approximately 18 keV. The total energy involved in the coincidence ($\sim$ 47 + 18 = 65 keV) agrees with the results from the integrated spectrum.

The long tail is somewhat marked but is believed to be "background", although its origin is rather obscure. Some of it doubtless is due to Υ-radiation in the room and to cosmic radiation, while a little can be ascribed to the source-contaminating β-rays of RaE (1.17 MeV) producing bremsstrahlung in their passage through the anthracene, this in turn being detected by the NaI(Tl) crystal. This effect was very marked when NaI(Tl) was used as the β-ray detector, due to the increased atomic number of the elements in the crystal. Indeed in this case "real

coincidences" were detected up to an apparent β-ray energy of ~1 MeV, and it was impossible to observe the true RaD β-spectrum.

The form of the spectrum agrees, within the rather wide limits of experimental accuracy, with that expected for an allowed β-transition (E_o = 18 keV, Z = 82), and from the theoretical shape it can be shown that about 20 - 30% of the spectrum must lie above 6 keV. The results of Richardson and Leigh-Smith (1937) and Falk-Vairant, Teillac and Victor (1951) are in reasonable agreement with this. The former authors deduce from cloud chamber observations that ~ 40% of the β-spectrum must lie above 5 keV, while the latter estimate from coincidence absorption measurements that up to 15% lies above 8 keV. A more detailed examination of the β-spectrum of RaD has been carried out in this Department by Insch, Balfour and Curran (1952) using a 2π source geometry with gas-filled proportional counters. These authors find an end-point at 18 ± 2.5 keV for the β-spectrum, and obtain good agreement between the observed shape and that calculated on Fermi theory for an allowed transition. Evidence is also found which supports the suggestion of two γ-rays of ~ 23 keV in cascade.

Some attempts were made to study the number of β-γ coincidences as a function of the bias level on the NaI(Tl) side of the system. Setting this to pass successively all radiations harder than 38, 44 and 49 keV, the ratio of

coincidences to γ-rays counted in the NaI(Tl) had the values 1/19, 1/20 and 1/16. This is roughly constant but on the whole favourable to the view that the hardest radiation (46.7 keV) is linked with the β-rays while the others (42.6 and 37 keV) are not. Since for other reasons we tend to give these levels life-times > 1 μsec., this is agreeable. The actual value of the ratio is low but checking approximately by making allowance for the solid angles for the β-rays and γ-rays and for the presence of non-coincident radiations, together with the fact that only β-rays of energy > 6 keV are detected, we find that it is well within a factor of 2 of the required number.

A cable giving a delay of ~ 3 μsec. to the β-ray or γ-ray channel was found to cut down the number of coincidences to the random value. The β-γ coincidences are thus confirmed to be time-coincident to well within 3 μsec., indicating that the life-time of the 46.7 keV level is certainly less than this.

Conclusion.

This work shows that the decay scheme of RaD is indeed extremely complex, although at present the proposed form given in Figure V.11 is consistent with all the above observations and, so far as is known, with those of other investigators. The metastability of at least one of the levels between ground and 46.7 keV seems to be established

with certainty and it adds considerably to the difficulties of fully investigating the radiation. The scheme is capable of explaining the fact that ~~β-radiations seem to be emitted in, on the average, 70% of the disintegrations~~ not more than 70% of the disintegrations appear to be converted in the L₁ shell. (Kinsey 1948), since clearly the transitions from 46.7 keV to ground may take place in such a cascade form that the γ-rays are all too soft to convert in the L-shell. Additional M-shell conversion is to be expected.

It is to be noted that our results do not rule out the possibility that β-rays of energy > 18 keV are emitted leaving the RaE nucleus excited in levels below 46.7 keV, and further work on the lines of the above β-γ coincidence method using γ-rays of precise energy as the coincidence control should help to solve this question. Further refinements to the experimental methods which will assist are possible. For example the 4π integrated spectrum can be examined as a function of the resolving time of the circuits. The lengthening of this time should make all pulses appear time-coincident and by modifying the spectrum form suggest more definitely the delayed radiations and give a measure of the life-times themselves.

In conclusion it can be said that the decay scheme given here, although offerred with a certain degree of reservation, is probably as simple as any capable of satisfying the experimental findings, and the actual mode

of disintegration when fully understood is likely to be at least as complex. The difficulties of investigating the extremely soft electron and electromagnetic radiations are considerable but further work with the existing techniques and some modifications of them should add more to our knowledge.

Since the work described above was completed, Butt and Brodie have investigated the electron emission down to very low energies and have detected additional weak lines ranging from about 7 to 12 keV. Their results would not appear to be discordant with any of the above findings. The tentative decay scheme of Figure V.11 differs from that given by them (see Feather 1949), and further experiments are necessary to decide which is correct. The decay scheme of Figure V.11 satisfies more readily the experimental results on γ-γ coincidences.

4. The Decay Scheme of Sm^{153}.

The investigations and results described here consist in the main of original work, although the writer is indebted to Dr. S.C. Curran for helpful suggestions and discussions. An account of this work has been submitted for publication (Bannerman 1952).

Introduction.

Previous work on the short-lived isotope of Samarium (47-hour Sm^{153}) is summarised in Nuclear Data (1950). Two main features of the decay, a γ-ray of energy $\sim$100 keV and a β-ray of energy $\sim$ 800 keV, have been well established by earlier workers. Hill (1948) in a study of the internal conversion electrons from Sm^{153} found conversion lines attributable to two γ-rays of energy 69.5 and 103 keV. Burson and Muehlhause (1948) found the end-point of the β-spectrum at 780 keV and γ-rays at 110 keV and 610 keV. From coincidence measurements they deduced the presence of an almost totally converted level in Eu^{153} in cascade with the 110 keV γ-ray and of energy less than 100 keV. The decay scheme incorporating these results (Nuclear Data 1950) is shown in Figure V.14a.

Later work by Hill and Shepherd (1950) shows only the presence of one γ-ray of energy 101.5 $\pm$ 0.3 keV, but shows two β-rays of energy 800 $\pm$ 10 keV and 680 $\pm$ 10 keV respectively. This difference corresponds to the γ-ray

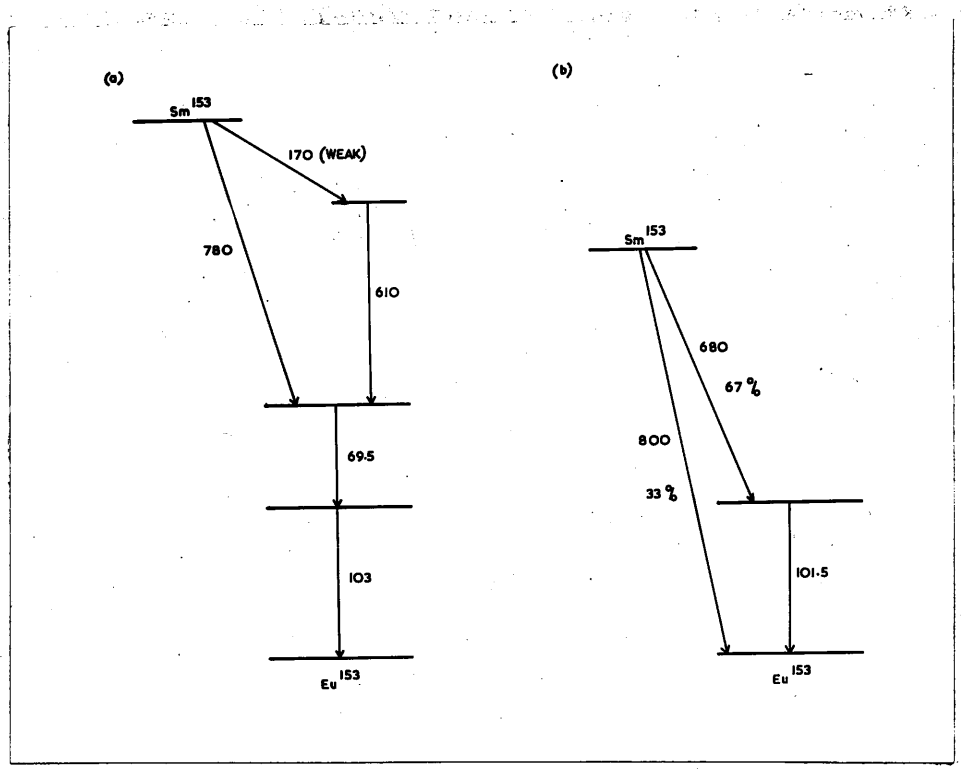

Figure V.14.

(a) The decay scheme of Sm^{153} proposed by Muehlhause.

(b) The decay scheme of Sm^{153} proposed by Hill and Shepherd.

In both schemes all energies are expressed in keV.

energy within the limits of experimental error, and would indicate a decay scheme of the form shown in Figure V.14b.

The integrated spectrum technique offers here an excellent means of distinguishing between the two proposed decay schemes. All γ-ray transitions, apart from the weak 610 keV one, are of low energy and the unconverted γ-rays as well as the X-rays arising from internal conversion will be almost 100% absorbed within a small NaI(Tl) crystal. The total disintegration energy, apart from that carried away by the neutrino, should therefore be trapped inside the crystal. We would then expect the observed spectrum to have one of two forms:-

(a) a β-spectrum of 780 keV carried forward in energy by $\sim$ 170 keV and giving an end-point at 950 keV (see Figure V.14a).

(b) two superimposed β-spectra, one extending from zero energy up to 800 keV and the other from $\sim$ 100 keV up to 800 keV (see Figure V.14b).

These two forms will be easily distinguishable and the observed spectrum shape should act as a test of the validity of either decay scheme.

The Integrated Spectrum.

The Sm^{153} was obtained by irradiating a sample of Sm_2O_3 powder in the Harwell pile. A thin source was prepared from this by evaporating to dryness a drop of samarium

nitrate spread on a nylon film with 10% insulin solution. The source thickness was estimated to be $\sim 5\ \mu g/cm^2$. The nylon film was then firmly clamped between the two cleaved halves of a 1 cm^3. crystal of NaI(Tl), and the whole surrounded by a thin layer of paraffin and an aluminium foil reflector. The crystal system was mounted on the photocathode of an E.M.I. 5311 photomultiplier tube and surrounded by 2 in. of lead shielding. The output from the multiplier was amplified and examined on the single-channel kicksorter.

The end-point of the spectrum was found to be at 800 ± 20 keV. The total disintegration energy of the transition is therefore ~ 800 keV in agreement with the decay scheme of Hill and Shepherd (Figure V.14b). The shape of the low energy region of the spectrum is shown in Figure V.15. All the features of the curve decayed with a 47-hour half-life, and so must be attributed to Sm^{153}. The main peak at 100 keV further confirms the scheme of Hill and Shepherd, but the other features indicate that the final decay scheme is more complex than their results suggest. In particular another energy level at ~ 170 keV appears to be indicated.

The γ-Ray Spectrum.

The γ-ray spectrum was examined with a NaI(Tl) crystal ($1 \times 1 \times 0.5$ cm^3.) surrounded by a thin film of paraffin and

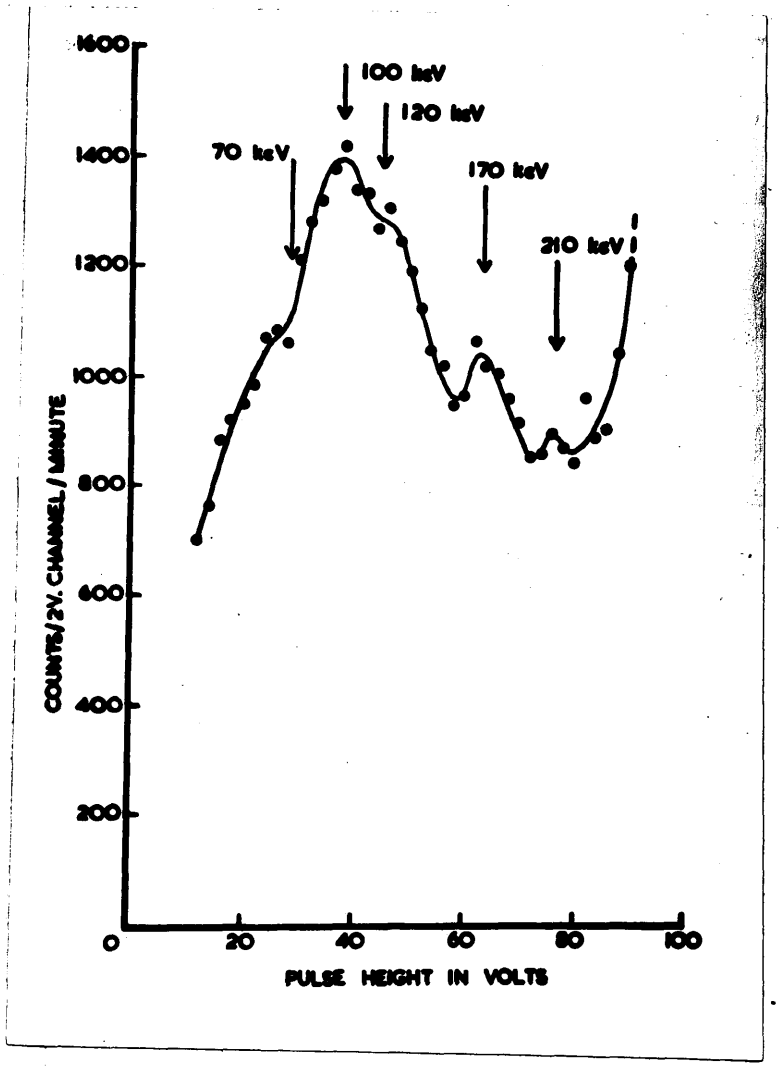

Figure V.15.

The low energy region of the Sm^{153} integrated spectrum, showing the complex nature of the curve. The final rise is produced by high energy pulses saturating in the amplifier.

an aluminium foil reflector, and mounted on an E.M.I. 5311 photomultiplier tube. The source was a small sample of Sm_2O_3 powder placed a few cm. from the crystal. The γ-ray beam from the source was uncollimated and the β-rays were screened off by Al absorbers.

The spectrum obtained (Figure V.16) showed two main peaks, one at 101 $\pm$ 2 keV and the other at 42 $\pm$ 0.5 keV. The first was calibrated with the 192 keV γ-ray line from In^{114} and the 73 keV X-rays from Hg^{203}. An accurate calibration of the second line was obtained using the 46.7 keV γ-ray line from RaD. This second line is obviously the X-ray arising from internal conversion in the K-shell of the product element Eu (energy of the Eu $K\alpha_1$ X-ray = 41.5 keV). A small peak was also found at $\sim$10 keV which decayed with the 47-hour half-life of Sm^{153}. It was shown by absorption measurements that this line could not be emitted by the source and it must therefore be an "iodine escape peak" (West, Meyerhof and Hofstadter 1951) produced in the crystal by the 41.5 keV X-rays. No evidence was found of any γ-rays above an energy of 101 keV, although a careful search was made in the 600 keV region. If a γ-ray of energy 610 keV is present its intensity must be less than 0.005% of the main transitions. The figure quoted for the intensity by Burson and Muehlhause (1948) is 0.003%.

In three different γ-ray distribution curves taken, the

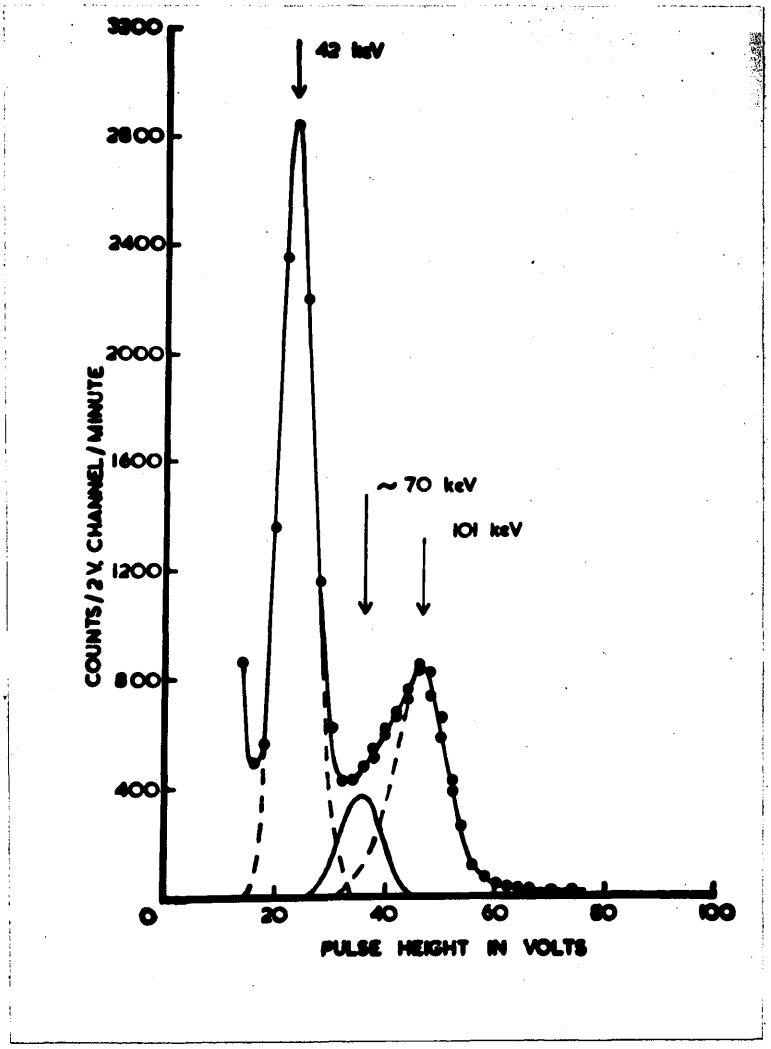

Figure V.16.

The γ-ray spectrum of Sm^{153}, detected in a small NaI(Tl) crystal. The peak at ~ 70 keV is obtained by subtracting symmetrically drawn curves for the 101 keV and 42 keV peaks (shown dotted) from the total spectrum.

101 keV γ-ray line showed an asymmetry on the low energy side of the peak, in contrast to the X-ray line which was symmetrical in all cases. If this asymmetry is assumed to be due to neither of the two lines, then subtraction of symmetrically drawn curves from the observed shape of the spectrum gives a small intermediate peak of energy about 70 keV (Figure V.16). This is most probably due to unconverted γ-rays from the reported 69.5 keV transition (Hill 1948).

The relative intensities of the γ-ray and X-ray lines, after correction for absorption, are shown in Table V.3. The value given for the 41.5 keV X-ray line includes the intensity of the 10 keV "iodine escape peak", which amounts to about one-fifth the intensity of the main X-ray peak. The intensity attributed to the 69.5 keV unconverted γ-ray line is not very accurate because of the method used in its estimation.

Table V.3.

γ- or X-Ray Energy	Relative Intensity
610 keV	< 0.005 %
101	26
69.5	4 ± 2
41.5	70

The γ-γ Coincidence Spectrum. /

The γ-γ Coincidence Spectrum.

If there is another highly converted transition in cascade with the 101 keV γ-ray, coincidences should be obtained between the X-rays from this transition and γ-rays and X-rays from the 101 keV transition. A small number of γ-γ coincidences should be observed as well if the cascade γ-ray is not totally converted. A search was made accordingly for such coincidences using two scintillation counters symmetrically arranged with respect to the source, each one being similar to the counter used in examining the γ-ray spectrum.

Coincidences were observed which decreased in number by a factor ~ 6 as the discriminator bias in one channel was increased beyond the X-ray energy of 41.5 keV. When the discriminator bias was increased beyond 100 keV the number of coincidences dropped to the random rate, showing that no false coincidences were being produced by bremsstrahlung from the screened out β-particles.

With the discriminator in one channel set to pass only 101 keV γ-ray pulses, a distribution curve was taken of the quanta giving rise to coincidences with the 101 keV γ-ray. This consisted of a single peak which coincided exactly with the Eu K X-ray peak. It was calculated from the geometry that one in every three 101 keV γ-quanta was accompanied by an X-ray in coincidence. Thus about 70% of the total K X-ray intensity is due to internal conversion of the 101 keV

γ-ray, the remaining 30% arising from the 69.5 keV transition. Allowing for the fluorescence yield in the K-shell of Eu and also for L-conversion (K/L~5/1, Hill and Shepherd 1950), a value $\alpha \sim 3$ is then obtained for the internal conversion coefficient of the 101 keV γ-ray. This result is in good agreement with the value $\alpha > 2.5$ given by Hill and Shepherd. No separate peak due to the 69.5 keV γ-ray was observed in the coincidence spectrum, but an upper limit of one-tenth the K X-ray peak can be given for its intensity, if present. This implies a value $\alpha > 10$ for the internal conversion coefficient - considerably greater when L-conversion is also taken into account.

The β-Ray Spectrum.

In examining the β-spectrum it is necessary to use a geometry giving a small solid angle, so that the number of coincidences from the source recorded in the counter is reduced to a negligible fraction of the total counting rate. This ensures that the true end-point of the spectrum is observed. A comparison of this result with the end-point of the integrated spectrum should decide whether there is a β-ray going directly to the ground state, or whether the most energetic β-ray leads to one of the excited states of Eu^{153}.

The β-spectrum from Sm^{153} was examined using the same crystal of NaI(Tl) as was used for the γ-ray spectrum.

Anthracene is normally preferable to NaI(Tl) because of its greater transparency to quanta, but in this case the highest γ-ray energy is well below the maximum of the β-spectrum and the greater ease involved in obtaining an accurate calibration of NaI(Tl) in the 1 MeV region is very desirable. The photoelectron peak from the 1.11 MeV γ-rays of Zn^{65} was used to calibrate the energy scale.

The source was prepared by evaporating to dryness a thin film of samarium nitrate in aqueous solution onto an aluminium foil, previously "wetted" with NaOH solution. The source thickness was again ~ 5 $\mu g/cm^2$. The whole counting system was surrounded by 2 in. of lead shielding, which reduced the background in the absence of the Sm^{153} source to 7 counts per minute.

The end-point of the β-spectrum taken under these conditions, with a solid angle $\sim 1\%$ of 4π, was found to be 800 ± 20 keV, in agreement with previous work. This is the same as the end-point found for the integrated spectrum, so the highest energy β-ray must go directly to the ground state of Eu^{153}. It therefore follows that there must be other β-rays of lower energy leading to the excited levels of Eu^{153}. These β-rays can be isolated by β-γ coincidence methods.

The β-γ Coincidence Spectrum.

A geometrical arrangement similar to that previously

used for observing γ-X coincidences was employed. In this case, however, a thin source replaced the Sm_2O_3 powder sample and the amount of absorber between the source and the NaI(Tl) crystal of the β-particle counter was reduced to a minimum. A similar geometry has been described more fully in the previous section on the decay scheme of RaD (see Figure V.13, inset). The whole system was surrounded by 2 in. of lead shielding.

All counts in the β-ray crystal due to γ-rays and X-rays from the Sm^{153} source were excluded by suitable biasing of the discriminator in the β-ray channel. The discriminator in the γ-ray channel was used in a similar manner to allow only counts produced by the 101 keV γ-rays to be recorded. The Zn^{65} 1.11 MeV γ-rays were again used to calibrate the β-ray crystal.

Under these conditions coincidences were observed giving a real-to-random counting ratio of 60/1. The β-ray spectrum obtained when controlled by these coincidences was found to have an end-point at 700 ± 20 keV. This result, taken in conjunction with the figure of 800 keV for the total disintegration energy, indicates clearly that the 101 keV γ-ray transition takes place to the ground state of Eu^{153}. A third β-ray of energy 630 keV must also exist leading to the 69.5 keV transition, but no attempt was made to isolate this.

Conclusion.

The decay scheme which follows from these results is illustrated in Figure V.17, together with approximate values for the relative intensities of the transitions. Referring again to the low energy region of the integrated spectrum (Figure V.15), we see that the proposed scheme can account directly for the peaks at 100 keV and 170 keV, since these will be the "zeros" of the two displaced β-spectra. Because of the method used of clamping a thin spread-out source between two blocks of NaI(Tl), a small fraction of the source material will inevitably be near the edge of the crystal. Thus there will be some escape of radiations due to the imperfect 4π geometry. The shoulders at $\sim$70 keV and $\sim$120 keV on the curve will arise if either a 101 keV γ-ray, or an X-ray from either transition escapes. If a β-particle escapes, the remaining radiation will tend to accentuate the rises at 100 keV and 170 keV. The peak at $\sim$210 keV, however, cannot be accounted for on this scheme. It may indicate the presence of a further excited level in Eu^{153} at $\sim$210 keV above the ground state.

The previous inconsistencies between the two alternative decay schemes have thus been resolved, and it is seen that the resultant scheme is in reality a combination of the two. The power of the integrated spectrum method in deciding between existing schemes and in providing a sound basis for establishing new ones is also well illustrated. An extension

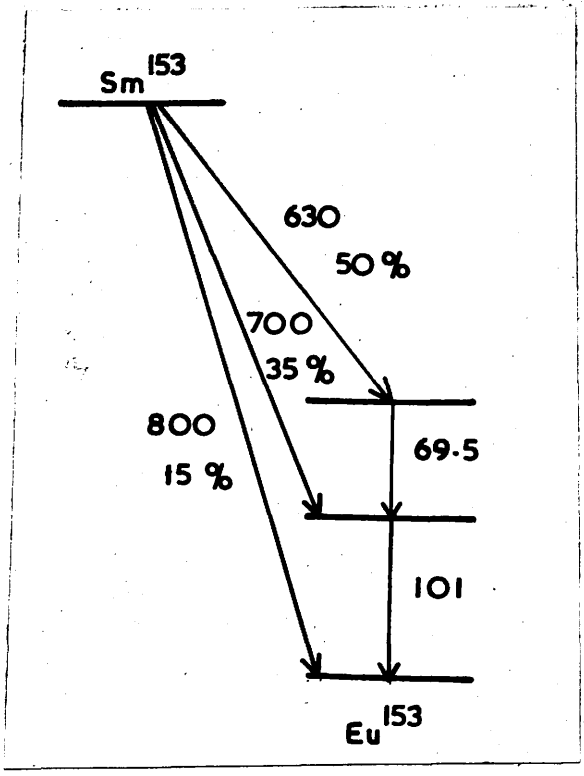

Figure V.17.

The proposed decay scheme of Sm^{153}, based on present work. All transition energies are expressed in keV.

of the present coincidence system should make it possible to isolate the 630 keV β-spectrum, although the almost total internal conversion of the 69.5 keV transition presents a serious problem. Possible transitions from a 210 keV level should also be investigated, but that to the 170 keV level (~ 40 keV) would be difficult to identify in the presence of the X-rays arising from internal conversion.

5. Conclusion.

(a) Improvements in Technique.

The work described in the previous pages has provided a good illustration of the power, as well as the weakness, of this new method of examining radioactive decay schemes. A summary of the advantages and disadvantages of this technique relative to the performance of other types of spectrometers has already been given as part of a detailed description of the scintillation counter (Part III.2c), but in general its superior efficiency is offset by its poorer resolving power, although the latter is often adequate.

An improvement in the resolving power can only be brought about by producing more photoelectrons per pulse at the photomultiplier cathode. This will involve a search for more efficient phosphors or for more sensitive photo-surfaces. It must be remembered however that increased cathode sensitivity is usually accompanied by an increase in thermal emission and hence in the noise level of the tube. Cooling would overcome this, but it represents an additional complexity. An increase in stopping power is also very desirable since this would allow the range of the integrated spectrum technique to be extended. Recent reports by Van Sciver and Hofstadter (1951) on the use of thallium activated CaI_2 and CsI as phosphors hold out some promise in this respect. These phosphors, however, are hygroscopic and still

suffer from the disadvantage of requiring special protective coatings. The alternative is to use liquid phosphors and to compensate for the reduced stopping power by making use of very large counting volumes, but this raises the problem of efficient light collection which is of vital importance in a proportional device.

The more immediate improvements planned are to the succeeding equipment and in particular to the kicksorter. These should enable more detailed information to be extracted from the data already supplied by the counters. Work is being carried out at the moment to make the two-channel system completely symmetrical so that one output is displayed on the X-axis and the other on the Y-axis of the oscilloscope screen. The pulse brightening will still be controlled by the output from the coincidence unit. If now the two counters (X and Y) are looking at a γ-ray source which produces a number of well-defined peaks in the spectrum, we shall obtain the following results. All non-coincident pulses will lie along either the X- or Y-axis at points corresponding to the respective γ-ray energies, and will be unbrightened. Coincident pulses will appear brightened at points whose X- and Y-coordinates correspond to the energies of the two γ-rays producing the coincidence. Thus if we scan the spectrum in the Y-direction as before, but at some suitable distance along the X-axis, we shall obtain the spectrum in coincidence with the γ-ray of the energy which corresponds

to that particular X-displacement. It therefore becomes possible to isolate the spectrum in coincidence with any γ-ray from the source, and this applies equally to β-γ coincidence measurements as well as to γ-γ. The additional advantage this gives in the examination of decay schemes is obvious, although the method is restricted to the region where the photoelectric effect predominates.

The extension of this method to higher γ-ray energies (e.g. to the γ-rays of La^{140}) requires the use of the Compton coincidence spectrometer in place of the single crystal spectrometer. Thus for β-γ work three counters will be needed, and for γ-γ work four. The resultant small solid angles will be a serious drawback. To overcome this disadvantage it is proposed to replace the present detecting crystal by a toroidal detector, consisting of a large "flat" of NaI(Tl) with a hole bored through the centre to allow the passage of the collimated γ-ray beam. It has been calculated that this should give an improvement of more than 10 in the coincidence counting rate without any loss in resolving power. Coincidence work between two such spectrometers should therefore become practicable. In addition to the application mentioned above, it should also be possible to carry out angular correlation studies with γ-rays of $\sim$1 MeV energy by isolating specific γ-rays in each spectrometer. The detection of fourfold coincidences should result in a negligible random background.

(b) Future Work.

The improved sensitivity and flexibility of the technique developed above has demonstrated that the assignment of some decay schemes is rather arbitrary, and is based mainly on the fitting of energy values into a level scheme, without much reference to relative intensities or to coincidence measurements. It would therefore appear to be a profitable, but rather tedious, task to examine systematically all existing decay schemes which rely on other techniques for their information.

In addition to this extension of the technique, a more detailed application of it is also possible. So far, of the three properties of nuclear energy levels, only the energy above the ground state has been determined from measurements of the transition energies. For a complete solution of the problem, the spin and parity of these levels should also be found. These can be obtained by determining the multipole order of γ-ray transitions and the degree of forbiddenness of β-ray transitions. These can be measured in various ways (Moon 1949). For example, the multipole order of a γ-ray transition can be obtained from a knowledge of the energy of the γ-ray, plus either the life-time (involving delayed coincidence measurements), or the values of the internal conversion coefficients, or the determination of angular correlations, etc. Information about β-ray

transitions can be obtained from measurements of the energy and the life-time (plus relative intensity if the spectrum is complex), or from the determination of spectrum shapes. It will be seen that all these measurements require an accurate determination of relative intensities and spectrum distributions and the use of well-defined geometries, particularly in coincidence experiments, in addition to the measurement of energies as previously. Future work should aim at this complete solution of the decay scheme by making use of a more refined and accurate technique.

Appendix I. The Detection of α-Particles.

In this appendix an account is given of some early work on α-particle detection. At that time ϒ-ray detection was still in the purely qualitative stage, and the most obvious application of the scintillation method was to the study of heavy low-energy particles using ZnS(Ag) as a phosphor. In the work described below the writer was employed in the construction of a scintillation counter to be used in conjunction with an α-particle spectrometer. The testing of the counter 'in situ' was carried out in collaboration with members of the group working on the H.T. Set.

1. The Nature of the Problem.

The purpose for which a scintillation counter was required was the detection of short-range α-particles produced in the artificial disintegration of nuclei. The particular reaction under consideration was the bombardment of Li^7 with protons. In this reaction a resonance in the production of ϒ-rays is observed at 440 keV proton energy and at this point the ϒ-ray spectrum consists of two lines at 14.5 MeV and 17.5 MeV respectively. If the compound nucleus (Be^8) is formed in a 17.5 MeV excited state then the 14.5 MeV transition will leave it in a 3 MeV excited state. The Be^8 nucleus may then split up into two α-particles of energy ~1.5 MeV.

The object of the experiment, then, was the detection of a group of 1.5 MeV α-particles. Magnetic resolution was to be employed as a means of determining the α-particle energy, and the scintillation counter was to be used simply as a detector mounted on the end of the resolver. The advantage in using a counter of this type is that the phosphor can be placed inside the vacuum system thus eliminating the problem of thin windows and allowing particles of low energy to be detected. Protons of as low an energy as 17 keV have been counted by this technique using a ZnS screen (Tollestrup 1948). In addition, the phosphor thickness required to stop the α-particles is very small and will have a low efficiency for detecting γ-rays. This is an advantage in such experiments, where low energy particles have to be counted against an intense γ-ray background. It will be seen later that good energy resolution is also required, and it was on this point that the scintillation counter proved unsatisfactory.

2. Description of the α-Particle Counter.

The phosphor used in this experiment was silver-activated zinc sulphide, ZnS(Ag), which is the most efficient of the ZnS phosphors for α-particle detection. Its advantages are a high physical light yield (~ 30%) and a fluorescence spectrum which matches the response of the photomultiplier tube used (R.C.A. 1P21). Further its

response to α-particles is linear over the energy range 0.1 to 5 MeV (Kallmann 1949). On the other hand, the technical light yield is lower because of the high refractive index (2.36) and the poor transparency of the phosphor, which becomes opaque in thicknesses greater than 50 mg/cm^2. However, the range of 1.5 MeV α-particles is less than 2 mg/cm^2. in the phosphor, and that of the Po α-particles used for testing is ~ 8 mg/cm^2., so that the phosphor need only be thick enough to stop these particles. Another drawback is that the phosphor is only available in powder form. This will produce a further decrease in the technical light yield, besides affecting the uniformity of the phosphor response. The decay time of ~ 5 μsec. is slow compared with organic phosphors, but is quite suitable for counting if no coincidence work is involved.

The ZnS(Ag) is mounted on a 1/4 in. thick glass disc which fits into the end of the magnetic resolver and terminates the vacuum system. The phosphor is thus inside the vacuum system while the photomultiplier tube observing it is outside. The phosphor screens are prepared by first spreading a thin layer of Apiezon B oil over the glass and then sprinkling the ZnS(Ag) powder onto this surface. The excess powder is shaken off by tapping and a fairly uniform screen is obtained, approximately one crystal layer thick (~ 10 mg/cm^2.). Examination under a microscope showed that

about 90% of the surface area was covered by ZnS(Ag) crystals. The low pressure oil acts as a binder for the crystals and also ensures good optical contact with the glass disc.

The photomultiplier tube used was an R.C.A. type 1P21. This is housed in a light-proof box which is bolted onto the end flange of the spectrometer. The box is constructed of soft iron to minimise the effect of the stray field of the spectrometer magnet on the photomultiplier tube. The 1P21 is mounted with its photocathode as close to the phosphor screen as possible and a light guide of reflecting Al foil was constructed to bridge the remaining gap ($\sim$ 1 cm.). When, in addition, a reflecting backing of Al leaf was used over the layer of ZnS(Ag), it was estimated that approximately a quarter of the emitted light reached the photocathode.

It was found in practice that the ZnS(Ag) gives off a phosphorescence after exposure to light. This diminishes rapidly at first, but after several hours appears to reach a steady level. In many cases this level is above the noise level of the photomultiplier tube and is the deciding factor in determining the signal-to-noise ratio. For ZnS(Ag) and a 1P21 photomultiplier tube operating at 75 volts/stage, it was found that the phosphor noise level corresponded to 20 keV α-particle pulses and the tube noise to 10 keV pulses. The signal-to-noise ratio should therefore be high for 1.5 MeV α-particles and the statistical component of the pulse-height spread should be relatively small.

3. Experimental Results.

A test of both the resolver and scintillation counter was carried out by examining the α-particles given off in the $F^{19}(p,\alpha)O^{16}$ reaction. This reaction has a resonance at 330 keV proton energy, at which a 1.8 MeV α-particle accompanied by a 6 MeV γ-ray is produced. The γ-rays were detected with a Geiger counter, and the proton current striking the target measured on a current integrator. The ratio of γ-ray counts (N_γ) to proton current was found to be constant, showing that N_γ could be taken as a measure of the number of disintegrations produced, and therefore of the total number of α-particles produced. To compensate for fluctuations in the proton beam during measurements, the ratio N_α/N_γ was used in plotting distribution curves, where N_α is the number of counts from the scintillation counter.

It was found that when the magnetic field was set to focus the 1.8 MeV α-particles onto the phosphor screen, a large number of scattered protons also reached the screen, although their energy was too low for them to come directly through the spectrometer. This effect is presumably due to multiple scattering of the protons at the walls of the spectrometer. The number of protons elastically scattered from the target is, of course, many orders of magnitude larger than the number of reaction particles produced.

An integral bias curve taken at this setting using a discriminator is illustrated in Figure 1 (II). The

α-particles show a tendency to form a plateau just before the sharp rise at about 7 V bias produced by the scattered protons. It should therefore be possible to discriminate against the background of protons by means of their pulse size. However, the pulse-height distribution from the scintillation counter shows rather a wide spread in energy response, and it is not possible to discriminate completely against the protons and yet be certain of detecting the α-particles with 100% efficiency. The poor energy resolution arises from the granular nature of the phosphor and is therefore inherent in this type of counter. The use of the scintillation counter as an α-particle detector on the magnetic resolver was therefore discontinued.

For the sake of completeness it should be mentioned here that this work was continued later with a gas-filled proportional counter in place of the scintillation counter. The window between the counter and the spectrometer consisted of a thin collodion film of about 3 mm. air equivalent thickness (~ 35% of the total α-particle range), which was supported on a grid made by drilling closely spaced 1 mm. diameter holes in a brass plate. The transparency of the grid was 45%. The integral bias curve obtained with this counter, under the same conditions as before, is shown in Figure 1 (I). It will be seen that the energy resolution of the proportional counter is much superior to that of the scintillation counter, and that it is now possible to

discriminate completely against the protons and still count the α-particles with 100% efficiency. This result, however, is only achieved at the expense of a reduction in the effective solid angle of the spectrometer by a factor of 45% due to the presence of the grid supporting the counter window.

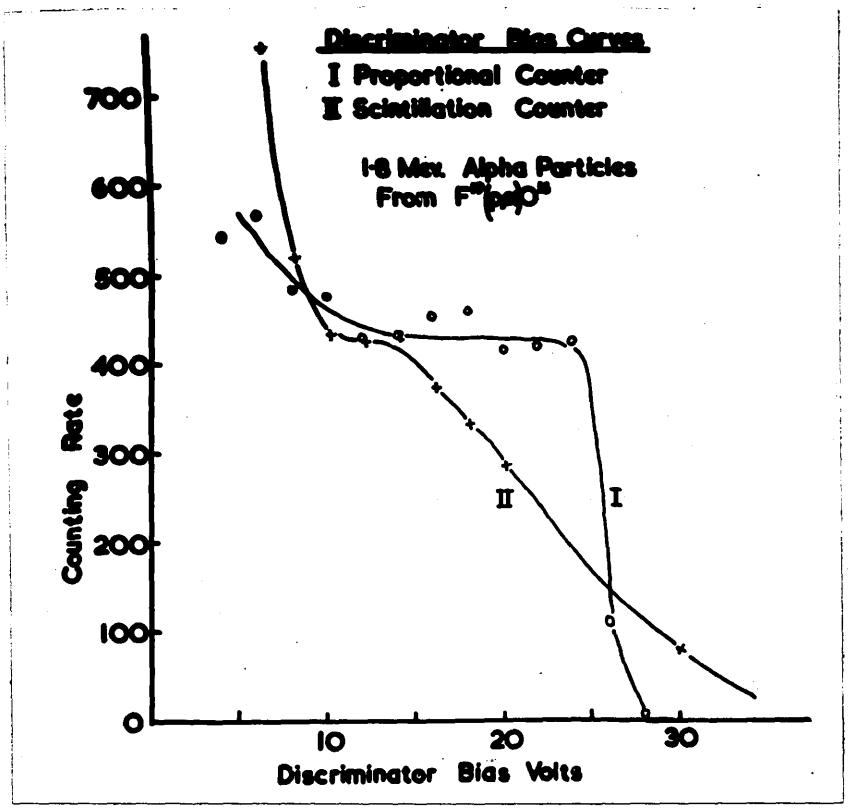

Figure 1.

Integral bias curves of 1.8 MeV α-particles observed (I) with a proportional counter, and (II) with a scintillation counter. The sharp rise below ~7 V bias is produced by scattered protons.

Appendix II. The Cleaning of Phosphor Crystals.

In order to obtain the best performance from a scintillation counter used in spectroscopic work, it is essential to see that the phosphor crystals are absolutely clean and optically transparent. This ensures that the maximum uniform light output, and hence the maximum signal-to-noise ratio and energy resolution, is obtained. Because of the importance which is attached to this point, some effort was made to find the most efficient method of cleaning for each different phosphor used. An account of the methods evolved by the writer for this purpose is given below. Mention is also made of any precautions necessary for storage and of the techniques employed in cutting and shaping the crystals. Of the phosphors listed, NaI(Tl) and anthracene have been used extensively, whilst the others mentioned were investigated but found to be inferior by comparison.

Silver-Activated Zinc Sulphide, ZnS(Ag).

Crystals of ZnS(Ag) are extremely difficult to produce in any appreciable size, even with large technical resources at one's disposal. This phosphor is usually obtained, therefore, as a coarse crystalline powder of grain size $\sim 40\ \mu$. It is highly stable and cleaning is not normally necessary, since phosphor screens are usually made up as required with fresh powder.

Scheelite, $CaWO_4$.

Crystals of calcium tungstate occur naturally as the mineral scheelite. They can also be grown artificially, and the latter form is preferable for scintillation work since perfectly clear regular crystals can be produced. Scheelite is chemically stable and very hard, so that after the initial grinding and polishing, the crystals can be kept clean merely by rubbing with a soft cloth or by immersing in any suitable solvent.

Naphthalene.

Naphthalene is chemically stable but has a high vapour pressure for a solid and if it is to be kept for more than a few days must be stored in an air-tight vessel. It is rather soft and is readily cut to a desired shape with a razor blade. Cleaning can be effected by a number of solvents, xylene in particular, but due to the high rate of evaporation of naphthalene the surfaces become dull again in a matter of minutes. Some attempt was made to overcome this by coating with solutions of perspex or distrene, but this was not very successful since the solvents also attacked the naphthalene. However, because of its low energy response compared with anthracene and NaI(Tl), naphthalene was not used much after these other phosphors became available commercially, and this problem ceased to be of importance.

Anthracene.

Anthracene crystals are stable in the ordinary atmosphere and so present no problems either of storage or of mounting. The vapour pressure is low and so loss due to evaporation is negligible over a period of years, and is much less than that involved in cleaning with solvents. Anthracene can be kept uncovered in vacuum for several days without appreciable loss provided the vessel is not too large and pumping is not continuous. It is more brittle than naphthalene and reasonable care must be taken in handling to avoid scratching or cracking the crystal. It can still be cut to a required shape fairly readily with a razor blade. Anthracene is best cleaned by immersing in chloroform for a minute or less, until all the crystal surfaces look perfectly clear. If the crystal is then removed from the chloroform and allowed to dry off with the minimum of handling, a clear surface having a highly-polished appearance is obtained. Other solvents (xylene, benzene, etc.) can be used for cleaning but they do not leave such a clear finish on the crystal.

Thallium-Activated Sodium Iodide, NaI(Tl).

Thallium-activated sodium iodide is hygroscopic and so requires to be kept out of contact with moist air at all times. Crystals are kept under liquid paraffin and also mounted on the photomultiplier tubes surrounded by a layer

of paraffin, which is usually maintained round the crystal by the close fitting Al foil reflector. The action of moisture on the crystal produces a yellow discolouration which can be cleaned off again and is therefore purely a surface effect. It is believed to be due to the liberation of free iodine by the action of light on the thin film of NaI solution formed on the crystal surface. This is supported by the fact that a solution of NaI can be kept in darkness without any change in colour but immediately turns yellow on exposure to light. Light was found to produce no observable change in NaI in the solid state.

NaI has a cubic structure and consequently has three planes of cleavage mutually at right-angles. It is a soft material and can be cut easily with a razor blade, but tends to be brittle in small pieces because of its cleavage planes. It is best shaped by cleaving rather than by cutting or sawing. A sharp-bladed instrument such as a wood chisel has been used successfully, and cubes and other rectangular shapes easily and quickly produced. All these operations should be carried out under liquid paraffin. It is also possible to machine crystals of NaI(Tl) if slow cutting speeds are used. In this Department a 1/2 in. diameter hole has been successfully drilled through the centre of a large block of NaI(Tl) for use in the Compton coincidence spectrometer.

Cleaning can be carried out with either acetone or ethyl alcohol, but both these liquids are immiscible with the liquid paraffin in which the NaI(Tl) is stored and this presents difficulties, particularly with small plate-shaped crystals. Either some paraffin remains on the crystal when it is put into the solvent and prevents portions of the surface from being cleaned or, when the crystal is returned to the paraffin, some drops of solvent remain on the surface and turn yellow in a few minutes because of the dissolved NaI they contain. The most successful method evolved so far for overcoming these difficulties makes use of an intermediate liquid which is miscible with both liquid paraffin and the solvent. Many liquids satisfy this criterion but only one was found to be suitable for each solvent in this particular case. The methods used can be illustrated as follows:-

(1) Paraffin → Amyl acetate → Acetone → Amyl acetate → Paraffin.

(2) Paraffin → Benzene → Alcohol → Benzene → Paraffin.

Of the two methods evolved the former is preferred. Initially the NaI(Tl) crystal is immersed in the paraffin in which it is normally kept. The crystal is then transferred to a vessel, usually a specimen tube, of amyl acetate and shaken up gently to remove the coating of paraffin. The amyl acetate has no observable action on the NaI(Tl) during the short period for which the crystal and amyl acetate are in

contact. The crystal is next transferred to the acetone where the actual cleaning takes place. The action is fairly rapid and, unless the crystal is very dirty, requires only a few seconds. The film of acetone clinging to the crystal is washed off in the next stage and in the final stage the amyl acetate is absorbed into the paraffin and mostly evaporates off from the surface. The crystal can then be transferred to a vessel of pure paraffin, if desired. At all times touching the crystal by hand must be avoided, and normally small forceps are used for manipulation. This method of cleaning has been found to be quick and reliable, and to involve the minimum handling of the crystal. Its only disadvantage lies unavoidably in the gradual dissolving away of the crystal of NaI(Tl).

Appendix III. Electronic Equipment.

In this appendix a more detailed account is given of some of the electronic equipment which was made up in this Department and used with the scintillation counter. No degree of originality is claimed for any of the circuits, although modifications had to be made in many cases in order to obtain a satisfactory performance. In particular, an appreciable amount of work was carried out on the kicksorter before it could be used as a reliable instrument.

The Coincidence Unit.

The circuit for this unit is shown in Figure 1. It is based on the Rossi circuit and consists of a 6SN7GT double triode (V_1 + V_2) which inverts the positive outputs of the two discriminators before applying them to the grids of the two EF50 valves (V_3 and V_4) which make up the Rossi pair. The positive output from the common anode load is fed out through a biased-off cathode-follower valve (V_5). This bias is adjusted so that only coincidence pulses appear at the output of the unit. A 1 K load is used across the input of channel 2 to match the characteristic impedance of the 3 μsec. delay line which is inserted when the random coincidence rate is being determined (see Figure III.3a). As this load would provide too large a pulse for the coincidence unit, a potentiometer is used and the setting adjusted to

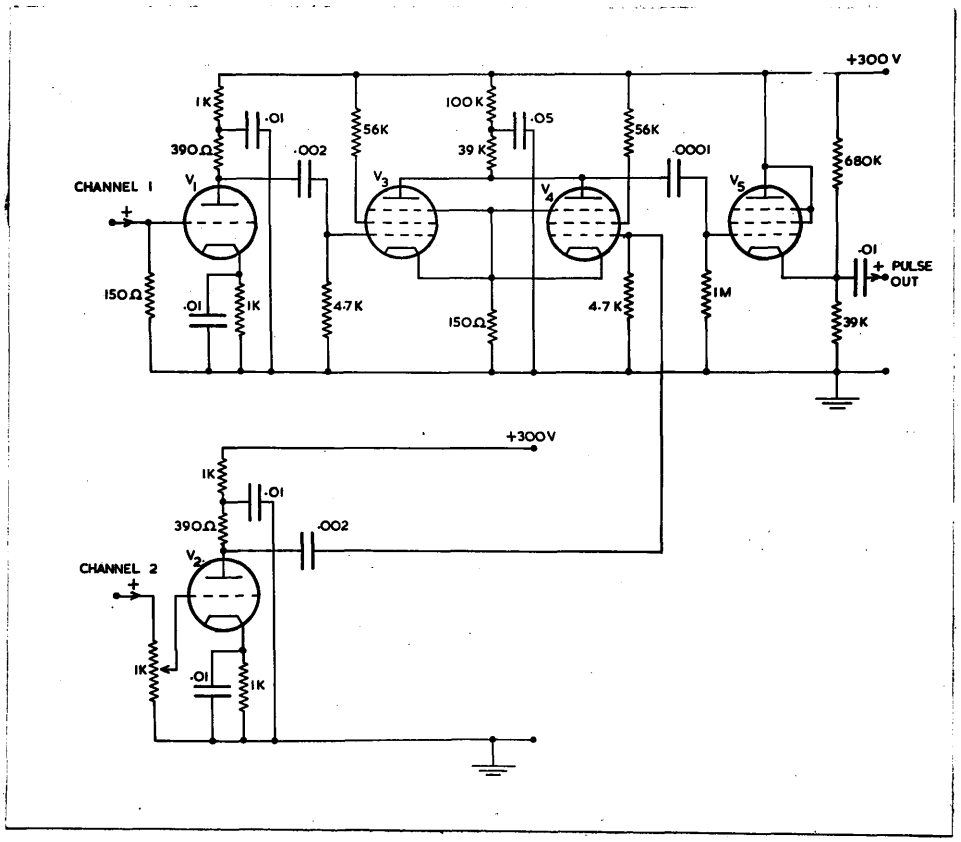

Figure 1.

The coincidence unit circuit diagram. V_1+V_2 = 6SN7GT: V_3, V_4, V_5 = EF50's.

make the input pulses in both channels equal. The resolving time was determined by feeding two independent random sources of pulses into the inputs and measuring both input counting rates and the coincidence counting rate. If the two input rates are N_1 and N_2 counts/sec. respectively, then the coincidence counting rate (N_{12} counts/sec.) is given by $N_{12} = 2N_1N_2\tau$, where τ is the resolving time of the coincidence unit in seconds. The value of τ found by this method was 0.5 μsec.

The Single-Channel Kicksorter.

The circuits of the two units, the pulse lengthening unit and the pulse brightening unit, are shown in Figure 2a and 2b. A brief outline of their functions has already been given in Part III.1b. The pulse lengthening unit consists essentially of a cathode-follower input valve (V_1) and a phase-splitting valve (V_4) which provides a push-pull output via the two cathode-followers V_5 and V_6. The grid of the valve V_4 is connected to the H.T.- line through the pentode V_3 which is normally just running. If now a negative pulse is applied to the grid of V_3, immediately after the arrival of a positive signal pulse on the grid of V_4, V_3 is cut off and because of the diode V_2 the grid of V_4 becomes completely isolated. The grid of V_4 remains at the maximum potential of the signal pulse just as long as the negative signal is applied to V_3. The output pulses are therefore lengthened

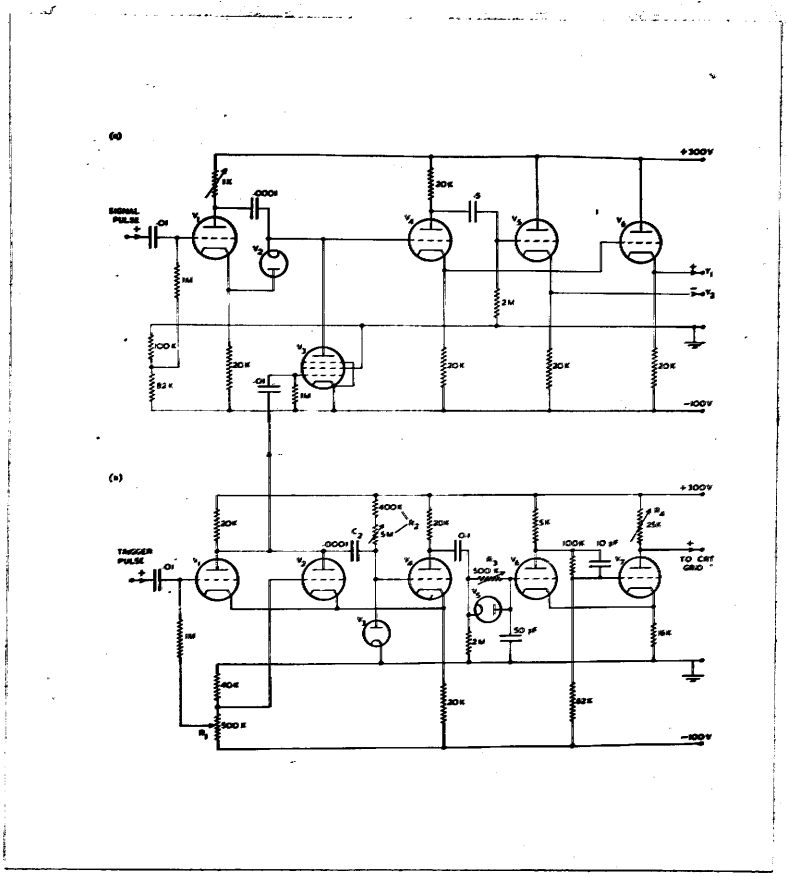

Figure 2.

The kicksorter circuit diagram.

(a) The pulse lengthening unit. V_1 = EF55: V_2 = VR92: V_3, V_4, V_5, V_6 = EF50's.

(b) The pulse brightening unit. V_1, V_2, V_4, V_6, V_7 = EF50's: V_3+V_5 = VR54. R_1 = trigger bias control: R_2 = pulse length control: R_3 = brightness delay control: R_4 = brightness amplitude control.

at their maximum value and the duration of the pulse is controlled by the length of the signal applied to the grid of V_3.

In the pulse brightening unit a positive pulse of fixed height and variable length is produced by the valves V_1 to V_4. The duration of this pulse is determined by the time constant R_2C_2 and the pulse length control is provided by the 5 M potentiometer making up R_2. The 400 K fixed resistor of R_2 is used to safeguard the two valves V_3 and V_4. The negative lengthening signal applied to the grid of V_3 in the pulse lengthening unit is taken from the common anode load of V_1 and V_2. The output from the anode of V_4 is fed through the cathode-coupled valves V_6 and V_7 onto the grid of the cathode-ray tube. A square positive pulse is produced with a variable delay on the front-edge provided by R_3, and a variable amplitude provided by the control R_4. The delay is incorporated to ensure that the signal pulse has reached its maximum value before the brightening pulse is applied. As will be seen from the above description the control R_2 varies the length of both signal and brightening pulses. The circuit is designed to cut off the brightening pulse at a fixed time interval before the back-edge of the signal pulse.

The cathode-ray tube used has a screen of silver-activated zinc sulphide to give it a fast response to the

pulsed electron beam. It is run off a 2 kV negative E.H.T. supply and the focus and brilliance controls are connected up in the standard manner. A diagram of the circuit used to produce the D.C. Y-deflection is shown in Figure 3. The 300 V supply is taken from the positive line of the power-pack used to run the two units of the kicksorter. By the use of a suitable dropping resistor (40 K), about 100 V is developed across the 50 K double-potentiometer (R_2 and R_3). This control provides the coarse push-pull Y-deflection of up to 100 V, both positive and negative. A fine control of 10 V range is provided by the potentiometer R_1. This control alters the mean potential of the Y-plates slightly, but the change is not sufficient to affect the focusing of the electron beam. The deflecting voltage applied to the Y-plates is read on the large-scale voltmeter V, and this is taken as a measure of the pulse-height of the portion of the spectrum opposite the photomultiplier slit. The X-plates are not used in this arrangement and they are tied together and connected to the astigmatism control to avoid defocusing the electron beam.

The response of the pulse lengthening unit was found to be linear from 0 V up to 60 V input, when the pulses were not lengthened. When the pulses were lengthened a non-linearity was observed for low inputs, and the form of the graph obtained is shown in Figure 4. The push-pull output

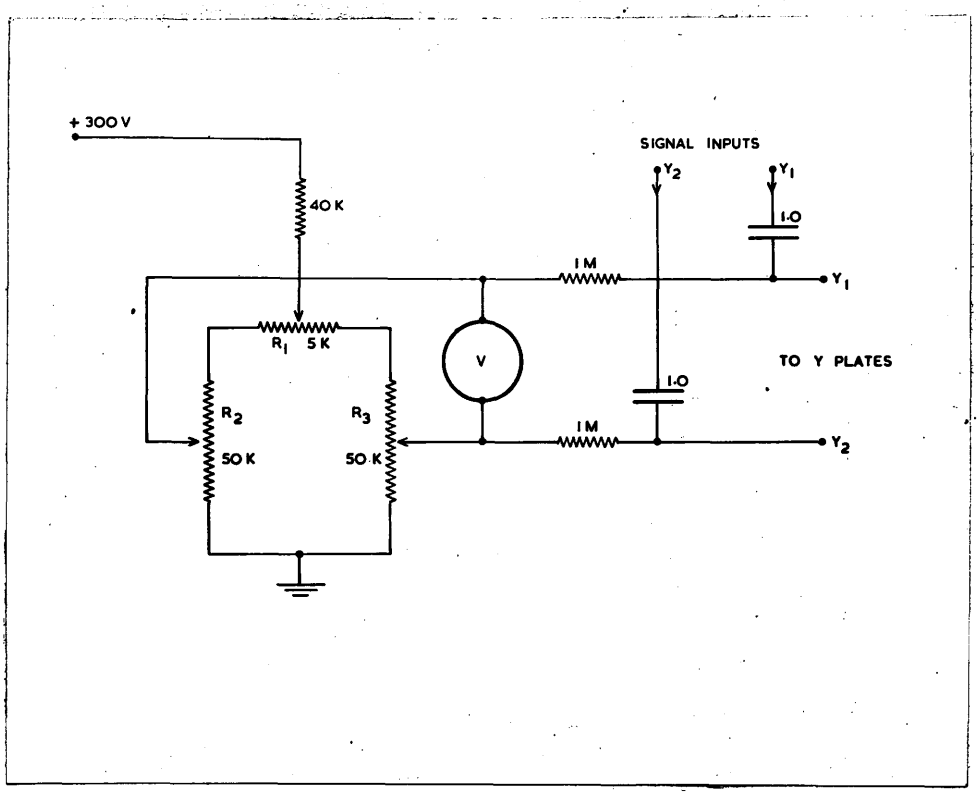

Figure 3.

The D.C. Y-deflection circuit.

R_1 = fine Y-shift control: R_2+R_3 = coarse Y-shift control:

V = large scale voltmeter.

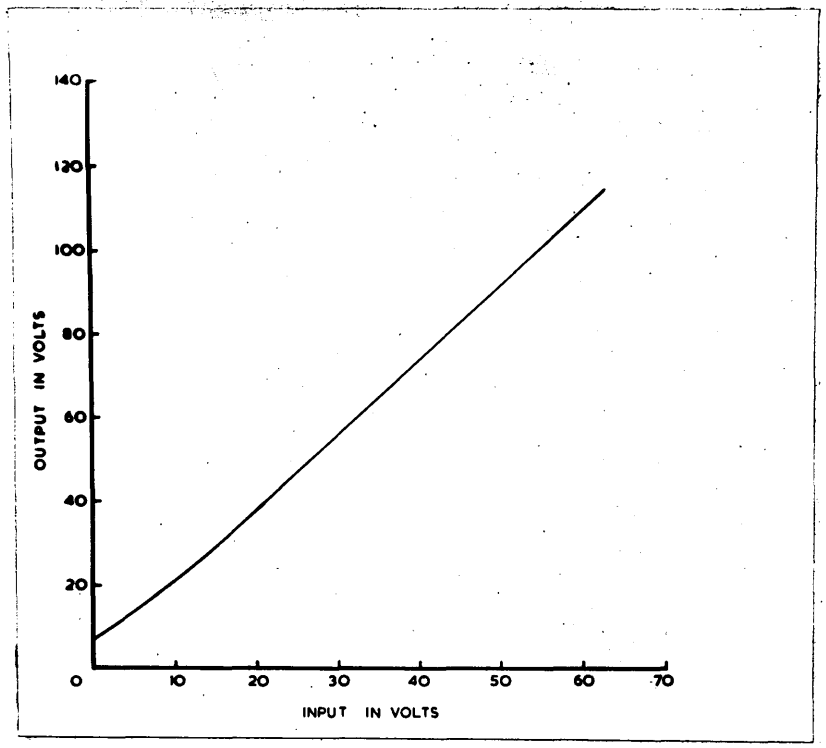

Figure 4.

The kicksorter calibration curve, showing the resultant Y-deflection plotted against the input voltage when a constant trigger pulse is applied to the pulse brightening unit. Note the non-linearity below ~15 V input.

pulses are approximately double the input pulses. The non-linearity is due to the sudden cut-off of the valve V_3 in the pulse lengthening unit by the negative signal from the brightening unit. This produces a slight positive increase in the grid voltage of V_4, if it has not already been driven positive by a large signal pulse. Thus for input pulses greater than $\sim$15 V, the response is found to be linear. For smaller pulses the output is greater than expected, until for zero signal input the cut-off effect produces an output pulse of 7 V.

The channel width of the kicksorter depends on three variables, the setting of the brilliance control, the amplitude of the brightening pulse and the gain of the 931A photomultiplier tube. Under normal working conditions the voltage on the 931A tube is kept constant at 1100 V, and the brilliance control is adjusted so that the zero spot on the screen is just visible. The brightness amplitude control R_4 (Figure 2b) is then used to vary the channel width. From a number of tests it was verified that the channel width is constant over the complete working range and that the shape of the channel is practically rectangular, i.e. all pulses within the channel limits are counted, but none outside. The width most commonly used is one of 2 V, although this can be reduced to 1 V if necessary for more accurate work. The channel width is set up by feeding

pulses of a constant height from a pulse generator into the kicksorter and varying the bias control until they appear opposite the slit. The brightness control is then adjusted so that the pulses are counted over a 2 V variation in bias. This adjustment need not be very accurate, since the important factor is the constancy of the channel width, not its absolute value.

References.

Allen,J.S. and Engelder,T.C., 1951, Rev. Sci. Instr., 22, 401.

Bannerman,R.C., Lewis,G.M. and Curran,S.C., 1951, Phil. Mag., 42, 1097.

Bannerman,R.C. and Curran,S.C., 1952, Phys. Rev., 85, 134.

Bannerman,R.C., 1952, Proc. Phys. Soc. (Submitted for publication as a letter).

Beach,L.A., Peacock,C.L. and Wilkinson,R.G., 1949, Phys. Rev., 76, 1624.

Bell,P.R., 1948, Phys. Rev., 73, 1405.

Bell,P.R. and Cassidy,J.M., 1949, Phys. Rev., 76, 183.

Bishop,G.R., Wilson,R. and Halban,H., 1950, Phys. Rev., 77, 416.

Brady,E.L. and Deutsch,M., 1948, Phys. Rev., 74, 1541.

Burson,S.B. and Muehlhause,C.O., 1948, Phys. Rev., 74, 1264.

Butt,D.K., 1950, Proc. Phys. Soc., A 63, 986.

Butt,D.K. and Brodie,W.D., 1951, Proc. Phys. Soc., A 64, 791.

Cockroft,A.L. and Curran,S.C., 1951, Rev. Sci. Instr., 22, 37.

Coltman,J.W. and Marshall,F.H., 1947, Nucleonics, 1, No. 3, 58.

Compton,A.H. and Allison,S.K., 1935, X-Rays (Van Nostrand).

Craig,H., 1952, Phys. Rev., 85, 688.

Cranberg,L., 1950, Phys. Rev., 77, 155.

Curran,S.C. and Baker,W.R., 1944, Rad. Lab. Report, 7.6.16. (A summary of this report is given by the same authors

in Rev. Sci. Instr., 19, 116 (1948).)

Curran,S.C., Angus,J. and Cockroft,A.L., 1949,
Phil. Mag., 40, 36.

Curran,S.C., Cockroft,A.L. and Insch,G.M., 1950,
Proc. Phys. Soc., A 63, 845.

De Benedetti,S., McGowan,F.K. and Francis,J.E., 1948,
Phys. Rev., 73, 1404.

Delsasso,L.A., Fowler,W.A. and Lauritsen,C.C., 1937,
Phys. Rev., 51, 391.

Deutsch,M., 1948, Nucleonics, 2, No. 3, 58.

Deutsch,M. and Metzger,F., 1948, Phys. Rev., 74, 1542.

Dunworth,J.V., 1940, Rev. Sci. Instr., 11, 167.

Ellis,C.D. and Skinner,H.W.B., 1924, Proc. Roy. Soc., 105, 60.

Falk-Vairant,P., Teillac,J. and Victor,C., 1951,
Comptes Rendus, 232, 1025.

Feather,N., 1938, Proc. Camb. Phil. Soc., 34, 599.

Feather,N., 1949, Nucleonics, 5, No. 1, 22.

Feather,N., Kyles,J. and Pringle,R.W., 1948,
Proc. Phys. Soc., A 61, 466.

Frilley,M., Gokhale,B.G. and Valadares,M., 1951,
Comptes Rendus, 232, 50 and 157.

Godfrey,T.N.K., Harrison,F.B. and Keuffel,J.W., 1951,
Phys. Rev., 84, 1248.

Hanson,A.O., 1949, Phys. Rev., 75, 1794.

Heitler,W., 1944, The Quantum Theory of Radiation,
(Oxford Univ. Press).

Hill,J.M. and Shepherd,L.R., 1950, Proc. Phys. Soc., A 63, 126.

Hill,R.D., 1948, Phys. Rev., 74, 78.

Hofstadter,R., 1948, Phys. Rev., 74, 100.

Hofstadter,R. and McIntyre,J.A., 1950a,
Nucleonics, 7, No. 3, 32.

Hofstadter,R. and McIntyre,J.A., 1950b, Phys. Rev., 78, 619.

Hopkins,J.I., 1951, Rev. Sci. Instr., 22, 29.

Hornyak,W.F., Lauritsen,T., Morrison,P. and Fowler,W.A., 1950,
Rev. Mod. Phys., 22, 291.

Insch,G.M., Balfour,J.G. and Curran,S.C., 1952,
Phys. Rev., 85, 805.

Johansson,S.A.E., 1950, Nature, 165, 396; Ark. Fys., 2, 216.

Johansson,S.A.E., 1952, Phil. Mag., 43, 249.

Jordan,W.H. and Bell,P.R., 1949, Nucleonics, 5, No. 4, 30.

Kallmann,H., 1947, Natur und Technik, July.

Kallmann,H., 1949, Phys. Rev., 75, 623.

Kallmann,H., 1950, Phys. Rev., 78, 621.

Kinsey,B., 1948, Can. J. Research, 26, 421.

Lind,D.A., Brown,J.R. and DuMond,J.W.M., 1949,
Phys. Rev., 76, 1838.

McIntyre,J.A. and Hofstadter,R., 1950, Phys. Rev., 78, 617.

McMillan,E., 1934, Phys. Rev., 46, 868.

Mandeville,C.E. and Scherb,M.V., 1948, Phys. Rev., 73, 1434.

Mitchell,A.C.G., Langer,L.M. and Brown,L.J., 1947,
Phys. Rev., 71, 140.

Moon,P.B., 1949, Artificial Radioactivity (C.U.P.).

Morton,G.A., 1948, R.C.A. Review, 10, 525.

Morton,G.A. and Mitchell,J.A., 1949, Nucleonics, 4, No. 1, 16.

Nuclear Data, 1950, National Bureau of Standards
Circular No. 499.

Osborne,R.K. and Peacock,W.C., 1946, Phys. Rev., 69, 679.

Persico,E. and Geoffrion,C., 1950, Rev. Sci. Instr., 21, 945.

Pringle,R.W., Roulston,K.I. and Taylor,H.W., 1950,
Rev. Sci. Instr., 21, 216.

Rall,W. and Wilkinson,R.G., 1947, Phys. Rev., 71, 321.

Richardson,H.O.W. and Leigh-Smith,A., 1937,
Proc. Roy. Soc., A 160, 454.

Robinson,B.L. and Madansky,L., 1951, Phys. Rev., 84, 1067.

Rothwell,P. and West,D., 1950, Proc. Phys. Soc., A 63, 539.

Rutherford,E., 1919, Phil. Mag., 37, 537.

Schardt,A.W. and Bernstein,W., 1951,
Rev. Sci. Instr., 22, 1020.

Slätis,H. and Siegbahn,K., 1949, Phys. Rev., 75, 318.

Taschek,R.F. and Gittings,H.T., 1948, Phys. Rev., 74, 1553.

Taylor,C.J., Jentschke,W.K., Remley,M.E., Eby,F.S. and
Kruger,P.G., 1951, Phys. Rev., 84, 1034.

Tollestrup,A.V., 1948, Phys. Rev., 74, 1561.

Van Sciver,W. and Hofstadter,R., 1951, Phys. Rev., 84, 1062.

Walker,R.L. and McDaniel,B.D., 1948, Phys. Rev., 74, 315.

Wattenberg,A., 1947, Phys. Rev., 71, 497.

West,H.J., Meyerhof,W.E. and Hofstadter,R., 1951,
Phys. Rev., 81, 141.

Wilson,H.W. and Curran,S.C., 1951, Phil.Mag., 42, 762.

Zworykin,V.K. and Rajchman,J.A., 1939, Proc. I.R.E., 27, 558.